# MEMOIRS

OF THE

# COLLEGE OF SCIENCE

KYOTO IMPERIAL UNIVERSITY

VOL. II NO. 2

MARCH 1917

KYOTO

# Reflexion and Refraction Phenomena relating to a Moving Medium.

By

**Kajuro Tamaki.**

(Received Nov. 21, 1916).

Since Fresnel[1] took up the problem of whether the motion of a mirror had any effect on the laws of reflexion and refraction, the problem has been investigated by many prominent physicists, Stokes[2], Voigt[3], Lodge[4], Hicks[5], Abraham[6], Einstein[7], Planck[8], Lorentz[9], Larmor[10], and others. The object of this paper is to report a study of the important phenomena of reflexion and refraction relating to a moving medium when the motion is not, as usual, confined to the direction normal to the surface of separation of two media. In this study the generalized Lorentz-Einstein transformation equations previously obtained by the present writer[11] are utilised.

## 1. Reflexion and Refraction in a Stationary Medium.

The phenomena of reflexion and refraction of light in a stationary medium are treated in several text-books of optics or of electricity[12]. For convenience of reference we shall here cite the results already established:

(i) Light polarized in the plane of incidence.

1 A. J. Fresnel, Annales de chimie, **9**, 57 (1818).
2 G. G. Stokes, Phil. Mag., **28**, 76 (1846); Math. Phys. Papers **1**, 140.
3 W. Voigt, Göttinger Nachr., 215 (1887).
4 O. Lodge, Phil. Trans., **184**, 793 (1893).
5 W. H. Hicks, Phil. Mag., **3**, 9 (1902).
6 M. Abraham, Ann. d. Phys., **14**, 236 (1904); Theorie d. Elektr., **2**, 327 (1908).
7 A. Einstein, Ann. d. Phys., **17**, 891 (1905).
8 M. Planck, Theorie der Wärmestrahlung, p. 71, Leipzig 1906.
9 H. A. Lorentz, Theory of Electrons, p. 60, Leipzig 1909.
10 J. Larmor, Phil. Mag., **28**, 702 (1914).
11 K. Tamaki, Mem. Col. Sci. Eng. Kyoto Imp. Univ., **3**, 103 (1911).
12 Cf. e.g. J. H. Jeans, Electr. Mag., p. 516, Cambridge 1908.

Let the boundary of a medium (1) and another one (2) be taken as the $yz$-plane, and let it intersect with the plane of incidence along the $y$-axis. The normal of the boundary plane drawn inwards to the medium (2) is taken as the $x$-axis, the $z$-axis being directed to the reader from the paper. Then the components of the electric force and the magnetic force for the incident light wave may be given by

$$\left.\begin{aligned} E_x &= 0, \\ E_y &= 0, \\ E_z &= E_{z0}^{i}\ e^{i2\pi\omega_i(t-\frac{x\cos\theta_i+y\sin\theta_i}{c_1})}, \\ H_x &= H_{x0}^{i}\ e^{i2\pi\omega_i(t-\frac{x\cos\theta_i+y\sin\theta_i}{c_1})}, \\ H_y &= H_{y0}^{i}\ e^{i2\pi\omega_i(t-\frac{x\cos\theta_i+y\sin\theta_i}{c_1})}, \\ H_z &= 0, \end{aligned}\right\} \quad \ldots\ldots\ (1.1)^1$$

where $\theta_i$ is the incident angle, $\omega_i$ the frequency and $c_1$ the velocity of propagation of wave in the medium (1), $E_{z0}^{i}, H_{x0}^{i}, H_{y0}^{i}$ being constants. In order that the above equations may satisfy the fundamental equations for the electromagnetic field, the following equations must be satisfied :

Fig. 1.

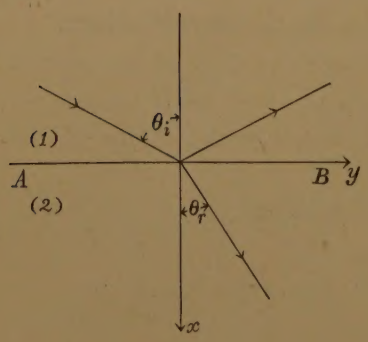


$$\frac{H_{x0}^{i}}{\sin\theta_i} = \frac{H_{y0}^{i}}{-\cos\theta_i} = \frac{E_{z0}^{i}}{\sqrt{\mu_1/\varepsilon_1}},$$

where $\varepsilon_1$ and $\mu_1$ are respectively the dielectric constant and permeability for the medium (1). Since in the case of light vibrations, $\mu_1$ does not differ much from unity, we may put

$$\frac{H_{x0}^{i}}{\sin\theta_i} = \frac{H_{y0}^{i}}{-\cos\theta_i} = \sqrt{\varepsilon_1}\ E_{z0}^{i}. \quad \ldots\ldots\ (1.2)$$

Similarly we have for the refracted wave

[1] The decimal system of paragraphing by Peano is adopted for numbering equations.

$$\left.\begin{aligned} E_x &= 0, \\ E_y &= 0, \\ E_z &= E_{z0}^{i}\, e^{i2\pi\omega_i(t-\frac{x\cos\theta_i + y\sin\theta_i}{c_1})}, \\ H_x &= H_{x0}^{i}\, e^{i2\pi\omega_i(t-\frac{x\cos\theta_i + y\sin\theta_i}{c_1})}, \\ H_y &= H_{y0}^{i}\, e^{i2\pi\omega_i(t-\frac{x\cos\theta_i + y\sin\theta_i}{c_1})}, \\ H_z &= 0, \end{aligned}\right\} \quad \ldots\ldots (1.3)$$

$$\frac{H_{x0}^{i}}{\sin\theta_i} = \frac{H_{y0}^{i}}{-\cos\theta_i} = \sqrt{\varepsilon_1}\, E_{z0}^{i}, \quad \ldots\ldots (1.4)$$

and for the refracted wave

$$\left.\begin{aligned} E_x &= 0, \\ E_y &= 0, \\ E_z &= E_{z0}^{r}\, e^{i2\pi\omega_r(t-\frac{x\cos\theta_r + y\sin\theta_r}{c_2})}, \\ H_x &= H_{x0}^{r}\, e^{i2\pi\omega_r(t-\frac{x\cos\theta_r + y\sin\theta_r}{c_2})}, \\ H_y &= H_{y0}^{r}\, e^{i2\pi\omega_r(t-\frac{x\cos\theta_r + y\sin\theta_r}{c_2})}, \\ H_z &= 0, \end{aligned}\right\} \quad \ldots\ldots (1.5)$$

$$\frac{H_{x0}^{r}}{\sin\theta_r} = \frac{H_{y0}^{r}}{-\cos\theta_r} = \sqrt{\varepsilon_2}\, E_{z0}^{r}. \quad \ldots\ldots (1.6)$$

These eqnations must be connected by the following relations:

$$\omega_i = \omega_l = \omega_r, \quad \ldots\ldots (1.7)$$

$$\theta_l = \pi - \theta_i, \quad \ldots\ldots (1.8)$$

$$\frac{\sin\theta_i}{\sin\theta_r} = \frac{c_1}{c_2} = n_{12}, \quad \ldots\ldots (1.9)$$

where $n_{12}$ is the refractive index of the medium (2) with respect to the medium (1). As is well known, equations (1.8) and (1.9) represent the reflexion and refraction law respectively. In addition to the above relations (1.7), (1.8), (1.9) we have the following ones:

$$\frac{E_{z0}^{l}}{E_{z0}^{i}} = \frac{\sin(\theta_r - \theta_i)}{\sin(\theta_r + \theta_i)}, \quad \ldots\ldots (1.10)$$

$$\frac{E_{z0}^{r}}{E_{z0}^{i}} = \frac{2\sin\theta_r\cos\theta_i}{\sin(\theta_r + \theta_i)}. \quad \ldots\ldots (1.11)$$

(ii) Light polarized perpendicular to the plane of incidence.

The geometrical relations among the incident, reflected and refracted rays are exactly similar to those in the first case, while the components of the electric and magnetic forces in those rays are connected by the equations

$$\frac{E^i_{x0}}{-\sin\theta_i} = \frac{E^i_{y0}}{\cos\theta_i} = \frac{H^i_{z0}}{\sqrt{\varepsilon_1}}, \quad \cdots\cdots (1.12)$$

$$\frac{E^l_{x0}}{-\sin\theta_l} = \frac{E^l_{y0}}{\cos\theta_l} = \frac{H^l_{z0}}{\sqrt{\varepsilon_1}}, \quad \cdots\cdots (1.13)$$

$$\frac{E^r_{x0}}{-\sin\theta_r} = \frac{E^r_{y0}}{\cos\theta_r} = \frac{H^r_{z0}}{\sqrt{\varepsilon_2}}, \quad \cdots\cdots (1.14)$$

$$\frac{H^l_{z0}}{H^i_{z0}} = \frac{2\cos\theta_i \sin\theta_r}{\sin(\theta_i+\theta_r)}, \quad \cdots\cdots (1.15)$$

$$\frac{H^r_{z0}}{H^i_{z0}} = \frac{2\sin\theta_i}{\sin 2\theta_i + \sin 2\theta_r}. \quad \cdots\cdots (1.16)$$

So far the discussion relates to a stationary medium; and in the next article we shall proceed into the case of a moving medium.

## 2. Aberration, Doppler Effect and Fresnel's Dragging Coefficient.

The aberration and the Doppler effect have been neatly treated by Einstein[1], as applications of his Principle of Relativity. Now, following his method, we shall deduce certain formulæ which are necessary in the succeding articles.

Let us consider a system $K'(x', y', z', t')$ moving with a constant velocity $v$ along a certain direction having direction cosines $l, m, n$ with respect to a stationary system $K(x, y, z, t)$. According to the generalized Lorentz-Einstein transformation[2] we have the following equations:

$$\left.\begin{aligned} x' &= x+(\gamma-1)\,l\,(lx+my+nz)-\gamma vlt, \\ y' &= y+(\gamma-1)\,m\,(lx+my+nz)-\gamma vmt, \\ z' &= z+(\gamma-1)\,n\,(lx+my+nz)-\gamma vnt, \\ t' &= \gamma\left\{t-\frac{v}{c^2}(lx+my+nz)\right\}, \end{aligned}\right\} \quad \cdots\cdots (2.1)$$

[1] A. Einstein, loc. cit.

[2] K. Tamaki, loc. cit., p. 106.

where

$$\gamma = \frac{1}{\sqrt{1-(v/c)^2}} = \frac{1}{\sqrt{1-\beta^2}}. \qquad \ldots\ldots (2.2)$$

The light disturbance in the $K'$-system may be expressed by the electric and magnetic force having the exponential factor $e^{i\Theta}$, where

$$\theta = 2\pi\omega'\left(t' - \frac{\lambda' x' + \mu' y' + \nu' z'}{c_1'}\right). \qquad \ldots\ldots (2.3)$$

If we substitute (2.1) in this expression we get

$$\begin{aligned}\theta = 2\pi\omega'\Big[&\gamma\left(1+\frac{v}{c_1'}\cos\chi'\right)t \\ &-x\left\{\gamma\frac{v}{c^2}l+\frac{\lambda'}{c_1'}+\frac{1}{c_1'}(\gamma-1)\,l\cos\chi'\right\} \\ &-y\left\{\gamma\frac{v}{c^2}m+\frac{\mu'}{c_1'}+\frac{1}{c_1'}(\gamma-1)\,m\cos\chi'\right\} \\ &-z\left\{\gamma\frac{v}{c^2}n+\frac{\nu'}{c_1'}+\frac{1}{c_1'}(\gamma-1)n\cos\chi'\right\}\Big], \qquad (2.4)\end{aligned}$$

where

$$\cos\chi' = l\lambda' + m\mu' + n\nu' \qquad \ldots\ldots (2.5)$$

is the cosine of the angle between the direction of propagation of the wave and the direction of motion of the system $K'$.

But since, by the Principle of Relativity, we must also have

$$\theta = 2\pi\omega\left(t - \frac{\lambda x + \mu y + \nu z}{c_1}\right), \qquad \ldots\ldots (2.6)$$

in the stationary system, comparing this with (2.4), we get

$$\omega = \omega'\gamma\left(1+\frac{v}{c_1'}\cos\chi'\right), \qquad \ldots\ldots (2.7)$$

and

$$\left.\begin{aligned}\omega\frac{\lambda}{c_1} &= \omega'\left\{\gamma\frac{v}{c^2}l+\frac{\lambda'}{c_1'}+\frac{1}{c_1'}(\gamma-1)\,l\cos\chi'\right\}, \\ \omega\frac{\mu}{c_1} &= \omega'\left\{\gamma\frac{v}{c^2}m+\frac{\mu'}{c_1'}+\frac{1}{c_1'}(\gamma-1)\,m\cos\chi'\right\}, \\ \omega\frac{\nu}{c_1} &= \omega'\left\{\gamma\frac{v}{c^2}n+\frac{\nu'}{c_1'}+\frac{1}{c_1'}(\gamma-1)\,n\cos\chi'\right\}.\end{aligned}\right\} \ldots (2.8)$$

If the angle between the directions of the motion and the propagation of light in the $K$-system be denoted by $\chi$, we have

$$\cos\chi = l\lambda + m\mu + n\nu. \qquad \ldots\ldots (2.9)$$

Multiplying $l, m, n$ to the equations (2.8) respectively and adding them together, we obtain

$$\frac{\omega}{c_1}\cos\chi = \omega'\gamma\left(\frac{v}{c^2} + \frac{1}{c_1'}\cos\chi'\right),$$

which combined with the equation (2.7) gives

$$\frac{\cos\chi}{c_1} = \frac{\cos\chi'/c_1' + v/c^2}{1 + v\cos\chi'/c_1'}, \qquad \ldots\ldots (2.10)$$

or, solving for $\cos\chi'/c_1'$

$$\frac{\cos\chi'}{c_1'} = \frac{\cos\chi/c_1 - v/c^2}{1 - v\cos\chi/c_1}. \qquad \ldots\ldots (2.11)$$

From either of these, it follows that

$$\left(1 + \frac{v}{c_1'}\cos\chi'\right)\left(1 - \frac{v}{c_1}\cos\chi\right) = 1 - \beta^2. \qquad \ldots\ldots (2.12)$$

Squaring and adding the equations (2.8) we get

$$\frac{\omega^2}{c_1^2} = \omega'^2\gamma^2\left\{\left(\frac{v}{c^2} + \frac{\cos\chi'}{c_1'}\right)^2 + (1-\beta^2)\frac{\sin^2\chi'}{c_1'^2}\right\}$$

which becomes by (2.7)

$$c_1 = c\,\frac{c + vn'\cos\chi'}{\sqrt{(v + cn'\cos\chi')^2 + (c^2 - v^2)\,n'^2\sin^2\chi'}}, \qquad (2.13)$$

where $n'$ is the refractive index of the moving medium.

This equation may be simplified if we neglect the terms containing higher orders of $\beta = v/c$, namely

$$\begin{aligned} c_1 &= \frac{c}{n'}(1 + \beta n'\cos\chi')\left(1 - \frac{1}{n'}\beta\cos\chi'\right) \\ &= \frac{c}{n'} + \left(1 - \frac{1}{n'^2}\right)v\cos\chi'. \qquad \ldots\ldots (2.14) \end{aligned}$$

The first term in the last equation is the velocity of light in the moving medium, and the coefficient of $v\cos\chi'$ in the second term is the well-known Fresnel's dragging coefficient.

When the light proceeds or receeds in the direction of motion of

the medium, as in the case of Fizeau's experiment, the above expression becomes

$$c_1 = \frac{c}{n'} \pm v\left(1 - \frac{1}{n'^2}\right),$$

which is exactly the same as that given in the usual text-books[1].

Multiplying $c_1$ to both sides of (2.10) we get, by the aid of (2.13),

$$\cos\chi = \frac{\beta + n'\cos\chi'}{\sqrt{(\beta + n'\cos\chi')^2 + (1-\beta^2)\,n'^2\sin^2\chi'}}$$

$$\fallingdotseq (\cos\chi' + \beta/n')(1 - \beta\cos\chi'/n')$$

$$\fallingdotseq \cos\chi' + \beta\sin^2\chi'/n'. \qquad \ldots\ldots (2.15)$$

Similarly we get

$$\cos\chi' \fallingdotseq \cos\chi - \beta\sin^2\chi/n'. \qquad \ldots\ldots (2.16)$$

Thus we see that up to the first power of $v$ we may write (2.14) in the form

$$c_1 = \frac{c}{n'} + \left(1 - \frac{1}{n'^2}\right) v\cos\chi. \qquad \ldots\ldots (2.17)$$

Hence the velocity in the moving medium measured in the stationary $K$-system is different in different directions. Fig. 2 shows the dependence of $c_1$ on directions. In this figure $ABCD$ is the circle of radius $c/n'$ and $EFG$ is that of radius $v\left(1 - \frac{1}{n'^2}\right)$. $GA$ represents the direction of motion of the medium. The curve $HBJD$ is the locus of the end points of $c_1$ drawn from $G$.

Fig. 2.

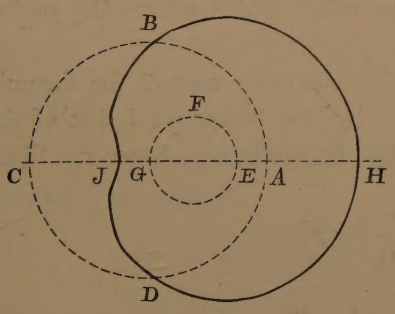


The equation (2.7) shows the Doppler effect. For instance, when a star $S$, as shown in Fig. 3, moving with a constant velocity $v$ along a certain direction $SS'$, is observed by an observer $O$, the frequency of any spectrum line of the star spectrum is given by

$$\omega = \omega_0 \frac{\sqrt{1 - (v/c)^2}}{1 - \frac{v}{c}\cos\chi}, \qquad \ldots\ldots (2.18)$$

1 E. g., W. Wood, Physical Optics p. 669, New York 1911.

where $\omega_0$ is the stationary frequency of the spectrum line and $\chi$ is the angle of the direction of the visual line and the reverse direction of the star's motion. The longitudinal Doppler effect[1] is given by

Fig. 3.

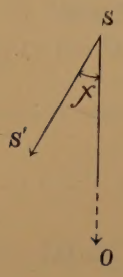


$$\omega = \omega_0 \frac{\sqrt{1-(v/c)^2}}{1 \mp v/c},$$

while the transverse Doppler effect[2] is given by

$$\omega = \omega_0 \sqrt{1-(v/c)^2}.$$

Let $T$, $T'$ and $\Lambda$, $\Lambda'$ be the periods and wave lengths in the two systems $K$ and $K'$ respectively. Then we get from (2.7)

$$T = T' \frac{\sqrt{1-(v/c)^2}}{1+\frac{v}{c_1'}\cos\chi'} = T' \frac{1-\frac{v}{c_1}\cos\chi}{\sqrt{1-(v/c)^2}}, \qquad (2.19)$$

$$\Lambda = \Lambda' \frac{c_1}{c_1'} \frac{\sqrt{1-(v/c)^2}}{1+\frac{v}{c_1'}\cos\chi'} = \Lambda' \frac{c_1}{c_1'} \frac{1-\frac{v}{c_1}\cos\chi}{\sqrt{1-(v/c)^2}}. \qquad (2.20)$$

These equations express the Doppler effect which affects the period and the wave length.

On account of the Doppler effect we must correct the formula (2.17), because $n'$ must be replaced by the refractive index of the wave of frequency actually observed by the stationary observer. Since by (2.20) we have

$$\Lambda \fallingdotseq \Lambda'\left(1-\frac{v}{c_1}\cos\chi\right)$$

we get

$$\begin{aligned} n &= n' + \frac{dn'}{d\Lambda'}(\Lambda - \Lambda') \\ &= n'\left(1-\frac{v}{c_1}\frac{\Lambda'}{n'}\frac{dn'}{d\Lambda'}\cos\chi\right) \\ &\fallingdotseq n'\left(1-\beta\frac{dn}{d\Lambda}\Lambda\cos\chi\right). \end{aligned}$$

Consequently (2.17) must be replaced by

[1] E. g., E. Cunningham, The Principle of Relativity, p. 60, Cambridge 1914.

[2] E. Cunningham, loc. cit., p. 61.

$$c_1 \doteqdot \frac{c}{n}\left(1-\beta\Lambda\frac{dn}{d\Lambda}\cos\chi\right)+\left(1-\frac{1}{n^2}\right)v\cos\chi$$

$$=\frac{c}{n}+v\left(1-\frac{1}{n^2}-\frac{\Lambda}{n}\frac{dn}{d\Lambda}\right)\cos\chi. \qquad \ldots\ldots (2.21)$$

This expression is nothing but that obtained by Lorentz[1] and Laub[2] and proved experimentally by Zeeman[3] in the case where $\chi = 0$.

By (2.8) and (2.11) we get

$$\frac{\sin\chi}{c_1}=\sqrt{1-\beta^2}\;\frac{\sin\chi'/c_1'}{1+\frac{v}{c_1'}\cos\chi'}$$

from which it follows that

$$\operatorname{tg}\chi=\frac{\sin\chi'\sqrt{1-(v/c)^2}}{\cos\chi'+\beta\,c_1'/c}=\frac{\sin\chi'\sqrt{1-(v/c)^2}}{\cos\chi'+\beta/n'}. \qquad (2.22)$$

This expression can be geometrically represented, as by Laue[4].

It is important to prove that the plane containing the directions of motion and propagation of light waves remain the same when referred to either system. Let $\xi, \eta, \varsigma$ be the direction cosines of the normal of the plane under consideration referred to the stationary system $K$, then we have

$$l\xi+m\eta+n\varsigma = 0,$$
$$\lambda\xi+\mu\eta+\nu\varsigma = 0,$$

so that we have

$$\frac{\xi}{m\nu-n\mu}=\frac{\eta}{n\lambda-l\nu}=\frac{\varsigma}{l\mu-m\lambda}.$$

Similarly we get

$$\frac{\xi'}{m\nu'-n\mu'}=\frac{\eta'}{n\lambda'-l\nu'}=\frac{\varsigma'}{l\mu'-m\lambda'},$$

where $\xi', \eta', \varsigma'$ are the corresponding quantities in the moving system. But from (2.8) we have

$$\frac{\omega}{c_1}(m\nu-n\mu)=\frac{\omega'}{c_1'}(m\nu'-n\mu'),$$

---

1 H. A. Lorentz, Versuch einer Theorie d. elektr. u. opt. Ersch. in bewegten Körpern, p. 101, Leiden 1895.

2 J. Laub, Ann. d. Phys. **23**, 743 (1908).

3 P. Zeeman, Nature, **97**, 540 (1916).

4 M. Laue, Das Relativitätsprinzip, p. 103, Braunschweig 1913.

$$\frac{\omega}{c_1}(n\lambda - l\nu) = \frac{\omega'}{c_1'}(n\lambda' - l\nu'),$$

$$\frac{\omega}{c_1}(l\mu - m\lambda) = \frac{\omega'}{c_1'}(l\mu' - m\lambda').$$

Hence we obtain

$$\xi/\xi' = \eta/\eta' = \varsigma/\varsigma',$$

the relation which we desired to prove.

## 3. Doppler Effect due to Reflexion at a Moving Plane.

Let $K'$-system be taken in the moving medium so that the $y'z'$-plane always coincides with the moving boundary plane and the $x'$-axis be drawn normally inwards to the second medium. In the annexed figure, $Oxyz$ is the stationary coordinate system and $O'x'y'z'$ the moving one at any instant. Let $OO'$ be the direction of motion of the boundary of the media, then the exponential factors for the incident and the reflected waves are given by

Fig. 4.

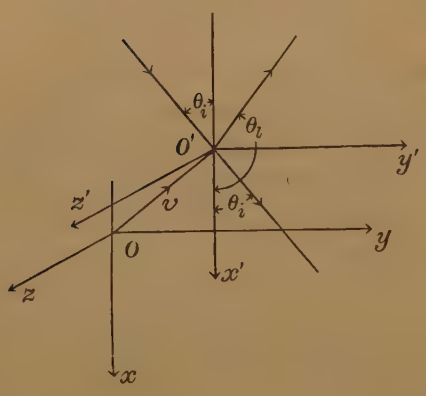


$$\left.\begin{aligned}\theta_i &= 2\pi\omega_i'\left(t' - \frac{\lambda_i'x' + \mu_i'y' + \nu_i'z'}{c_1'}\right),\\ \theta_l &= 2\pi\omega_l'\left(t' - \frac{\lambda_l'x' + \mu_l'y' + \nu_l'z'}{c_1'}\right),\end{aligned}\right\} \quad \ldots\ldots (3.1)$$

the suffices $i$ and $l$ signifying their reference to the incident and reflected wave respectively. Similarly in the stationary system we must have

$$\left.\begin{aligned}\theta_i &= 2\pi\omega_i\left(t - \frac{\lambda_i x + \mu_i y + \nu_i z}{c_1}\right),\\ \theta_l &= 2\pi\omega_l\left(t - \frac{\lambda_l x + \mu_l y + \nu_l z}{c_1}\right).\end{aligned}\right\} \quad \ldots\ldots (3.2)$$

If the incident wave propagates in the $x'y'$-plane in the $K'$-system, the incident angle being $\theta_i'$, we have

$$\lambda_i' = \cos\theta_i',\ \mu_i' = \sin\theta_i',\ \nu_i' = 0. \qquad \ldots\ldots (3.3)$$

Since the angle $\theta_l'$ between the direction of propagation of the reflected wave and the $x'$-axis is given by (1.8), namely by

$$\theta_l' = \pi - \theta_i',$$

we get

$$\left.\begin{aligned} \lambda_l' &= \cos\theta_l' = -\cos\theta_i', \\ \mu_l' &= \sin\theta_l' = \ \ \sin\theta_i', \\ \nu_l' &= 0. \end{aligned}\right\} \qquad \ldots\ldots (3.4)$$

If $\chi_i'$ and $\chi_l'$ are the angles between the direction of motion and that of propagation of the incident and that of reflected waves respectively, we have

$$\cos\chi_i' = l\lambda_i' + m\mu_i' + n\nu_i',$$
$$\cos\chi_l' = l\lambda_l' + m\mu_l' + n\nu_l',$$

and we get by (3.3) and (3.4)

$$\left.\begin{aligned} \cos\chi_i' &= \ \ l\cos\theta_i' + m\sin\theta_i', \\ \cos\chi_l' &= -l\cos\theta_i' + m\sin\theta_i'. \end{aligned}\right\} \qquad \ldots\ldots (3.5)$$

The corresponding quantities $\chi_i$ and $\chi_l$ in the $K$-system are given by

$$\left.\begin{aligned} \cos\chi_i &= l\lambda_i + m\mu_i + n\nu_i, \\ \cos\chi_l &= l\lambda_l + m\mu_l + n\nu_l, \end{aligned}\right\} \qquad \ldots\ldots (3.6)$$

and the following relations hold true in virtue of (2.10) and (2.11)

$$\left.\begin{aligned} \frac{\cos\chi_i}{c_1} &= \frac{\cos\chi_i'/c_1' + v/c^2}{1 + v\cos\chi_i'/c_1'}, \\ \frac{\cos\chi_l}{c_1} &= \frac{\cos\chi_l'/c_1' + v/c^2}{1 + v\cos\chi_l'/c_1'}, \end{aligned}\right\} \qquad \ldots\ldots (3.7)$$

$$\left.\begin{aligned} \frac{\cos\chi_i'}{c_1'} &= \frac{\cos\chi_i/c_1 - v/c^2}{1 - v\cos\chi_i/c_1}, \\ \frac{\cos\chi_l'}{c_1'} &= \frac{\cos\chi_l/c_1 - v/c^2}{1 - v\cos\chi_l/c_1}, \end{aligned}\right\} \qquad \ldots\ldots (3.8)$$

$$\frac{1 + v\cos\chi_i'/c_1'}{1 + v\cos\chi_l'/c_1'} = \frac{1 - v\cos\chi_i/c_1}{1 - v\cos\chi_l/c_1}. \qquad \ldots\ldots (3.9)$$

Let the angle of incidence be $\theta_i$ and that between the incident plane and the $xy$-plane be $\varphi_i$, then

$$\left.\begin{aligned} \lambda_i &= \cos\theta_i, \\ \mu_i &= \sin\theta_i \cos\varphi_i, \\ \nu_i &= \sin\theta_i \sin\varphi_i. \end{aligned}\right\} \qquad \ldots\ldots (3.10)$$

Now by the transformation equations (2.1) and the conditional equations (3.4) we get

$$\left.\begin{aligned} \omega_i &= \omega_i'\gamma\left(1+\frac{v}{c_1'}\cos\chi_i'\right), \\ \omega_i\frac{\lambda_i}{c_1} &= \omega_i'\left\{\gamma\frac{v}{c^2}l + \frac{\cos\theta_i'}{c_1'} + \frac{1}{c_1'}(\gamma-1)l\cos\chi_i'\right\}, \\ \omega_i\frac{\mu_i}{c_1} &= \omega_i'\left\{\gamma\frac{v}{c^2}m + \frac{\sin\theta_i'}{c_1'} + \frac{1}{c_1'}(\gamma-1)m\cos\chi_i'\right\}, \\ \omega_i\frac{\nu_i}{c_1} &= \omega_i'\left\{\gamma\frac{v}{c^2}n + \frac{1}{c_1'}(\gamma-1)n\cos\chi_i'\right\}. \end{aligned}\right\} \qquad (3.11)$$

Similarly we get

$$\left.\begin{aligned} \omega_i &= \omega_i'\gamma\left\{1+\frac{v}{c_1'}\cos\chi_i'\right\}, \\ \omega_i\frac{\lambda_i}{c_1} &= \omega_i'\left\{\gamma\frac{v}{c^2}l - \frac{\cos\theta_i'}{c_1'} + \frac{1}{c_1'}(\gamma-1)l\cos\chi_i'\right\}, \\ \omega_i\frac{\mu_i}{c_1} &= \omega_i'\left\{\gamma\frac{v}{c^2}m + \frac{\sin\theta_i'}{c_1'} + \frac{1}{c_1'}(\gamma-1)m\cos\chi_i'\right\}, \\ \omega_i\frac{\nu_i}{c_1} &= \omega_i'\left\{\gamma\frac{v}{c^2}n + \frac{1}{c_1'}(\gamma-1)n\cos\chi_i'\right\}. \end{aligned}\right\} \qquad (3.12)$$

Since we have by (1.7)

$$\omega_i' = \omega_i' \qquad \ldots\ldots (3.13)$$

the first equations in (3.11) and (3.12) can be combined into the single equation

$$\omega_i = \omega_i\frac{1+\frac{v}{c_1'}\cos\chi_i'}{1+\frac{v}{c_1'}\cos\chi_i'},$$

which becomes by (3.9)

$$\omega_i = \omega_i\frac{1-\frac{v}{c_1}\cos\chi_i}{1-\frac{v}{c_1}\cos\chi_i}. \qquad \ldots\ldots (3.14)$$

[1] M. Abraham, loc. cit. p. 329.

The last equation in (3.11), by the aids of (2.7) and (3.8), may be written

$$\frac{\nu_i}{n} = (1-\gamma)\cos\chi_i + \gamma\beta\frac{c_1}{c}. \qquad \ldots\ldots (3.15)$$

Similarly the corresponding equation in (3.12) becomes

$$\frac{\nu_l}{n} = (1-\gamma)\cos\chi_i + \gamma\beta\frac{c_1}{c}. \qquad \ldots\ldots (3.16)$$

Combining the two middle equations with the last one in (3.11) we get

$$\left.\begin{aligned} \frac{\cos\theta_i'}{c_1'} &= l\,\frac{\lambda_i/l-\nu_i/n}{\gamma c_1\left(1-\frac{v}{c_1}\cos\chi_i\right)}, \\ \frac{\sin\theta_i'}{c_1'} &= m\,\frac{\mu_i/m-\nu_i/n}{\gamma c_1\left(1-\frac{v}{c_1}\cos\chi_i\right)}. \end{aligned}\right\} \qquad \ldots\ldots (3.17)$$

Squaring and adding these last equations we obtain

$$c_1' = c_1\frac{\gamma\left(1-\frac{v}{c_1}\cos\chi_i\right)}{\sqrt{(\lambda_i/l-\nu_i/n)^2l^2+(\mu_i/m-\nu_i/n)^2m^2}}. \qquad (3.18)$$

Substituting the value of $\nu_i/n$ given by (3.15) in (3.17) we get

$$\left.\begin{aligned} \frac{\cos\theta_i'}{c_1'} &= \frac{\lambda_i-l(1-\gamma)\cos\chi_i-l\gamma\beta c_1/c}{\gamma c_1\left(1-\frac{v}{c_1}\cos\chi_i\right)} \\ \frac{\sin\theta_i'}{c_1'} &= \frac{\mu_i-m(1-\gamma)\cos\chi_i-m\gamma\beta c_1/c}{\gamma c_1\left(1-\frac{v}{c_1}\cos\chi_i\right)} \end{aligned}\right\} \ldots (3.19)$$

and consequently

$$\left.\begin{aligned} \frac{\cos\chi_i'}{c_1'} &= \frac{(l\lambda_i+m\mu_i)-(l^2+m^2)(1-\gamma)\cos\chi_i-(l^2+m^2)\gamma\beta c_1/c}{\gamma c_1\left(1-\frac{v}{c_1}\cos\chi_i\right)}, \\ \frac{\cos\chi_i'}{c_1'} &= \frac{(m\mu_i-l\lambda_i)+(l^2-m^2)(1-\gamma)\cos\chi_i+(l^2-m^2)\gamma\beta c_1/c}{\gamma c_1\left(1-\frac{v}{c_1}\cos\chi_i\right)}. \end{aligned}\right\}$$

$$\ldots\ldots (3.20)$$

By the last equation we get

$$\cos\chi_i = \frac{(m\mu_i - l\lambda_i) + \gamma\beta\frac{c_1}{c}(1 + l^2 - m^2) + \left\{(1-\gamma)(l^2-m^2) - \gamma\beta^2\right\}\cos\chi_i}{\gamma\left\{1 + \beta^2(l^2-m^2)\right\} + \frac{v}{c_1}(m\mu_i - l\lambda_i) + \frac{v}{c_1}\left\{(1-\gamma)(l^2-m^2) - \gamma\right\}\cos\chi_i}, \quad \ldots\ldots (3.21)$$

and consequently

$$1 - \frac{v}{c}\cos\chi_i = \frac{\gamma(1-\beta^2)\left(1 - \frac{v}{c_1}\cos\chi_i\right)}{\gamma\left\{1 + \beta^2(l^2-m^2)\right\} + \frac{v}{c_1}(m\mu_i - l\lambda_i) + \frac{v}{c_1}\left\{(1-\gamma)(l^2-m^2) - \gamma\right\}\cos\chi_i},$$

by which (3.14) becomes

$$\omega_i = \omega_i\gamma\left[\gamma\left\{1 + \beta^2(l^2-m^2)\right\} + \frac{v}{c_1}(m\mu_i - l\lambda_i) + \frac{v}{c_1}\left\{(1-\gamma)(l^2-m^2) - \gamma\right\}\cos\chi_i\right]. \quad \ldots\ldots (3.22)$$

Let the direction of motion of the boundary plane be specified as shown in Fig. 5, then we have

$$\left.\begin{aligned} l &= \cos\theta, \\ m &= \sin\theta\cos\Phi, \\ n &= \sin\theta\sin\Phi, \end{aligned}\right\} \quad (3.23)$$

Fig. 5.

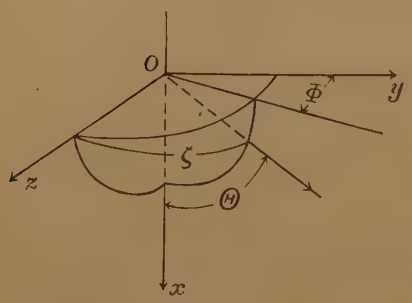


and consequently it follows that

$$\left.\begin{aligned} l^2 - m^2 &= 1 - \sin^2\theta(1 + \cos^2\Phi), \\ m\mu_i - l\lambda_i &= \cos\Phi\cos\varphi_i\sin\theta\sin\theta_i \\ &\quad - \cos\theta\cos\theta_i, \\ \cos\chi_i &= \cos\theta\cos\theta_i + \sin\theta\sin\theta_i \times \\ &\quad \times\cos(\Phi - \varphi_i). \end{aligned}\right\} \quad \ldots\ldots (3.24)$$

Hence the equation (3.22) becomes

$$\begin{aligned} \omega_i = \omega_i\gamma[&\gamma\{1 + \beta^2(1 - \sin^2\theta\,\overline{1 + \cos^2\Phi})\} + \beta(\cos\Phi\cos\varphi_i\sin\theta\sin\theta_i \\ &- \cos\theta\cos\theta_i) + \beta\{(1-\gamma)(1 - \sin^2\theta\,\overline{1 + \cos^2\Phi}) - \gamma\}\{\cos\theta\cos\theta_i \\ &+ \sin\theta\sin\theta_i\cos(\Phi - \varphi_i)\}]. \end{aligned} \quad \ldots\ldots (3.25)$$

When the plane of incidence coincides with the $xy$-plane we have $\varphi_i = 0$ and the last equation simplifies into

$$\omega_t = \omega_i\gamma[\gamma\{1+\beta^2(1-\sin^2\theta\sqrt{1+\cos^2\Phi})\}+\beta(\cos\Phi\cos\varphi_i\sin\theta\sin\theta_i - \cos\theta\cos\theta_i)+\beta\{(1-\gamma)(1-\sin^2\theta\sqrt{1+\cos^2\Phi})-\gamma\}\{\cos\theta\cos\theta_i + \sin\theta\sin\theta_i\cos\Phi\}]. \quad \ldots\ldots (3.26)$$

If the angle between the direction of motion and the $z$-axis is denoted by $\varsigma$ we have

$$\cos\varsigma = \sin\theta\sin\Phi \quad \ldots\ldots (3.27)$$

and the last equation may be written

$$\omega_t = \omega_i\gamma[\gamma\{1+\beta^2(1-2\sin^2\theta+\cos^2\varsigma)\} +\beta(1-\gamma)\sin\theta_i\sqrt{\sin^2\theta-\cos^2\varsigma}\,(2\cos^2\theta+\cos^2\varsigma) +\beta\cos\theta_i\cos\theta\{(1-\gamma)(1-2\sin^2\theta+\cos^2\varsigma)-(1+\gamma)\}]. \quad (3.28)$$

The equations (3.25) and (3.28) give the Doppler effect on the frequency due to reflexion at a moving plane. It is important to notice that it does not depend at all on the nature of the boundary plane, because this effect is kinematical.

Let us consider some special cases. When the motion of the boundary plane is confined in the incident plane, (3.26) simplifies into

$$\omega_t = \omega_i\gamma[\gamma\{1+\beta^2(1-2\sin^2\theta)\}-\beta\cos(\theta+\theta_i) +\beta\{(1-\gamma)(1-2\sin^2\theta)-\gamma\}\cos(\theta-\theta_i)], \quad \ldots\ldots (3.29)$$

and according as the motion is in the plane perpendicular to the incident plane or in the plane of boundary we get

$$\omega_t = \omega_i\gamma[\gamma(1+\beta^2\cos^2\theta)-\beta\cos\theta_i\cos\theta +\beta\{(1+\gamma)\cos^2\theta-\gamma\}\cos\theta_i\cos\theta] = \omega_i\gamma[\gamma(1+\beta^2\cos^2\theta)+\beta\cos\theta_i\cos\theta\{(1-\gamma)\cos^2\theta-(1+\gamma)\}], \quad \ldots\ldots (3.30)$$

or

$$\omega_t = \omega_i\gamma[\gamma(1-\beta^2\cos^2\Phi)+\beta\sin\theta_i\cos\Phi(1-\gamma)\sin^2\Phi]. \quad \ldots\ldots (3.31)$$

The change of frequency expressed by the last equation may be called the generalized transverse Doppler effect. When $\Phi = \pi/2$ we get the usual transverse Doppler effect

$$\omega_t = \omega_i\gamma^2 = \omega_i/(1-\beta^2).$$

When the motion is along the $x$-axis, i.e. along the inwards drawn

normal of the boundary plane, we get, by putting $\theta = 0$, $\varsigma = \pi/2$ in (3.27)

$$\omega_l = \omega_i\gamma[\gamma(1+\beta^2) - 2\gamma\beta\cos\theta_i]$$

$$= \omega_i \frac{1+\beta^2-2\beta\cos\theta_i}{1-\beta^2}, \qquad \ldots\ldots (3.32)$$

which is idential with that obtained by Harnack[1] and Edser[2]. Finally, when the motion occurs along the $y$-axis, we get, by putting $\varsigma = \theta = \pi/2$ in (3.27),

$$\omega_l = \omega_i\gamma[\gamma(1-\beta^2)] = \omega_i, \qquad \ldots\ldots (3.33)$$

which shows that there takes place no change of frequency; while, when the motion is along the $z$-axis, we get

$$\omega_l = \omega_i\gamma^2 = \omega_i/(1-\beta^2), \qquad \ldots\ldots (3.34)$$

which is the usual transverse Doppler effect already obtained.

## 4. Law of Reflexion at a Moving Plane.

Let us put

$$\left.\begin{aligned} \lambda_i &= -\cos\theta_i, \\ \mu_i &= \sin\theta_i\cos\varphi_i, \\ \nu_i &= \sin\theta_i\sin\varphi_i, \end{aligned}\right\} \qquad \ldots\ldots (4.1)$$

then, if we neglect $\beta^2$, the last two equations in (3.11) and (3.12) immediately give the important result:

$$\varphi_i = \varphi_l. \qquad \ldots\ldots (4.2)$$

Hence we see that, as far as the first order effect is considered, the usual reflection law which states that the reflected ray always lies in the plane of incidence also holds good even when the reflecting surface is in motion. The azimuth angle of the plane of incidence which would coincide with the $x'y'$-plane in the moving system can be obtained from (3.11) or (3.12). Thus

$$\operatorname{tg}\varphi_l = \operatorname{tg}\varphi_i = \beta\sin\dot{\Phi}\sin\theta/\sin\theta_i$$
$$= \beta\cos\varsigma/\sin\theta_i. \qquad \ldots\ldots (4.3)$$

---

1 A. Harnack, Ann. d. Phys., **39**. 1056 (1912).

2 E. Edser, Phil. Mag., **28**, 520 (1914).

If we adopt the aether hypothesis, we may suppose that there is an aether drift of the velocity $v\cos\varsigma$ in the negative direction of the $z$-axis, instead of considering that the reflecting surface is actually moving with the same velocity component $v\cos\varsigma$ in the positive direction of the $z$-axis. Then, since $y$-component of the velocity of light is $c\sin\theta_i$, the relation given by the equation (4.3) can be easily interpreted by means of the annexed figure

Fig. 6.

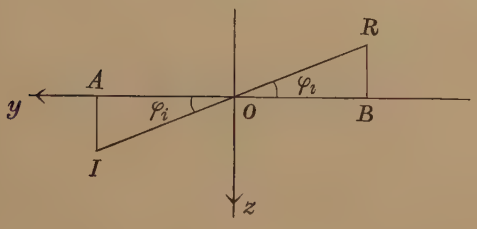


in which $AO=OB=c\sin\theta_i$ and $IA=BR=v\cos\varsigma$.

But, when the second order effect is taken into account, we find that there is a small deviation of the reflected ray from the incident plane. For we get, by (3.11) and (3.12), after easy transformations

$$\operatorname{tg}\varphi_i=\frac{\sin\Theta\sin\Phi}{\sin\theta_i\sin\varphi_i}\{\gamma\beta+(1-\gamma)\cos\chi_i\},$$

$$\operatorname{tg}\varphi_i=\frac{\sin\Theta\sin\Phi}{\sin\theta_i\sin\varphi_i}\{\gamma\beta+(1-\gamma)\cos\chi_i\},$$

and therefore, if $\delta$ is the angle of deviation, we obtain from the last two equations

$$\operatorname{tg}\delta=\frac{\sin\Theta\sin\Phi}{\sin\theta_i\sin\varphi_i}(1-\gamma)(\cos\chi_i-\cos\chi_i)$$

which is approximately equal to

$$\operatorname{tg}\delta=2(1-\gamma)\frac{\sin\Theta\sin\Phi\cos\chi_i}{\sin\theta_i\sin\varphi_i}. \qquad \ldots\ldots (4.4)$$

Now let us consider the angle of reflexion. From the second equation in (3.12) we obtain

$$\cos\theta_i=\frac{\begin{array}{c}\cos\theta_i+\cos\Theta[(\cos\Theta\cos\theta_i+\sin\Theta\cos\Phi\sin\theta_i)\{\gamma\beta^2+(1-\gamma)^2\times\\ \times(1-\sin^2\Theta\,\overline{1+\cos^2\Phi}\}-2\beta\gamma-2(1-\gamma)\cos\Theta\cos\theta_i-2\beta\gamma\times\\ \times(1-\gamma)\{1-\sin^2\Theta\,(1+\cos^2\Phi)\}]\end{array}}{\begin{array}{c}\gamma^2\{1+\beta^2(1-\sin^2\Theta\,\overline{1+\cos^2\Phi})\}+\beta\gamma[\cos\Phi\sin\Theta\sin\theta_i\\ -\cos\Theta\cos\theta_i+\{(1-\gamma)(1-\sin^2\Theta\,\overline{1+\cos^2\Phi})-\gamma\}\times\\ \times\{\cos\Theta\cos\theta_i+\sin\Theta\cos\Phi\sin\theta_i\}]\end{array}}$$

$$\ldots\ldots (4.5)$$

or

$$\cos\theta_t = \frac{\begin{array}{c}\cos\theta_i+\cos\theta[(\cos\theta\cos\theta_i+\sin\theta_i\sqrt{\sin^2\theta-\cos^2\zeta})\{\gamma\beta^2 \\ +(1-\gamma)^2(1-2\sin^2\theta+\cos^2\zeta)\}-2\beta\gamma-2(1-\gamma)\times \\ \times\cos\theta\cos\theta_i-2\beta\gamma(1-\gamma)(1-2\sin^2\theta+\cos^2\zeta)]\end{array}}{\begin{array}{c}\gamma^2\{1+\beta^2(1-2\sin^2\theta+\cos^2\zeta)\}+\beta\gamma[\sin\theta_i\sqrt{\sin^2\theta-\cos^2\zeta} \\ -\cos\theta\cos\theta_i+\{(1-\gamma)(1-2\sin^2\theta+\cos^2\zeta)-\gamma\}\times \\ \times\{\cos\theta_i\cos\theta+\sin\theta_i\sqrt{\sin^2\theta-\cos^2\zeta}\}]\end{array}}$$

provided the incident plane is taken to coincide with the $xy$-plane.

When the motion is confined in the coordinate planes $xy, yz$ and $zx$ respectively, we get

$$\cos\theta_t = \frac{\begin{array}{c}\cos\theta_i+\cos\theta[\cos(\theta-\theta_i)\{\gamma\beta^2+(1-\gamma)^2\cos^2\theta\}-2\beta\gamma \\ -2(1-\gamma)\cos\theta\cos\theta_i-2\beta\gamma(1-\gamma)\cos 2\theta]\end{array}}{\begin{array}{c}\gamma^2(1+\beta^2\cos 2\theta)+\beta\gamma[-\cos(\theta+\theta_i)+\{(1-\gamma)\cos 2\theta \\ -\gamma\}\cos(\theta-\theta_i)]\end{array}} \qquad \ldots\ldots (4.7)$$

$$\cos\theta_t = \frac{\cos\theta_i}{\gamma^2(1-\beta^2\cos^2\Phi)+\beta\gamma\cos\Phi\sin\theta_i(1-\gamma)\sin^2\Phi}, \qquad \ldots\ldots (4.8)$$

$$\cos\theta_t = \frac{\begin{array}{c}\cos\theta_i+\cos\theta[\cos\theta\cos\theta_i\{\gamma\beta^2+(1+\gamma)^2\cos^2\theta\}-2\beta\gamma \\ -2(1-\gamma)\cos\theta\cos\theta_i-2\beta\gamma(1-\gamma)\cos^2\theta]\end{array}}{\begin{array}{c}\gamma^2(1+\beta^2\cos^2\theta)+\beta\gamma[-\cos\theta\cos\theta_i \\ +\{(1-\gamma)\cos^2\theta-\gamma\}\cos\theta\cos\theta_i]\end{array}},$$

and when the motion takes place along the coordinate axes $x, y$ and $z$ respectively, we obtain

$$\cos\theta_t = \frac{\cos\theta_i(\beta^2+\gamma)-2\beta(2-\gamma)}{\gamma(1+\beta^2)-2\beta\gamma\cos\theta_i}, \qquad \ldots\ldots (4.10)$$

$$\cos\theta_t = \cos\theta_i, \qquad \ldots\ldots (4.11)$$

$$\cos\theta_t = \cos\theta_i/\gamma^2. \qquad \ldots\ldots (4.12)$$

If we put $\gamma = 1$ as an approximation, (4.10) becomes

$$\cos\theta_t = \frac{(1+\beta^2)\cos\theta_i-2\beta}{1+\beta^2-2\beta\cos\theta}, \qquad \ldots\ldots (4.13)$$

which may be written in the form

$$\operatorname{tg}(\theta_t/2) = \frac{1+\beta}{1-\beta}\operatorname{tg}(\theta_i/2) = \frac{c+v}{c-v}\operatorname{tg}\left(\frac{\theta_i}{2}\right). \qquad (4.14)$$

The equation (4.13) is exactly equal to those obtained by Harnack[1] and Edser[2], while (4.14) is the equation obtained by Hicks[3]. By the same approximation (4.12) becomes equal to (4.11), i.e.

$$\theta_l = \theta_i. \qquad \ldots\ldots (4.15)$$

Hence we see that the law of reflexion is not affected by the motion taking place in the boundary plane. It has already been shown by Stokes[4], Lodge[5] and Edser[6] that the motion at right angles to the plane of incidence cannot affect the law of reflexion. But (4.12) tells us that it affects the law when $\gamma$ is taken into account.

Moreover, when we retain $\beta^2$ in $\gamma$, (4.10) becomes

$$\cos\theta_l = \frac{(2+3\beta^2)\cos\theta_i - 4\beta}{2+3\beta^2-4\beta\cos\theta_i}.$$

This shows that there is a small discrepancy between the above result and that already obtained by different authors.

## 5. Doppler Effect due to Refraction by a Moving Medium.

Let us consider what change would occur in frequency when light is refracted by a moving medium. If the moving medium is carried along with the dashed system, the index of exponential factor for the refracted wave can be expressed by

$$\theta_r' = 2\pi\omega_r'\left(t' - \frac{\lambda_r'x' + \mu_r'y' + \nu_r'z'}{c_2'}\right), \qquad \ldots\ldots (5.1)$$

and in this case the corresponding expression referred to the stationary system $K$ is given by

$$\theta_r = 2\pi\omega_r\left(t - \frac{\lambda_r x + \mu_r y + \nu_r z}{c_2}\right), \qquad \ldots\ldots (5.2)$$

where the suffix $r$ signifies that it relates to the refracted wave and the suffix 2 to the medium (2).

1 A. Harnack, loc. cit., p. 1057.
2 D. Edser, loc. cit., p. 519.
3 W. H. Hicks, Phil. Mag., **3**, 16 (1902).
4 G. G. Stokes, Math. Phys. Papers I. p. 145.
5 O. Lodge, Phil. Trans., **184**, 795 (1893).
6 E. Edser, loc. cit. p. 521.

When the light is incident to the boundary plane with an angle $\theta_i'$ in the $x'y'$-plane, the reflected and refracted lights are confined in the same plane, and we have

$$\left.\begin{aligned} &\frac{\sin\theta_i'}{\sin\theta_r'} = \frac{c_1'}{c_2'} = n_{12}, \\ &\lambda_r' = \cos\theta_r' = \sqrt{1-\left(\frac{c_2'}{c_1'}\right)^2 \sin^2\theta_i'}, \\ &\mu_r' = \sin\theta_r' = \frac{c_2'}{c_1'}\sin\theta_i', \\ &\nu_r' = 0. \end{aligned}\right\} \quad \cdots\cdots (5.3)$$

Putting

$$\left.\begin{aligned} \cos\chi_r &= l\lambda_r + m\mu_r + n\nu_r, \\ \cos\chi_r' &= l\lambda_r' + m\mu_r' + n\nu_r', \end{aligned}\right\} \quad \cdots\cdots (5.4)$$

we get from (5.1) and (5.2) by transformation equations

$$\left.\begin{aligned} \omega_r &= \omega_r'\gamma\left(1+\frac{v}{c_2'}\cos\chi_r'\right), \\ \omega_r\frac{\lambda_r}{c_2} &= \omega_r'\left\{\gamma\frac{v}{c^2}l + \frac{\lambda_r'}{c_2'} + \frac{1}{c_2'}(\gamma-1)l\cos\chi_r'\right\}, \\ \omega_r\frac{\mu_r}{c_2} &= \omega_r'\left\{\gamma\frac{v}{c^2}m + \frac{\mu_r'}{c_2'} + \frac{1}{c_2'}(\gamma-1)m\cos\chi_r'\right\}, \\ \omega_r\frac{\nu_r}{c_2} &= \omega_r'\left\{\gamma\frac{v}{c^2}n + \frac{\nu_r'}{c_2'} + \frac{1}{c_2'}(\gamma-1)n\cos\chi_r'\right\}. \end{aligned}\right\} \quad (5.5)$$

But since we have by (1.7) and (3.11)

$$\omega_i = \omega_i'\gamma\left(1+\frac{v}{c_1'}\cos\chi_i'\right) = \omega_r'\gamma\left(1+\frac{v}{c_1'}\cos\chi_i'\right),$$

the first equation in (5.5) may be written

$$\omega_r = \omega_i\frac{1+\frac{v}{c_2'}\cos\chi_r'}{1+\frac{v}{c_1'}\cos\chi_i'}. \quad \cdots\cdots (5.6)$$

Moreover, observing the expression (2.11), we get

$$\frac{\cos\chi_i'}{c_1'} = \frac{\cos\chi_i/c_1 - v/c^2}{1-\frac{v}{c_1}\cos\chi_i},$$

$$\frac{\cos\chi_r'}{c_2'} = \frac{\cos\chi_r/c_2 - v/c^2}{1-\frac{v}{c_2}\cos\chi_r},$$

and consequently

$$1+\frac{v}{c_2'}\cos\chi_r' = \frac{1-\beta^2}{1-\frac{v}{c_2}\cos\chi_r},$$

$$1+\frac{v}{c_1'}\cos\chi_i' = \frac{1-\beta^2}{1-\frac{v}{c_1}\cos\chi_i}.$$

Hence (5.6) may also be written

$$\omega_r = \omega_i \frac{1-\frac{v}{c_1}\cos\chi_i}{1-\frac{v}{c_2}\cos\chi_r}, \qquad \ldots\ldots (5.7)$$

which gives the Doppler effect on frequency; and we see that there exists an exact similarity between this equation and the equation (3.14).

Substituting the values of (5.3) in (5.4) and dividing by $c_2'$ we get

$$\frac{\cos\chi_r'}{c_2'} = l\sqrt{\left(\frac{1}{c_2'}\right)^2-\left(\frac{\sin\theta_i'}{c_1'}\right)^2}+m\left(\frac{\sin\theta_i'}{c_1'}\right)$$

which becomes, by (3.17),

$$\frac{\cos\chi_r'}{c_2'} = l\left[\left(\frac{1}{c_2'}\right)^2-\frac{(\mu_i-m\nu_i/n)^2}{\gamma^2c_1^2\left(1-\frac{v}{c_1}\cos\chi_i\right)^2}\right]^{\frac{1}{2}}+m\frac{\mu_i-\nu_i m/n}{\gamma c_1\left(1-\frac{v}{c_1}\cos\chi_i\right)}.$$

Again by (3.18) and (1.5) this equation transforms into

$$\begin{aligned}\frac{\cos\chi_r'}{c_2'} = {} & \frac{\cos\theta}{\gamma c(1-\beta\cos\chi_i)}\left[n^2\{\cos\theta_i-(1-\gamma)\cos\theta\cos\chi_i-\gamma\beta\cos\theta\}^2\right.\\ & \left.+(n^2-1)\{\sin\theta_i-(1-\gamma)\sin\theta\cos\Phi\cos\chi_i-\gamma\beta\sin\theta\cos\Phi\}^2\right]^{\frac{1}{2}}\\ & +\frac{\sin\theta\cos\Phi}{\gamma c(1-\beta\cos\chi_i)}\{\sin\theta_i-(1-\gamma)\sin\theta\cos\Phi\cos\chi_i-\gamma\beta\sin\theta\cos\Phi\},\end{aligned}$$

$$\ldots\ldots (5.8)$$

where we have assumed that the first medium is the air and the incident plane is made to coincide with the $xy$-plane, $n$ being put for $n_{12}$.

Employing this value for $\cos\chi_r'/c_2'$ and eliminating $\cos\chi_i/c_1'$ in (5.6), we get

$$\omega_r = \omega_i\gamma[\gamma(1-\beta\cos\chi_i)+\beta\cos\theta\{n^2(\cos\theta_i-\sqrt{1-\gamma}\cos\theta\cos\chi_i$$
$$-\gamma\beta\cos\theta)^2+(n^2-1)(\sin\theta_i-\sqrt{1-\gamma}\sin\theta\cos\Phi\cos\chi_i$$
$$-\gamma\beta\sin\theta\cos\Phi)^2\}^{\frac{1}{2}}+\beta\sin\theta\cos\Phi\{\sin\theta_i-\sqrt{1-\gamma}\sin\theta\cos\Phi\cos\chi_i$$
$$-\beta\gamma\sin\theta\cos\Phi\}]. \qquad \ldots\ldots (5.9)$$

When $n = 1$, the last equation reduces to

$$\omega_r = \omega_i[1+\beta\gamma\sin^2\theta\sin^2\Phi\{(1-\gamma)\cos\chi_i+\beta\gamma\}].$$

But, by (3.15), $(1-\gamma)\cos\chi_i+\beta\gamma = \nu_i/n$, and since the $xy$-plane is the plane of incidence, $\nu_i = 0$. Therefore we see that, when $n$ is equal to unity, (5.9) reduces to $\omega_r = \omega_i$, which is as it ought to be, for in this case light is propagating in a single homogeneous medium.

When the terms containing higher orders of $\beta$ are neglected, equation (5.9) becomes

$$\omega_r = \omega_i[1-\beta\cos\theta\{\cos\theta_i-(n^2-\sin^2\theta_i)^{\frac{1}{2}}\}], \ldots\ldots(5.10)$$

which is quite independent of the azimuth of the plane containing the motion. If the boundary plane is moving parallel to itself we get from the last equation

$$\omega_r = \omega_i[1-\beta\{\cos\theta_i-(n^2-\sin^2\theta_i)^{\frac{1}{2}}\}], \quad \ldots\ldots (5.11)$$

while (5.10) becomes

$$\omega_r = \omega_i, \qquad \ldots\ldots (5\ 12)$$

i.e. no change of frequency takes place when the boundary plane is moving in its own plane.

## 6. Law of Refraction by a Moving Medium.

The law of refraction by a moving medium can be treated as in article 4 for the reflexion phenomena. For the sake of simplicity, let us confine ourselves to the first order effect alone. Putting

$$\left.\begin{aligned}\lambda_r &= \cos\theta_r,\\ \mu_r &= \sin\theta_r\cos\varphi_r,\\ \nu_r &= \sin\theta_r\sin\varphi_r,\end{aligned}\right\} \qquad \ldots\ldots (6.1)$$

and starting from the equation (5.5) and similar sets we easily arrive at the result

$$\varphi_r = \varphi_i = \varphi_i. \qquad \ldots\ldots (6.2)$$

This tells us that the reflected and refracted rays are all contained in the plane of incidence, even when the mediums are in motion, provided $\beta^2$ and the higher terms are neglected.

Let us put

$$A\cos\Psi = \{n^2\cos\theta_i(\cos\theta_i - 2\beta\cos\Theta) + (n^2-1)\sin\theta_i(\sin\theta_i - 2\beta\sin\Theta\cos\Phi)\}^{\frac{1}{2}}$$
$$A\sin\Psi = \cos\Phi(\sin\theta_i - \beta\sin\Theta\cos\Phi), \qquad \ldots\ldots (6.3)$$

then the equation (5.8) takes the following simpler form

$$\frac{\cos\chi_r'}{c_2'} = \frac{A\cos(\Theta-\Psi)}{c(1-\beta\cos\chi_i)}. \qquad \ldots\ldots (6.4)$$

Therefore the equation (3.8) may be written

$$\frac{\cos\chi_r}{c_2} = \frac{1}{c}\frac{A\cos(\Theta-\Psi)+\beta}{1-\beta\cos\chi_i+\beta A\cos(\Theta-\Psi)}. \quad \ldots (6.5)$$

Accordingly the second equation in (5.5) becomes

$$\frac{\cos\theta_r}{c_2} = \frac{1}{c}\frac{A\cos\Psi+\beta\cos\Theta}{1-\beta\cos\chi_i+\beta A\cos(\Theta-\Psi)}.$$

But since we have by (2.17)

$$c_2 = \frac{c}{n} + v\left(1-\frac{1}{n^2}\right)\cos\chi_r, \qquad \ldots\ldots (6.6)$$

the last equation may be written

$$\cos\theta_r = \frac{1}{n}\frac{A\cos\Psi+\beta\cos\Theta+\beta\left(1-\frac{1}{n^2}\right)A^2\cos\Psi\cos(\Theta-\Psi)}{1-\beta\cos\chi_i+\beta A\cos(\Theta-\Psi)}$$

and we get

$$\sin^2\theta_r = \frac{n^2 - A^2\cos^2\Psi - 2\beta n^2\cos\chi_i - 2\beta A\cos\Psi\cos\Theta + 2\beta A\cos(\Theta-\Psi)\left\{n^2-\left(1-\frac{1}{n^2}\right)A^2\cos^2\Psi\right\}}{n^2\{1-\beta\cos\chi_i+\beta A\cos(\Theta-\Psi)\}^2}.$$

But since, by (6.3), we have

$$n^2 - A^2\cos^2\Psi = \sin^2\theta_i + 2\beta n^2\cos\chi_i - 2\beta\sin\Theta\cos\Phi\sin\theta_i,$$

$$n^2-\left(1-\frac{1}{n^2}\right)A^2\cos^2\Psi = 1+\left(1-\frac{1}{n^2}\right)\sin^2\theta_i+2\beta(n^2-1)\cos\chi_i$$
$$-2\beta\left(1-\frac{1}{n^2}\right)\sin\theta\cos\Phi,$$

the numerator of $\sin^2\theta_r$ becomes

$$\sin^2\theta_i+2\beta n\left(1-\frac{1}{n^2}\right)\sin^2\theta_i\cos\chi_r,$$

because we may put

$$\beta A\sin\Psi = \beta\cos\Phi\sin\theta_i,$$
$$\beta A\cos(\theta-\Psi) = \beta n\cos\chi_r,$$

in virtue of (6.3) and (6.5).

Consequently we get

$$\sin\theta_r = \frac{1}{n}\frac{\sin\theta_i+\beta n\left(1-\frac{1}{n^2}\right)\sin\theta_i\cos\chi_r}{1-\beta\cos\chi_i+\beta n\cos\chi_r}.$$

However, as a rough approximation, we may put

$$\beta n\cos\chi_r = \beta\cos\chi_i.$$

Therefore finally we obtain

$$\sin\theta_r = \frac{\sin\theta_i}{n}\left\{1+\beta n\left(1-\frac{1}{n^2}\right)\cos\chi_r\right\}, \quad \ldots\ldots (6.7)$$

which may be also written

$$\sin\theta_r = \frac{\sin\theta_i}{n}\left\{1+\beta\left(1-\frac{1}{n^2}\right)\cos\chi_i\right\}, \quad \ldots\ldots (6.8)$$

without sensible error. The equations (6.7) and (6.8) give the angle of refraction $\theta_r$ when the medium is in motion. When $v=0$ they become

$$\sin\theta_r = \frac{1}{n}\sin\theta_i,$$

which is the usual refraction law of Snell (1.9).

It is interesting to note that the equation (6.7) can be obtained at once from

$$\frac{\sin\theta_r}{\sin\theta_i} = \frac{c_2}{c},$$

if we substitute the value of $c_2$ given by (6.6).

The equation (6.8) affords us an easy method of finding the refracted ray geometrically. In the annexed figure, let $AB$ be the boundary of the two media and $IA$, $I'B$ be two incident rays such that, when $AC$ is perpendicular to $BC$, $BC=kc$, where $c$ is the velocity of light in the upper medium and $k$ a certain constant. Draw a circle with the radius $k\{c+\beta(1-1/n^2)\times \times\cos\chi_s\}/n$ and $A$ as its centre. Next draw a tangent from $B$ to the circle thus obtained and find the touching point. Then, by Huyghens Principle, it remains to draw a line passing through $A$ and $D$ to find the required ray.

Fig. 7.

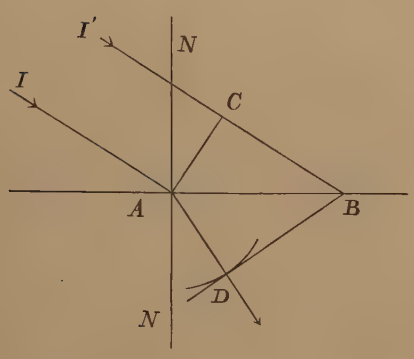


Again, it is interesting to observe that when the motion of the medium is at right angles to the plane of incidence the equation (6.7) degenerates to (1.9).

## 7. Generalized Transformation Equations for Field Vectors.

So far we have investigated the kinematical relations only. In order to enter the dynamical region, it is here convenient, as preliminary, to make some digression.

If we adopt Minkowski's notation for the time coordinate, namely

$$\left.\begin{aligned} ict &= \rho, \\ ict' &= \rho', \end{aligned}\right\} \qquad \ldots\ldots\ (7.1)$$

where $i=\sqrt{-1}$ and $c$ is the velocity of light in vacuum, the generalised Lorentz-Einstein transformation equations (2.1) can be written

$$\begin{aligned} x' &= x\{1+(\gamma-1)l^2\}+ylm\,(\gamma-1) &&+zln\,(\gamma-1) &&+\rho i\beta\gamma l, \\ y' &= xlm(\gamma-1) &&+y\{1+(\gamma-1)m^2\}+zmn(\gamma-1) &&+\rho i\beta\gamma m, \\ z' &= xln\,(\gamma-1) &&+ymn(\gamma-1) &&+z\{1+(\gamma-1)n^2\}+\rho i\beta\gamma n, \\ \rho' &= -xi\beta\gamma l &&-yi\beta\gamma m &&-zi\beta\gamma n &&+\rho\gamma. \end{aligned}$$

Since $(x, y, z, \rho)$ is a 4-vector, we can transform any 4-vector from

the stationary system $K$ to the moving system $K'$, and vice versa by the following scheme[1]:

| | $x'$ | $y'$ | $z'$ | $\rho'$ |
|---|---|---|---|---|
| $x$ | $1+(\gamma-1)l^2$ | $(\gamma-1)lm$ | $(\gamma-1)ln$ | $-il\beta\gamma$ |
| $y$ | $(\gamma-1)lm$ | $1+(\gamma-1)m^2$ | $(\gamma-1)mn$ | $-im\beta\gamma$ |
| $z$ | $(\gamma-1)ln$ | $(\gamma-1)mn$ | $1+(\gamma-1)n^2$ | $-in\beta\gamma$ |
| $\rho$ | $il\beta\gamma$ | $im\beta\gamma$ | $in\beta\gamma$ | $\gamma$ |

(7.2)

Let $A$ be the determinant built up by the coefficients in (7.2), then it is easy to prove that $A=1$, which is the characteristic property of the Lorentz-Einstein transformation[2]. Let $A_{14}^{14}$ etc., be the cofactors of the determinant $A$ obtained by cancelling the two columns and rows suffixed. Then any 6-vector may be transformed by the following scheme[3]:

| | $M_{x\rho}'$ | $M_{y\rho}'$ | $M_{z\rho}'$ | $M_{yz}'$ | $M_{zx}'$ | $M_{xy}'$ |
|---|---|---|---|---|---|---|
| $M_{x\rho}$ | $A_{14}^{14}$ | $A_{24}^{14}$ | $A_{34}^{14}$ | $A_{23}^{14}$ | $A_{31}^{14}$ | $A_{12}^{14}$ |
| $M_{y\rho}$ | $A_{14}^{24}$ | $A_{24}^{24}$ | $A_{34}^{24}$ | $A_{23}^{24}$ | $A_{31}^{24}$ | $A_{12}^{24}$ |
| $M_{z\rho}$ | $A_{14}^{34}$ | $A_{24}^{34}$ | $A_{34}^{34}$ | $A_{23}^{34}$ | $A_{31}^{34}$ | $A_{12}^{34}$ |
| $M_{yz}$ | $A_{14}^{23}$ | $A_{24}^{23}$ | $A_{34}^{23}$ | $A_{23}^{23}$ | $A_{31}^{23}$ | $A_{12}^{23}$ |
| $M_{zx}$ | $A_{14}^{31}$ | $A_{24}^{31}$ | $A_{34}^{31}$ | $A_{23}^{31}$ | $A_{31}^{31}$ | $A_{12}^{31}$ |
| $M_{xy}$ | $A_{14}^{12}$ | $A_{24}^{12}$ | $A_{34}^{12}$ | $A_{23}^{12}$ | $A_{31}^{12}$ | $A_{12}^{12}$ |

Substituting the values of the cofactors in the above scheme we get[4]

| | $M_{x\rho}'$ | $M_{y\rho}'$ | $M_{z\rho}'$ | $M_{yz}'$ | $M_{zx}'$ | $M_{xy}'$ |
|---|---|---|---|---|---|---|
| $M_{x\rho}$ | $l^2+(1-l^2)\gamma$ | $-lm(\gamma-1)$ | $-ln(\gamma-1)$ | $0$ | $-ni\beta\gamma$ | $mi\beta\gamma$ |
| $M_{y\rho}$ | $-lm(\gamma-1)$ | $m^2+(1-m^2)\gamma$ | $-mn(\gamma-1)$ | $ni\beta\gamma$ | $0$ | $-li\beta\gamma$ |
| $M_{z\rho}$ | $-ln(\gamma-1)$ | $-mn(\gamma-1)$ | $n^2+(1-n^2)\gamma$ | $-mi\beta\gamma$ | $li\beta\gamma$ | $0$ |
| $M_{yz}$ | $0$ | $-ni\beta\gamma$ | $mi\beta\gamma$ | $l^2+(1-l^2)\gamma$ | $-lm(\gamma-1)$ | $-ln(\gamma-1)$ |
| $M_{zx}$ | $ni\beta\gamma$ | $0$ | $-li\beta\gamma$ | $-lm(\gamma-1)$ | $m^2+(1-m^2)\gamma$ | $-mn(\gamma-1)$ |
| $M_{xy}$ | $-mi\beta\gamma$ | $li\beta\gamma$ | $0$ | $-ln(\gamma-1)$ | $-mn(\gamma-1)$ | $n^2+(1-n^2)\gamma$ |

..... (7.3)

Now the Maxwell-Hertz fundamental equations for the electromagnetic field are

---

1 K. Tamaki, loc. cit., p. 143; **5**, 245 (1913).

2 M. Laue, loc. cit., p. 95.

3 K. Tamaki, loc. cit., p. 147.

4 K. Tamaki, ibid.

$$\left.\begin{aligned} \text{curl}\,\mathbf{E} &= -\frac{1}{c}\frac{\partial \mathbf{B}}{\partial t}, \\ \text{curl}\,\mathbf{H} &= \frac{1}{c}\frac{\partial \mathbf{D}}{\partial t}, \\ \text{div}\,\mathbf{D} &= 0, \\ \text{div}\,\mathbf{B} &= 0, \end{aligned}\right\} \quad \ldots\ldots (7{\cdot}4)$$

where $\mathbf{E}, \mathbf{D}, \mathbf{H}, \mathbf{B}$ are the vectors expressing the electric force, electric displacement, magnetic force and magnetic induction respectively. Let

$$\left.\begin{aligned} M_{x\rho} &= -iE_x, & M_{y\rho} &= -iE_y, & M_{z\rho} &= -iE_z, \\ M_{yz} &= B_x, & M_{zx} &= B_y, & M_{xy} &= B_z, \end{aligned}\right\} \quad \ldots (7{\cdot}5)$$

then since

$$\begin{aligned} -\frac{\partial}{\partial y} iE_z + \frac{\partial}{\partial z} iE_y + \frac{\partial}{\partial \rho} B_x &= 0, \\ \frac{\partial}{\partial x} iE_z \qquad - \frac{\partial}{\partial z} iE_x + \frac{\partial}{\partial \rho} B_y &= 0, \\ -\frac{\partial}{\partial x} iE_y + \frac{\partial}{\partial y} iE_x \qquad + \frac{\partial}{\partial \rho} B_z &= 0, \\ \frac{\partial}{\partial x} B_x + \frac{\partial}{\partial y} B_y + \frac{\partial}{\partial z} B_z \qquad &= 0, \end{aligned}$$

wet get

$$div\,\mathbf{M}^* = 0, \qquad \ldots\ldots (7{\cdot}6)$$

where $\mathbf{M}^*$ is the reciprocal vector of $\mathbf{M}$. The remaining equations in (7.4) may be written

$$\begin{aligned} +\frac{\partial}{\partial y} H_z - \frac{\partial}{\partial z} H_y - \frac{\partial}{\partial \rho} iD_x &= 0, \\ -\frac{\partial}{\partial x} H_z \qquad + \frac{\partial}{\partial z} H_x - \frac{\partial}{\partial \rho} iD_y &= 0, \\ +\frac{\partial}{\partial x} H_y - \frac{\partial}{\partial y} H_x \qquad - \frac{\partial}{\partial \rho} iD_z &= 0, \\ \frac{\partial}{\partial x} iD_x + \frac{\partial}{\partial y} iD_y + \frac{\partial}{\partial z} iD_z \qquad &= 0. \end{aligned}$$

Therefore if we put

$$\left.\begin{aligned} N_{x\rho} &= -iD_x, & N_{y\rho} &= -iD_y, & N_{z\rho} &= -iD_z, \\ N_{yz} &= H_x, & N_{zx} &= H_y, & N_{xy} &= H_z, \end{aligned}\right\} \quad \ldots (7{\cdot}7)$$

this system of equations can be represented by the single vector equation

$$Div\,\mathbf{N} = 0. \qquad \ldots\ldots (7.8)$$

If the medium is moving together with the dashed system, there are the following relations among the vectors

$$\left.\begin{aligned} \mathbf{D}' &= \varepsilon\,\mathbf{E}', \\ \mathbf{B}' &= \mu\,\mathbf{H}'. \end{aligned}\right\} \qquad \ldots\ldots (7.9)$$

From (7.3) and (7.5) we get the relations

$$\left.\begin{aligned} E_x' &= E_x\{l^2+(1-l^2)\gamma\} - E_y lm(\gamma-1) - E_z ln(\gamma-1) - B_y n\beta\gamma + B_z m\beta\gamma, \\ E_y' &= -E_x lm(\gamma-1) + E_y\{m^2+(1-m^2)\gamma\} - E_z mn(\gamma-1) \\ &\qquad + B_x n\beta\gamma - B_z l\beta\gamma, \\ E_z' &= -E_x ln(\gamma-1) - E_y mn(\gamma-1) + E_z\{n^2+(1-n^2)\gamma\} \\ &\qquad - B_x m\beta\gamma + B_y l\beta\gamma, \end{aligned}\right\} \qquad \ldots\ldots (7.10)$$

$$\left.\begin{aligned} B_x' &= -E_y n\beta\gamma - E_z m\beta\gamma + B_x\{l^2+(1-l^2)\gamma\} - B_y lm(\gamma-1), \\ &\qquad - B_z ln(\gamma-1), \\ B_y' &= -E_x n\beta\gamma + E_z l\beta\gamma - B_x lm(\gamma-1) + B_y\{m^2+(1-m^2)\gamma\} \\ &\qquad - B_z mn(\gamma-1), \\ B_z' &= E_x m\beta\gamma - E_y l\beta\gamma - B_x ln(\gamma-1) - B_y mn(\gamma-1) \\ &\qquad + B_z\{n^2+(1-n^2)\gamma\}, \end{aligned}\right\} \qquad \ldots\ldots (7.11)$$

and the corresponding inverse transformations. Similarly from (7.3) and (7.7) we obtain

$$\left.\begin{aligned} D_x' &= D_x\{l^2+(1-l^2)\gamma\} - D_y lm(\gamma-1) - D_z ln(\gamma-1) \\ &\qquad - H_y n\beta\gamma + H_z m\beta\gamma, \\ D_y' &= -D_x lm(\gamma-1) + D_y\{m^2+(1-m^2)\gamma\} - D_z mn(\gamma-1) \\ &\qquad + H_x n\beta\gamma - H_z l\beta\gamma, \\ D_z' &= -D_x ln(\gamma-1) - D_y mn(\gamma-1) + D_z\{n^2+(1-n^2)\gamma\} \\ &\qquad - H_x m\beta\gamma + H_y l\beta\gamma, \end{aligned}\right\} \qquad \ldots\ldots (7.12)$$

$$\left.\begin{aligned} H_x' = {} & D_y n\beta\gamma - D_z m\beta\gamma + H_x\{l^2+(1-l^2)\gamma\} - H_y lm(\gamma-1) \\ & + H_z mn(\gamma-1), \\ H_y' = {} & -D_x n\beta\gamma + D_z l\beta\gamma - H_x lm(\gamma-1) + H_y\{m^2+(1-m^2)\gamma\} \\ & - H_z mn(\gamma-1), \\ H_z' = {} & D_x m\beta\gamma - D_y l\beta\gamma - H_x ln(\gamma-1) - H_y mn(\gamma-1) \\ & + H_z\{n^2+(1-n^2)\gamma\}, \end{aligned}\right\} \quad \ldots\ldots (7.13)$$

and the corresponding inverse transformations.

## 8. Decomposition of the Electric and Magnetic Forces into Two Parts.

A plane light wave having the electric force and the magnetic force **H** may be regarded as composed of two parts, namely

$$\left.\begin{aligned} \mathbf{E} &= \mathbf{E}_{\parallel} + \mathbf{E}_{\perp}, \\ \mathbf{H} &= \mathbf{H}_{\parallel} + \mathbf{H}_{\perp}, \end{aligned}\right\} \quad \ldots\ldots (8.1)$$

where the components with the sign $\parallel$ belong to the component wave which would be polarized in the plane of incidence referred to the moving $K'$-system, while those marked with $\perp$ belong to that which would be polarized at right angles to the plane of incidence in the $K'$-system. It is required to find the relation between the above two parts.

For the sake of simplicity, let us hereafter confine ourselves to the first order effect only. In this case, the equations (7.12) and (7.13) may be simplified to

$$\left.\begin{aligned} E_x' &= E_x - \beta(H_y n - H_z m), \\ E_y' &= E_y - \beta(H_z l - H_x n), \\ E_z' &= E_z - \beta(H_x m - H_y l), \\ H_x' &= H_x + \beta(E_y n - E_z m), \\ H_y' &= H_y + \beta(E_z l - E_x n), \\ H_z' &= H_z + \beta(E_x m - E_y l), \end{aligned}\right\} \quad \ldots\ldots (8.2)$$

where $l, m, n$ are the direction cosines of the direction of motion. Hence we must have

$$\left.\begin{aligned} E_{x\parallel}' &= E_{x\parallel} - \beta(nH_{y\parallel} - mH_{z\parallel}), \\ E_{y\parallel}' &= E_{y\parallel} - \beta(lH_{z\parallel} - nH_{x\parallel}), \\ E_{z\parallel}' &= E_{z\parallel} - \beta(mH_{x\parallel} - lH_{y\parallel}), \\ H_{x\parallel}' &= H_{x\parallel} + \beta(nE_{y\parallel} - mE_{z\parallel}), \\ H_{y\parallel}' &= H_{y\parallel} + \beta(lE_{z\parallel} - nE_{x\parallel}), \\ H_{z\parallel}' &= H_{z\parallel} + \beta(mE_{x\parallel} - lE_{y\parallel}), \end{aligned}\right\} \quad \ldots\ldots (8.3)$$

and

$$\left.\begin{aligned} E_{x\perp}' &= E_{x\perp} - \beta(nH_{y\perp} - mH_{z\perp}), \\ E_{y\perp}' &= E_{y\perp} - \beta(lH_{z\perp} - nH_{x\perp}), \\ E_{z\perp}' &= E_{z\perp} - \beta(mH_{x\perp} - lH_{y\perp}), \\ H_{x\perp}' &= H_{x\perp} + \beta(nE_{y\perp} - mE_{z\perp}), \\ H_{y\perp}' &= H_{y\perp} + \beta(lE_{z\perp} - nE_{x\perp}), \\ H_{z\perp}' &= H_{z\perp} + \beta(mE_{x\perp} - lE_{y\perp}). \end{aligned}\right\} \quad \ldots\ldots (8.4)$$

But, since the component waves with the suffix $\parallel$ and $\perp$ are polarized in and perpendicular to the $x'y'$-plane, i.e. the plane of incidence in the $K'$-system, they are given by

$$\left.\begin{aligned} E_{x\parallel}' &= 0, \quad & H_{x\parallel}' &= H_{x0}', \\ E_{y\parallel}' &= 0, \quad & H_{y\parallel}' &= H_{y0}', \\ E_{z\parallel}' &= E_{z0}', \quad & H_{z\parallel}' &= 0, \end{aligned}\right\} \quad \ldots\ldots (8.5)$$

and

$$\left.\begin{aligned} E_{x\perp}' &= E_{x0}', \quad & H_{x\perp}' &= 0, \\ E_{y\perp}' &= E_{y0}', \quad & H_{y\perp}' &= 0, \\ E_{z\perp}' &= 0, \quad & H_{z\perp}' &= H_{z0}', \end{aligned}\right\} \quad \ldots\ldots (8.6)$$

where we have omitted the exponential factors. Therefore we must have

$$\left.\begin{aligned} E_{x\parallel} &= \beta(nH_{y\parallel} - mH_{z\parallel}), \\ E_{y\parallel} &= \beta(lH_{z\parallel} - nH_{x\parallel}), \\ E_{z\parallel} &= \beta(mH_{x\parallel} - lH_{y\parallel}), \end{aligned}\right\} \quad \ldots\ldots (8.7)$$

and

$$\left.\begin{aligned} H_{x\perp} &= \beta(mE_{z\perp} - nE_{y\perp}), \\ H_{y\perp} &= \beta(nE_{x\perp} - lE_{z\perp}), \\ H_{z\perp} &= \beta(lE_{y\perp} - mE_{x\perp}). \end{aligned}\right\} \quad \ldots\ldots (8.8)$$

Substituting the values given by (8.5) in the inverse transformation equations of (8.3), namely

$$\begin{aligned}
E_{x\parallel} &= E_{x\parallel}' + \beta(nH_{y\parallel}' - mH_{z\parallel}'),\\
E_{y\parallel} &= E_{y\parallel}' + \beta(lH_{z\parallel}' - nH_{x\parallel}'),\\
E_{z\parallel} &= E_{z\parallel}' + \beta(mH_{x\parallel}' - lH_{y\parallel}')\\
H_{x\parallel} &= H_{x\parallel}' - \beta(nE_{y\parallel}' - mE_{z\parallel}'),\\
H_{y\parallel} &= H_{y\parallel}' - \beta(lE_{z\parallel}' - nE_{x\parallel}'),\\
H_{z\parallel} &= H_{z\parallel}' - \beta(mE_{x\parallel}' - lE_{y\parallel}'),
\end{aligned}$$

we get

$$\left.\begin{aligned}
E_{x\parallel} &= \beta nH_{y0}', & H_{x\parallel} &= H_{x0}' + \beta mE_{z0}',\\
E_{y\parallel} &= -\beta nH_{x0}', & H_{y\parallel} &= H_{y0}' - \beta lE_{z0}',\\
E_{z\parallel} &= E_{z0}' + \beta(mH_{x0}' - lH_{y0}'), & H_{z\parallel} &= 0.
\end{aligned}\right\} \quad (8.9)$$

Similarly we obtain from (8.4) and (8.6)

$$\left.\begin{aligned}
E_{x\perp} &= E_{x0}' - \beta mH_{z0}', & H_{x\perp} &= -\beta nE_{y0}',\\
E_{y\perp} &= E_{y0}' + \beta lH_{z0}', & H_{y\perp} &= \beta nE_{x0}',\\
E_{z\perp} &= 0, & H_{z\perp} &= H_{z0}' - \beta(mE_{x0}' - lE_{y0}').
\end{aligned}\right\} \quad (8.10)$$

Now let us consider the following two cases separately:

(i) The light is polarized in the plane of incidence.

In this case, when the $xy$-plane is taken as the plane of incidence we have

$$\left.\begin{aligned}
E_{x\parallel} + E_{x\perp} &= 0, & H_{x\parallel} + H_{x\perp} &= H_{x0},\\
E_{y\parallel} + E_{y\perp} &= 0, & H_{y\parallel} + H_{y\perp} &= H_{y0},\\
E_{z\parallel} + E_{z\perp} &= E_{z0}, & H_{z\parallel} + H_{z\perp} &= 0.
\end{aligned}\right\} \quad \ldots\ldots (8.11)$$

Since $H_{z\parallel}=0$, the equation (8.7) and (8.8) give $H_{y\parallel}=E_{x\parallel}/\beta n$ and $H_{y\perp}=\beta nE_{x\perp}$. Therefore, substituting these values in the expression for $H_{y0}$ in (8.11), we get

$$H_{y0} = \frac{1}{\beta n} E_{x\parallel} + \beta nE_{x\perp},$$

which may be written

$$H_{y0} = \left(\frac{1}{\beta n} - \beta n\right) E_{x\parallel} \doteqdot E_{x\parallel}/\beta n,$$

as we have $E_{x\parallel}+E_{x\perp}=0$. On the other hand, if we start from the expression for $H_{x0}$ in (8.11), we get

$$H_{x0} = -\frac{1}{\beta n} E_{y\parallel} - \beta nE_{y\perp}$$

$$= \left(\beta n - \frac{1}{\beta n}\right) E_{y\parallel}$$

$$\fallingdotseq -\frac{1}{\beta n} E_{y\parallel}.$$

Consequently we obtain

$$\left.\begin{aligned} E_{x\parallel} &= \beta n H_{y0} = -\beta \frac{nl}{m} H_{x0}, \\ E_{y\parallel} &= -\beta n H_{x0} = \beta \frac{mn}{l} H_{y0}, \\ E_{z\parallel} &= E_{z0}, \\ H_{x\parallel} &= H_{x0} = -\frac{m}{l} H_{y0}, \\ H_{y\parallel} &= H_{y0} = -\frac{l}{m} H_{x0}, \\ H_{z\parallel} &= 0, \end{aligned}\right\} \quad \ldots\ldots (8.13)$$

$$\left.\begin{aligned} E_{x\perp} &= -\beta n H_{y0} = \beta \frac{nl}{m} H_{x0}, \\ E_{y\perp} &= \beta n H_{x0} = -\beta \frac{mn}{l} H_{y0}, \\ E_{z\perp} &= 0, \\ H_{x\perp} &= H_{y\perp} = H_{z\perp} = 0. \end{aligned}\right\} \quad \ldots\ldots (8.13)$$

(ii) The light is polarized at right angles to the plane of incidence. In this case we have

$$\left.\begin{aligned} E_{x\parallel} + E_{x\perp} &= E_{x0}, \quad H_{x\parallel} + H_{x\perp} = 0, \\ E_{y\parallel} + E_{y\perp} &= E_{y0}, \quad H_{y\parallel} + H_{y\perp} = 0, \\ E_{z\parallel} + E_{z\perp} &= 0, \quad H_{z\parallel} + H_{z\perp} = H_{z0}, \end{aligned}\right\} \quad \ldots\ldots (8.14)$$

and it can be easily shown that

$$\left.\begin{aligned} E_{x\parallel} &= E_{y\parallel} = E_{z\parallel} = 0, \\ H_{x\parallel} &= \beta n E_{y0} = -\beta n \frac{l}{m} E_{x0}, \\ H_{y\parallel} &= -\beta n E_{x0} = \beta n \frac{m}{l} E_{y0}, \\ H_{z\parallel} &= 0. \end{aligned}\right\} \quad \ldots\ldots (8.15)$$

$$\left.\begin{aligned} E_{x\perp} &= E_{x0}, \\ E_{y\perp} &= E_{y0}, \\ E_{z\perp} &= 0, \\ H_{x\perp} &= -\beta n E_{y0} = -\beta n \frac{l}{m} E_{x0}, \\ H_{y\perp} &= \beta n E_{x0} = -\beta n \frac{m}{l} E_{y0}, \\ H_{z\perp} &= H_{z0}. \end{aligned}\right\} \quad \ldots\ldots (8.16)$$

## 9. Change of Amplitude due to Reflexion at a Moving Surface.

In order to investigate the change of amplitude due to reflexion at a moving surface, it is necessary to know the corresponding change in the dashed system. But this can be easily found from the results enumerated in § 1, if we know the values

$$\varkappa_1 \equiv \frac{\sin(\theta_r' - \theta_i')}{\sin(\theta_r' + \theta_i')}, \qquad \varkappa_2 \equiv \frac{\operatorname{tg}(\theta_r' - \theta_i')}{\operatorname{tg}(\theta_r' + \theta_i')}.$$

When the plane of incidence is so taken as to coincide with the $xy$-plane we may put, by (3.17), (3.18) and (1.9)

$$\begin{aligned} \cos\theta_i' &= c_1' \cos\theta_i / c(1 - \beta\cos\chi_i) = \cos\theta_i, \\ \sin\theta_i' &= c_1' \sin\theta_i / c\,(1 - \beta\cos\chi_i) = \sin\theta_i, \\ \cos\theta_r' &= (1 - \sin^2\theta_r')^{\frac{1}{2}} = \left(1 - \frac{1}{n^2}\sin^2\theta_i\right)^{\frac{1}{2}}, \\ \sin\theta_r' &= \qquad\qquad = \frac{1}{n}\sin\theta_i. \end{aligned}$$

Consequently we get

$$\varkappa_1 \equiv \frac{\sin(\theta_r' - \theta_i')}{\sin(\theta_r' + \theta_i')} = \frac{\cos\theta_i - (n^2 - \sin^2\theta_i)^{\frac{1}{2}}}{\cos\theta_i + (n^2 - \sin^2\theta_i)^{\frac{1}{2}}}, \quad \ldots\ldots (9.1)$$

$$\varkappa_2 \equiv \frac{\operatorname{tg}(\theta_r' - \theta_i')}{\operatorname{tg}(\theta_r' + \theta_i')} = \frac{(n^2 - \sin^2\theta_i)^{\frac{1}{2}} - n^2\cos\theta_i}{(n^2 - \sin^2\theta_i)^{\frac{1}{2}} + n^2\cos\theta_i}. \quad \ldots (9.2)$$

Now we have, as the inverse transformation of (8.3),

$$\left.\begin{aligned} E_{x\parallel} &= E_{x\parallel}' + \beta(nH_{y\parallel}' - mH_{z\parallel}'), & H_{x\parallel} &= H_{x\parallel}' - \beta(nE_{y\parallel}' - mE_{z\parallel}'), \\ E_{y\parallel} &= E_{y\parallel}' + \beta(lH_{z\parallel}' - nH_{x\parallel}'), & H_{y\parallel} &= H_{y\parallel}' - \beta(lE_{z\parallel}' - nE_{x\parallel}'), \\ E_{z\parallel} &= E_{z\parallel}' + \beta(mH_{x\parallel}' - lH_{y\parallel}'), & H_{z\parallel} &= H_{z\parallel}' - \beta(mE_{x\parallel}' - lE_{y\parallel}'). \end{aligned}\right\} \quad \ldots\ldots (9.3)$$

But since we have by (1.1)

$$\begin{aligned} E_{x\parallel}' &= 0, & H_{x\parallel}' &= H_{x0}', \\ E_{y\parallel}' &= 0, & H_{y\parallel}' &= H_{y0}', \\ E_{z\parallel}' &= E_{z0}', & H_{z\parallel}' &= 0, \end{aligned}$$

the above equations simplify to

$$\begin{aligned} E_{x\parallel} &= \beta n H_{y0}', & H_{x\parallel} &= H_{x0}' + \beta m E_{z0}', \\ E_{y\parallel} &= -\beta n H_{x0}', & H_{y\parallel} &= H_{y0}' - \beta l E_{z0}', \\ E_{z\parallel} &= E_{z0}' + \beta(mH_{x0}' - lH_{y0}'), & H_{z\parallel} &= 0. \end{aligned}$$

Moreover, according to (1.10), we have

$$E_{z0}^{\prime\prime} = \varkappa_1 E_{z0}^{\prime}$$

and by (1.2)

$$\begin{aligned} H_{x0}^{\prime\prime} &= E_{z0}^{\prime\prime} \sin\theta_i', & H_{x0}^{\prime\prime} &= E_{z0}^{\prime\prime} \sin\theta_t', \\ H_{y0}^{\prime\prime} &= -E_{z0}^{\prime\prime} \cos\theta_i', & H_{y0}^{\prime\prime} &= -E_{z0}^{\prime\prime} \cos\theta_t'. \end{aligned}$$

Hence, substituting these relations in the last equations, we get

$$\begin{aligned} E_{x\parallel}^{\,i} &= -\beta n E_{z0}^{\prime\prime} \cos\theta_i', & H_{x\parallel}^{\,i} &= E_{z0}^{\prime\prime} \sin\theta_i' + \beta m E_{z0}^{\prime\prime}, \\ E_{y\parallel}^{\,i} &= -\beta n E_{z0}' \sin\theta_i', & H_{y\parallel}^{\,i} &= -E_{z0}^{\prime\prime} \cos\theta_i' - \beta l E_{z0}^{\prime\prime}, \\ E_{z\parallel}^{\,i} &= E_{z0}^{\prime\prime} + \beta(m \sin\theta_i' + l \cos\theta_i') E_{z0}^{\prime\prime}, & H_{z\parallel}^{\,i} &= 0, \end{aligned}$$

and

$$\begin{aligned} E_{x\parallel}^{\,t} &= -\beta n \varkappa_1 E_{z0}^{\prime\prime} \cos\theta_t', & H_{x\parallel}^{\,t} &= \varkappa_1 E_{z0}^{\prime\prime} \sin\theta_t' + \beta m \varkappa_1 E_{z0}^{\prime\prime}, \\ E_{y\parallel}^{\,t} &= -\beta n \varkappa_1 E_{z0}^{\prime\prime} \sin\theta_t', & H_{y\parallel}^{\,t} &= -\varkappa_1 E_{z0}^{\prime\prime} \cos\theta_t' - \beta l \varkappa_1 E_{z0}^{\prime\prime}, \\ E_{z\parallel}^{\,t} &= \varkappa_1 E_{z0}^{\prime\prime} + \beta(l \cos\theta_t' + m \sin\theta_t') \varkappa_1 E_{z0}^{\prime\prime}, & H_{z\parallel}^{\,t} &= 0. \end{aligned}$$

Combining these last sets of equations, we obtain

$$\left.\begin{aligned} E_{x\parallel}^{\,t} &= \frac{\cos\theta_t'}{\cos\theta_i'} \varkappa_1 E_{x\parallel}^{\,i}, & H_{x\parallel}^{\,t} &= \frac{\beta m + \sin\theta_t'}{\beta m + \sin\theta_i'} \varkappa_1 H_{x\parallel}^{\,i}, \\ E_{y\parallel}^{\,t} &= \frac{\sin\theta_t'}{\sin\theta_i'} \varkappa_1 E_{y\parallel}^{\,i}, & H_{y\parallel}^{\,t} &= \frac{\beta l + \cos\theta_t'}{\beta l + \cos\theta_i'} \varkappa_1 H_{y\parallel}^{\,i}, \\ E_{z\parallel}^{\,t} &= \frac{1 + \beta\cos\chi_t'}{1 + \beta\cos\chi_i'} \varkappa_1 E_{z\parallel}^{\,i}, & H_{z\parallel}^{\,t} &= H_{z\parallel}^{\,i} = 0. \end{aligned}\right\} \quad (9.4)$$

Similarly, substituting the values

$$E_{x\perp}' = E_{x0}', \qquad H_{x\perp}' = 0,$$
$$E_{y\perp}' = E_{y0}', \qquad H_{y\perp}' = 0,$$
$$E_{z\perp}' = 0, \qquad H_{z\perp}' = H_{z0}',$$

in the inverse transformation equations of (8.4), namely

$$\left.\begin{aligned} E_{x\perp} &= E_{x\perp}'+\beta(nH_{y\perp}'-mH_{z\perp}'), & H_{x\perp} &= H_{x\perp}'-\beta(nE_{y\perp}'-mE_{z\perp}'),\\ E_{y\perp} &= E_{y\perp}'+\beta(lH_{z\perp}'-nH_{x\perp}'), & H_{y\perp} &= H_{y\perp}'-\beta(lE_{z\perp}'-nE_{x\perp}'),\\ E_{z\perp} &= E_{z\perp}'+\beta(mH_{x\perp}'-lH_{y\perp}'), & H_{z\perp} &= H_{z\perp}'-\beta(mE_{x\perp}'-lE_{y\perp}'), \end{aligned}\right\} \quad \ldots\ldots (9.5)$$

we get

$$E_{x\perp} = E_{x0}'-\beta mH_{z0}', \quad H_{x\perp} = -\beta nE_{y0}',$$
$$E_{y\perp} = E_{y0}'+\beta lH_{z0}', \quad H_{y\perp} = \beta nE_{x0}',$$
$$E_{z\perp} = 0, \qquad H_{z\perp} = H_{z0}'-\beta(mE_{x0}'-lE_{y0}').$$

According to § 1 (ii) we have

$$H_{x0}^{il} = \varkappa_2 H_{z0}^{il}$$

and

$$E_{x0}^{il} = -H_{z0}^{il} \sin\theta_i', \quad E_{z0}^{ll} = -H_{z0}^{ll} \sin\theta_l',$$
$$E_{y0}^{il} = +H_{z0}^{il} \cos\theta_i', \quad E_{y0}^{ll} = +H_{z0}^{ll} \cos\theta_l'.$$

Hence we get

$$\left.\begin{aligned} E_{x\perp}^{\,l} &= \frac{\sin\theta_l'+\beta m}{\sin\theta_i'+\beta m}\varkappa_2 E_{x\perp}^{\,i}, & H_{x\perp}^{\,l} &= \frac{\cos\theta_l'}{\cos\theta_i'}\varkappa_2 H_{x\perp}^{\,i},\\ E_{y\perp}^{\,l} &= \frac{\cos\theta_l'+\beta l}{\cos\theta_i'+\beta l}\varkappa_2 E_{y\perp}^{\,i}, & H_{y\perp}^{\,l} &= \frac{\sin\theta_l'}{\sin\theta_i'}\varkappa_2 H_{y\perp}^{\,i},\\ E_{z\perp}^{\,l} &= E_{z\perp}^{\,i} = 0, & H_{z\perp}^{\,l} &= \frac{1+\beta\cos\chi_l'}{1+\beta\cos\chi_i'}\varkappa_2 H_{z\perp}^{\,i}. \end{aligned}\right\} (9.6)$$

Adding the corresponding equations in (9.4) and (9.6), we obtain

$$\left.\begin{aligned}
E_x^{\,l} &= \frac{\cos\theta_l'}{\cos\theta_i'}\varkappa_1 E_{x\parallel}^{\,i} + \frac{\sin\theta_l'+\beta m}{\sin\theta_i'+\beta m}\varkappa_2 E_{x\perp}^{\,i},\\
E_y^{\,l} &= \frac{\sin\theta_l'}{\sin\theta_i'}\varkappa_1 E_{y\parallel}^{\,i} + \frac{\cos\theta_l'+\beta l}{\cos\theta_i'+\beta l}\varkappa_2 E_{y\perp}^{\,i},\\
E_z^{\,l} &= \frac{1+\beta\cos\chi_l'}{1+\beta\cos\chi_i'}\varkappa_1 E_{z\parallel}^{\,i},\\
H_x^{\,l} &= \frac{\sin\theta_l'+\beta m}{\sin\theta_i'+\beta m}\varkappa_1 H_{x\parallel}^{\,i} + \frac{\cos\theta_l'}{\cos\theta_i'}\varkappa_2 H_{x\perp}^{\,i},\\
H_y^{\,l} &= \frac{\cos\theta_l'+\beta l}{\cos\theta_i'+\beta l}\varkappa_1 H_{y\parallel}^{\,i} + \frac{\sin\theta_l'}{\sin\theta_i'}\varkappa_2 H_{y\perp}^{\,i},\\
H_z^{\,l} &= \frac{1+\beta\cos\chi_l'}{1+\beta\cos\chi_i'}\varkappa_2 H_{z\perp}^{\,i}.
\end{aligned}\right\} \quad \cdots\cdots(9.7)$$

Now we are in a position to calculate the amplitude change due to reflexion by a moving surface. Let us consider the case under two headings :

(i) The plane of polarization is parallel to the plane of incidence.

In this case we have obtained in the preceding article the relations (8.12) and (8.13). Substituting their values in the last equations we get

$$\begin{aligned}
E_x^{\,l} &= \beta n(\varkappa_2-\varkappa_1)H_{y0}^{\,i},\\
E_y^{\,l} &= \beta n\left(-\varkappa_1+\frac{\cos\theta_l+\beta l}{\cos\theta_i+\beta l}\varkappa_2\right)H_{x0}^{\,i},\\
E_z^{\,l} &= \frac{1+\beta\cos\chi_l}{1+\beta\cos\chi_i}\varkappa_1 E_{z0}^{\,i},\\
H_x^{\,l} &= \varkappa_1 H_{x0}^{\,i},\\
H_y^{\,l} &= \frac{\cos\theta_l+\beta l}{\cos\theta_i+\beta l}\varkappa_1 H_{y0}^{\,i},\\
H_z^{\,l} &= 0,
\end{aligned}$$

which become by (9.1) and (9.2)

$$E_x^{\,l} = \frac{2\beta(n^2-1)\sin^2\theta_i\sin\Theta\sin\Phi}{(n^2-1)\sin^2\theta_i+(n^2+1)\cos\theta_i(n^2-\sin^2\theta_i)^{\frac{1}{2}}}H_{y0}^{\,i},$$

$$E_y^{\,l} = \frac{2\beta(n^2-1)\cos\theta_i(n^2-\sin^2\theta_i)^{\frac{1}{2}}\sin\Theta\sin\Phi}{(n^2-1)\sin^2\theta_i+(n^2+1)\cos\theta_i(n^2-\sin^2\theta_i)^{\frac{1}{2}}}H_{x0}^{\,i},$$

$$E_z^{\,l} = \frac{1+\beta\cos\chi_l}{1+\beta\cos\chi_i}\frac{\cos\theta_i-(n^2-\sin^2\theta_i)^{\frac{1}{2}}}{\cos\theta_i+(n^2-\sin^2\theta_i)^{\frac{1}{2}}}E_{z0}^{\,i},$$

$$H_x^l = \frac{\cos\theta_i - (n^2 - \sin^2\theta_i)^{\frac{1}{2}}}{\cos\theta_i + (n^2 - \sin^2\theta_i)^{\frac{1}{2}}} H_{x0}^i,$$

$$H_y^l = \frac{\cos\theta_l + \beta l}{\cos\theta_i + \beta l} \frac{\cos\theta_i - (n^2 - \sin^2\theta_i)^{\frac{1}{2}}}{\cos\theta_i - (n^2 - \sin^2\theta_i)^{\frac{1}{2}}} H_{y0}^i,$$

$$H_z^l = 0.$$

It is important to remember that we have adjusted the plane of incidence to be parallel to the $xy$-plane, so that by (4.3) we must have $\beta \sin\theta \sin\Phi = 0$. Hence we get

$$\left.\begin{aligned} E_x^l &= 0, & H_x^l &= \frac{\sin\theta_l + \beta m}{\sin\theta_i + \beta m} \varkappa_1 H_{x0}^i, \\ E_y^l &= 0, & H_y^l &= \frac{\cos\theta_l + \beta l}{\cos\theta_i + \beta l} \varkappa_1 H_{y0}^i, \\ E_z^l &= \frac{1 + \beta\cos\chi_l}{1 + \beta\cos\chi_i} \varkappa_1 E_{z0}^i, & H_z^l &= 0. \end{aligned}\right\} \quad (9.8)$$

When $v = 0$, these equations reduce to

$$\begin{aligned} E_x^l &= 0, & H_x^l &= \varkappa_1 H_{x0}^i, \\ E_y^l &= 0, & H_y^l &= -\varkappa_1 H_{y0}^i, \\ E_z^l &= \varkappa_1 E_{z0}^i, & H_z^l &= 0, \end{aligned}$$

which are the relations among the components in the case of reflexion at the stationary surface, for we can easily arrive at these results from (1.2), (1.4) and (1.10). The equation (9.8) also shows that, even after the reflexion, the plane of polarization and the orthogonality of the electric and magnetic forces remain the same.

(ii) The plane of polarization is perpendicular to the plane of incidence.

In this case we get from (8.15), (8.16) and (9.7)

$$\left.\begin{aligned} E_x^l &= \frac{\sin\theta_l + \beta m}{\sin\theta_i + \beta m} \varkappa_2 E_{x0}^i, & H_x^l &= 0, \\ E_y^l &= \frac{\cos\theta_l + \beta l}{\cos\theta_i + \beta l} \varkappa_2 E_{y0}^i, & E_y^l &= 0, \\ E_z^l &= 0, & H_z^l &= \frac{1 + \beta\cos\chi_l}{1 + \beta\cos\chi_i} \varkappa_2 H_{z0}^i. \end{aligned}\right\} \quad (9.9)$$

Remarks made on (9.8) may be applied to (9.9) also. Comparing (9.9) and (9.8), it will be seen that we can arrive at results in case

(ii) from those in (i) by the substitution of $x_2$ in place of $x_1$ and interchanging the electric force and the magnetic force.

## 10. Change of Amplitude due to Reflexion at a Moving Perfect Mirror.

When the medium (2) possesses conductivity we must use the equation

$$\text{curl}\,\mathbf{H} = \frac{1}{c}\left(\frac{\partial \mathbf{D}}{\partial t} + \sigma \mathbf{E}\right),$$

instead of

$$\text{curl}\,\mathbf{H} = \frac{1}{c}\frac{\partial \mathbf{D}}{\partial t},$$

where $\sigma$ is the specific conductivity. Consequently, for the electromagnetic wave of the frequency $\omega$, we must replace $\varepsilon_2$ by $\varepsilon_2 + \sigma/i\omega$; and, accordingly, we must have

$$c_2^2 = \frac{c^2}{\varepsilon_2 + \sigma/i\omega},$$

$$\sin\theta_r = \sin\theta_i\, c_2/c_1 = \sin\theta_i \sqrt{\frac{\varepsilon_1}{\varepsilon_2 + \sigma/i\omega}}.$$

Hence, if we put

$$n = \sqrt{\frac{\varepsilon_2 + \sigma/i\omega}{\varepsilon_1}}, \qquad \ldots\ldots (10.1)$$

we may use the results already obtained, even when the second medium is conducting.

When the frequency of light wave is so high that $\sigma/\omega$ is negligibly small, (10.1) may be written

$$n = \sqrt{\varepsilon_2/\varepsilon_1}. \qquad \ldots\ldots (10.2)$$

Then, for such a light wave, the conducting medium acts as if it were the usual dispersive one without conductivity. On the contrary, for the light waves of lower frequency we must neglect the first term in comparison with the second one, so that we have

$$n = \sqrt{\frac{\sigma}{i\omega\varepsilon_1}} = \sqrt{-i\frac{\sigma}{\varepsilon_1\omega}} = (1-i)\sqrt{\frac{\sigma}{2\varepsilon_1\omega}}. \qquad \ldots (10.3)$$

For the perfect mirror for which $\sigma$ may be regarded as infinitely great, we may put $n=\infty$. This signifies that the velocity of the pro-

pagation of light in the second medium is zero, or, in other words, that the light is perfectly reflected by the mirror.

In the last article we made it evident that, when an incident wave

$$\begin{aligned} E_x^i &= 0, & H_x^i &= H_{x0}^i, \\ E_y^i &= 0, & H_y^i &= H_{y0}^i, \\ E_z^i &= E_{z0}^i, & H_z^i &= 0, \end{aligned}$$

is reflected at a moving boundary, we get the reflected wave given by (9.8). Squaring and adding the components of the magnetic force in (9.8) we get

$$\begin{aligned} (H^l)^2 &= \varkappa_1^2 \left\{ \left( \frac{\sin\theta_l + \beta m}{\sin\theta_i + \beta m} H_{x0}^i \right)^2 + \left( \frac{\cos\theta_l + \beta l}{\cos\theta_i + \beta l} H_{y0}^i \right)^2 \right\} \\ &= (\varkappa_1 H^i)^2 \{ (\sin\theta_l + \beta m)^2 (1 + \beta m/\sin\theta_i)^{-2} \\ &\qquad + (\cos\theta_l + \beta l)^2 (1 + \beta l/\cos\theta_i)^{-2} \} \\ &\fallingdotseq (\varkappa_1 H^i)^2 \{ (\sin^2\theta_l + 2\beta m \sin\theta_l)(1 - 2\beta m/\sin\theta_i) \\ &\qquad + (\cos^2\theta_l + 2\beta l \cos\theta_l)(1 - 2\beta l/\cos\theta_i) \} \\ &\fallingdotseq (\varkappa_1 H^i)^2 \{ 1 + 2\beta\cos\chi_l - 2\beta\cos\chi_i \} \\ &\fallingdotseq \left\{ \varkappa_1 H_i \frac{1 + \beta\cos\chi_l}{1 + \beta\cos\chi_i} \right\}^2 \\ &= \left\{ \frac{1 + \beta\cos\chi_l}{1 + \beta\cos\chi_i} \varkappa_1 E^i \right\}^2. \end{aligned}$$

Hence we see that the absolute value of the magnetic force is equal to that of the electric force. Therefore, if we denote the amplitudes of the incident and the reflected waves by $A_i$ and $A_l$, respectively, we have

$$A_l = \frac{1 + \beta\cos\chi_l}{1 + \beta\cos\chi_i} \varkappa_1 A_i. \qquad \ldots\ldots (10.4)$$

But this can be written

$$A_l = \frac{\omega_l}{\omega_i} \varkappa_1 A_i, \qquad \ldots\ldots (10.5)$$

for we have by (3.14)

$$\frac{\omega_l}{\omega_i} = \frac{1 - \beta\cos\chi_i}{1 - \beta\cos\chi_l},$$

which may, without sensible error, be written

$$\frac{\omega_l}{\omega_i} = \frac{1+\beta\cos\chi_l}{1+\beta\cos\chi_i}.$$

For the perfect mirror, since we may put $n$ infinitely great, (9.1) gives

$$x_1 = -1.$$

Consequently the relation between the amplitudes is given by

$$A_l = -\frac{\omega_l}{\omega_i} A_i. \qquad \ldots\ldots (10.6)$$

Thus we see that the ratio of the amplitudes is equal to that of the frequencies with the negative sign. Since (9.2) also becomes $x_2 = -1$ for an infinitely great value of $n$, the equation (10.6) eqally applies to the light wave polarized at right angles to the plane of incidence.

Formerly Sir Joseph Larmor[1], Poynting[2], and Wood[3] were of the opinion that there takes place no change of amplitude of light vibration by the reflexion at a moving mirror, while Edser[4] obtained the relation

$$A_l = -\frac{c^2+v^2+2cv\cos\theta_i}{c^2-v^2} A_i, \qquad \ldots\ldots (10.7)$$

when the mirror is moving normally to itself and towards the direction of the advancing wave. The agreement of our results with Edser's can easily be shown by the substitution of the value of $\omega_l/\omega_i$ given by (3.31) in (10.6) and then changing the sign of $v$. If we put $\theta_i = 0$, and neglect $v^2$ in (10.7) we get

$$A_l = -\left(1+2\frac{v}{c}\right) A_i,$$

which agrees with Lorentz's result[5] in the case of normal incidence.

## 11. Change of Amplitude due to Refraction by a Moving Boundary.

Proceeding as in the case of § 9, it is easy to get the amplitudes of the electric and magnetic forces of the refracted wave. In this case we must use

1 J. Larmor, Ency. Brit. **32**, 121 (1902).
2 J. Poynting, Pressure of Light, p. 86, London 1919.
3 W. Wood, Loc. cit., p. 699.
4 E. Edser, loc. cit., p. 523.
5 H. A. Lorentz, Theory of Electrons, p. 61.

$$\left.\begin{aligned}
E_{x\parallel} &= E_{x\parallel}' + \beta(nH_{y\parallel}' - mH_{z\parallel}'),\\
E_{y\parallel} &= E_{y\parallel}' + \beta(lH_{z\parallel}' - nH_{x\parallel}'),\\
E_{z\parallel} &= E_{z\parallel}' + \beta(mH_{x\parallel}' - lH_{y\parallel}'),\\
H_{x\parallel} &= H_{x\parallel}' + \beta(mD_{z\parallel}' - nD_{y\parallel}'),\\
H_{y\parallel} &= H_{y\parallel}' + \beta(nD_{x\parallel}' - lD_{z\parallel}'),\\
H_{z\parallel} &= H_{z\parallel}' + \beta(lD_{y\parallel}' - mD_{x\parallel}'),
\end{aligned}\right\} \quad \ldots\ldots (11.1)$$

instead of (9.3). In these equations $\mathbf{D}'$ may be substituted by $\epsilon_2 \mathbf{E}'$. Employing the relations given by (1.12), (1.14) and (1.16) we obtain

$$\left.\begin{aligned}
E_{x\parallel}^{\,r} &= \frac{n\cos\theta_r'}{\cos\theta_i'} k_1 E_{x\parallel}^{\,i}, & H_{x\parallel}^{\,r} &= \frac{\sin\theta_r' + n\beta m}{\sin\theta_i' + \beta m} k_1 n H_{x\parallel}^{\,i},\\
E_{y\parallel}^{\,r} &= \frac{n\sin\theta_r'}{\sin\theta_i'} k_1 E_{y\parallel}^{\,i}, & H_{y\parallel}^{\,r} &= \frac{\cos\theta_r' + n\beta l}{\cos\theta_i' + \beta l} k_1 n H_{y\parallel}^{\,i},\\
E_{z\parallel}^{\,r} &= \frac{1 + n\beta\cos\chi_r'}{1 + \beta\cos\chi_i'} k_1 E_{z\parallel}^{\,i}, & H_{z\parallel}^{\,r} &= 0,
\end{aligned}\right\} \quad \ldots\ldots (11.2)$$

where

$$k_1 = \frac{2\cos\theta_i'\sin\theta_r'}{\sin(\theta_i' + \theta_r')} = \frac{2\cos\theta_i\sin\theta_r}{\sin(\theta_i + \theta_r)}. \quad \ldots\ldots (11.3)$$

Similarly we get

$$\left.\begin{aligned}
E_{x\perp}^{\,r} &= \frac{\sin\theta_r' + n\beta m}{n(\sin\theta_i' + \beta m)} k_2 E_{x\perp}^{\,i}, & H_{x\perp}^{\,r} &= \frac{n\sin\theta_r'}{\sin\theta_i'} k_2 H_{x\perp}^{\,i},\\
E_{y\perp}^{\,r} &= \frac{\cos\theta_r' + n\beta l}{n(\cos\theta_i' + \beta l)} k_2 E_{y\perp}^{\,i}, & H_{y\perp}^{\,r} &= \frac{n\cos\theta_r'}{\cos\theta_i'} k_2 H_{y\perp}^{\,i},\\
E_{z\perp}^{\,r} &= 0, & H_{z\perp}^{\,r} &= \frac{1 + n\beta\cos\chi_r'}{1 + \beta\cos\chi_i'} k_2 H_{z\perp}^{\,i},
\end{aligned}\right\} \quad \ldots\ldots (11.4)$$

where

$$k_2 = \frac{2\sin 2\theta_i'}{\sin 2\theta_i' + \sin 2\theta_r'} = \frac{2\sin 2\theta_i}{\sin 2\theta_i + \sin 2\theta_r}. \quad \ldots (11.5)$$

Adding (11.2) and (11.4) we obtain

$$\left.\begin{aligned}
E_x^{\,r} &= \frac{n\cos\theta_r'}{\cos\theta_i'} k_1 E_{x\parallel}^{\,i} + \frac{\sin\theta_r' + n\beta m}{n(\sin\theta_i' + \beta m)} k_2 E_{x\perp}^{\,i},\\
E_y^{\,r} &= \frac{n\sin\theta_r'}{\sin\theta_i'} k_1 E_{y\parallel}^{\,i} + \frac{\cos\theta_r' + \beta l n}{n(\cos\theta_i' + \beta l)} k_2 E_{y\perp}^{\,i},\\
E_z^{\,r} &= \frac{1 + n\beta\cos\chi_r'}{1 + \beta\cos\chi_i'} k_1 E_{z\parallel}^{\,i},
\end{aligned}\right\} \quad (11.6)$$

$$\left.\begin{aligned} H_x^r &= \frac{\sin\theta_r' + n\beta m}{\sin\theta_i' + \beta m}\, nk_1 H_{x\parallel}^i + \frac{n\sin\theta_r'}{\sin\theta_i'}\, k_2 H_{x\perp}, \\ H^r &= \frac{\cos\theta_r' + n\beta l}{\cos\theta_i' + \beta l}\, nk_1 H_{y\parallel}^i + \frac{n\cos\theta_r'}{\cos\theta_i'}\, k_2 H_{y\perp}^i, \\ H_z^r &= \frac{1 + n\beta\cos\chi_r'}{1 + \beta\cos\chi_i'}\, k_2 H_{z\perp}^i. \end{aligned}\right\}$$

Consequently we get

$$\left.\begin{aligned} E_x^r &= 0, & H_x^r &= \frac{\sin\theta_r' + n\beta m}{\sin\theta_i' + \beta m}\, nk_1 H_{x0}^i, \\ E_y^r &= 0, & H_y^r &= \frac{\cos\theta_r' + n\beta l}{\cos\theta_i' + \beta l}\, nk_1 H_{y0}^i, \\ E_z^r &= \frac{1 + n\beta\cos\chi_r'}{1 + \beta\cos\chi_i'}\, k_1 E_{z0}^i, & H_z^r &= 0, \end{aligned}\right\} \quad \ldots\ldots (11.7)$$

for the light wave polarized parallel to the plane of incidence and

$$\left.\begin{aligned} E_x^r &= \frac{\sin\theta_r' + n\beta m}{n(\sin\theta_i' + \beta m)}\, k_2 E_{x0}^i, & H_x^r &= 0, \\ E_y^r &= \frac{\cos\theta_r' + n\beta l}{n(\cos\theta_i' + \beta l)}\, k_2 E_{y0}^i, & H_y^r &= 0, \\ E_z^r &= 0. & H_z^r &= \frac{1 + n\beta\cos\chi_r'}{1 + \beta\cos\chi_i'}\, k_2 H_{z0}^i, \end{aligned}\right\} \quad \ldots\ldots (11.8)$$

for the light wave polarized perpendicularly to the plane of incidence.

Squaring the components of the magnetic force in (11.7) and adding we get

$$\begin{aligned} (H^r)^2 &= \{(\sin\theta_r' + \beta mn)^2(1 + \beta m/\sin\theta_i')^{-2} \\ &\qquad + (\cos\theta_r' + \beta ln)^2(1 + \beta l/\cos\theta_i')^{-2}\} k_1^2 n^2 E_{x0}^{i2} \\ &\fallingdotseq \{1 + 2n\beta\cos\chi_r' - 2\beta m\sin\theta_i'\,(\sin\theta_r'/\sin\theta_i')^2 \\ &\qquad - 2\beta l\cos\theta_i'\,(\cos\theta_r'/\sin\theta_i')^2\}\,(k_1 n E_{x0}^i)^2 \\ &\fallingdotseq (1 + 2n\beta\cos\chi_r')(1 - 2\beta\cos\chi_i')(k_1 n E_{x0}^i)^2 \\ &\fallingdotseq \left\{\frac{1 + n\beta\cos\chi_r'}{1 + \beta\cos\chi_i'}\, nk_1 E_{x0}^i\right\}^2. \end{aligned}$$

Hence we see that

$$H^r = nE^r = \sqrt{\varepsilon_2}\, E^r. \quad \ldots\ldots (11.9)$$

This relation can be deduced from (11.8) also.

If $A_i$ and $A_r$ denote the amplitudes of the electric forces for the incident and refracted waves respectively we may put

$$A_r = \frac{1+n\beta\cos\chi_r'}{1+\beta\cos\chi_i'}\,kA_i, \qquad \ldots\ldots \text{(11.10)}$$

where $k$ must be taken equal to $k_1$ and $k_2/n$ respectively for the wave polarized parallel to and perpendicular to the incident plane. But, since we may put

$$\frac{1+n\beta\cos\chi_r'}{1+\beta\cos\chi_i'} \doteq \frac{1+n\beta\cos\chi_r}{1+\beta\cos\chi_i} \doteq \frac{1-\beta\cos\chi_i}{1-n\beta\cos\chi_r},$$

the last equation may be written

$$A_r = \frac{\omega_r}{\omega_i}\,kA_i, \qquad \ldots\ldots \text{(11.11)}$$

on account of the equation (5.7). By (5.10) this again may be written

$$A_r = [1-\beta\cos\theta\{\cos\theta_i-(n^2-\sin^2\theta_i)^{\frac{1}{2}}\}]kA_i. \quad \text{(11.12)}$$

When the mediums are at rest this equation reduces to

$$A_r = kA_i,$$

and when $n = 1$,

$$A_r = A_i.$$

## 12. Polarization of Light by Reflexion at a Moving Surface.

It is well known that when the natural light with the components of electric and magnetic forces

$$\left.\begin{aligned}
E_x^i &= -E_\parallel^i \sin\theta_i\, e^{i2\pi\omega_i(t-\frac{x\cos\theta_i+y\sin\theta_i}{c_1})},\\
E_y^i &= E_\parallel^i \cos\theta_i\, e^{i2\pi\omega_i(t-\frac{x\cos\theta_i+y\sin\theta_i}{c_1})},\\
E_z^i &= E_\perp^i\, e^{i2\pi\omega_i(t-\frac{x\cos\theta_i+y\sin\theta_i}{c_1})},\\
H_x^i &= E_\perp^i\sqrt{\varepsilon_1}\sin\theta_i\, e^{i2\pi\omega_i(t-\frac{x\cos\theta_i+y\sin\theta_i}{c_1})},\\
H_y^i &= -E_\perp^i\sqrt{\varepsilon_1}\cos\theta_i\, e^{i2\pi\omega_i(t-\frac{x\cos\theta_i+y\sin\theta_i}{c_1})},\\
H_z^i &= E_\parallel^i\sqrt{\varepsilon_1}\, e^{i2\pi\omega_i(t-\frac{x\cos\theta_i+y\sin\theta_i}{c_1})}
\end{aligned}\right\} \quad \text{(12.1)}$$

is incident at a boundary plane of the two stationary media (1) and (2), we get the reflected wave with the components

$$\left.\begin{aligned}
E_x^l &= -E_\parallel^l \sin\theta_l\, e^{i2\pi\omega_l\left(t-\frac{x\cos\theta_l+y\sin\theta_l}{c_1}\right)},\\
E_y^l &= E_\parallel^l \cos\theta_l\, e^{i2\pi\omega_l\left(t-\frac{x\cos\theta_l+y\sin\theta_l}{c_1}\right)},\\
E_z^l &= E_\perp^l\, e^{i2\pi\omega_l\left(t-\frac{x\cos\theta_l+y\sin\theta_l}{c_1}\right)},\\
H_x^l &= E_\perp^l\sqrt{\varepsilon_1}\sin\theta_l\, e^{i2\pi\omega_l\left(t-\frac{x\cos\theta_l+y\sin\theta_l}{c_1}\right)},\\
H_y^l &= -E_\perp^l\sqrt{\varepsilon_1}\cos\theta_l\, e^{i2\pi\omega_l\left(t-\frac{x\cos\theta_l+y\sin\theta_l}{c_1}\right)},\\
H_z^l &= E_\parallel^l\sqrt{\varepsilon_1}\, e^{i2\pi\omega\left(t-\frac{x\cos\theta_l+y\sin\theta_l}{c_1}\right)}
\end{aligned}\right\} \quad (12.2)$$

and the refracted wave with the components

$$\left.\begin{aligned}
E_x^r &= -E_\parallel^r \sin\theta_r\, e^{i2\pi\omega_r\left(t-\frac{x\cos\theta_r+y\sin\theta_r}{c_2}\right)},\\
E_y^r &= E_\parallel^r \cos\theta_r\, e^{i2\pi\omega_r\left(t-\frac{x\cos\theta_r+y\sin\theta_r}{c_2}\right)},\\
E_z^r &= E_\perp^r\, e^{i2\pi\omega_r\left(t-\frac{x\cos\theta_r+y\sin\theta_r}{c_2}\right)},\\
H_x^r &= E_\perp^r\sqrt{\varepsilon_2}\sin\theta_r\, e^{i2\pi\omega_r\left(t-\frac{x\cos\theta_r+y\sin\theta_r}{c_2}\right)},\\
H_y &= -E_\perp^r\sqrt{\varepsilon_2}\cos\theta_r\, e^{i2\pi\omega_r\left(t-\frac{x\cos\theta_r+y\sin\theta_r}{c_2}\right)},\\
H_z^r &= E_\parallel^r\sqrt{\varepsilon_2}\, e^{i2\pi\omega_r\left(t-\frac{x\cos\theta_r+y\sin\theta_r}{c_2}\right)},
\end{aligned}\right\} \quad (12.3)$$

where

$$\left.\begin{aligned}
&\omega_i = \omega_l = \omega_r,\\
&\theta_l = \pi-\theta_i,\\
&\frac{\sin\theta}{\sin\theta} = n = \sqrt{\frac{\varepsilon_2}{\varepsilon_1}},\\
&E_\perp^l = \varkappa_1 E_\perp^i, \qquad E_\perp^r = k_1 E_\perp^i,\\
&E_\parallel^l = \varkappa_2 E_\parallel^i, \qquad E_\parallel^r = k_2 E_\parallel^i,
\end{aligned}\right\} \quad \cdots\cdots \quad (12.4)$$

$\varkappa_1$, $\varkappa_2$, $k_1$ and $k_2$ being given by (9.1), (9.2), (11.3) and (11.5).

In the case where the media and consequently the boundary plane is in motion, the component electric and magnetic forces for the reflected and refracted waves are given in articles 9 and 11 respectively. According to the results (9.8) and (9.9) we get

$$
\left.\begin{aligned}
E_x^{\,l} &= -E_\parallel^{\,l}\sin\theta_i\,\frac{\sin\theta_l+\beta m}{\sin\theta_i+\beta m}\,e^{i2\pi\omega_l\left(t-\frac{x\cos\theta_l+y\sin\theta_l}{c_1}\right)},\\
E_y^{\,l} &= E_\parallel^{\,l}\cos\theta_i\,\frac{\cos\theta_l+\beta l}{\cos\theta_i+\beta l}\,e^{i2\pi\omega_l\left(t-\frac{x\cos\theta_l+y\sin\theta_l}{c_1}\right)},\\
E_z &= E_\perp^{\,l}\,\frac{1+\beta\cos\chi_l}{1+\beta\cos\chi_i}\,e^{i2\pi\omega_l\left(t-\frac{x\cos\theta_l+y\sin\theta_l}{c_1}\right)},
\end{aligned}\right\}
$$

$$
\left.\begin{aligned}
H_x^{\,l} &= E_\perp^{\,l}\sqrt{\varepsilon_1}\sin\theta_i\,\frac{\sin\theta_l+\beta m}{\sin\theta_i+\beta m}\,e^{i2\pi\omega_l\left(t-\frac{x\cos\theta_l+y\sin\theta}{c_1}\right)},\\
H_y^{\,l} &= -E_\perp^{\,l}\sqrt{\varepsilon_1}\cos\theta\,\frac{\cos\theta_l+\beta l}{\cos\theta_i+\beta l}\,e^{i2\pi\omega\left(t-\frac{x\cos\theta_l+y\sin\theta}{c_1}\right)},\\
H_z^{\,l} &= E_\parallel^{\,l}\sqrt{\varepsilon_1}\,\frac{1+\beta\cos\chi_l}{1+\beta\cos\chi_i}\,e^{i2\pi\omega_l\left(t-\frac{x\cos\theta_l+y\sin\theta_l}{c_1}\right)},
\end{aligned}\right\}
$$

..... (12.5)

and by (11.7) and (11.8)

$$
\left.\begin{aligned}
E_x^{\,r} &= -E_\parallel^{\,r}\sin\theta_i\,\frac{\sin\theta_r'+n\beta m}{\sin\theta_i'+\beta m}\,e^{i2\pi\omega_r\left(t-\frac{x\cos\theta_r+y\sin\theta_r}{c_2}\right)},\\
E_y^{\,r} &= E_\parallel^{\,r}\cos\theta_i\,\frac{\cos\theta_r'+n\beta l}{\cos\theta_i'+\beta l}\,e^{i2\pi\omega_r\left(t-\frac{x\cos\theta_r+y\sin\theta_r}{c_2}\right)},\\
E_z^{\,r} &= E_\perp^{\,r}\,\frac{1+n\beta\cos\chi_r'}{1+\beta\cos\chi_i'}\,e^{i2\pi\omega_r\left(t-\frac{x\cos\theta_r+y\sin\theta_r}{c_2}\right)},
\end{aligned}\right\}
$$

$$
\left.\begin{aligned}
H_x^{\,r} &= E_\perp^{\,r}\sqrt{\varepsilon_2}\sin\theta_i\,\frac{\sin\theta_r+n\beta m}{\sin\theta_i+\beta m}\,e^{i2\pi\omega_r\left(t-\frac{x\cos\theta_r+y\sin\theta_r}{c_2}\right)},\\
H_y^{\,r} &= -E_\perp^{\,r}\sqrt{\varepsilon_2}\cos\theta_i\,\frac{\cos\theta_r+n\beta l}{\cos\theta_i+\beta l}\,e^{i2\pi\omega_r\left(t-\frac{x\cos\theta_r+y\sin\theta_r}{c_2}\right)},\\
H_z^{\,r} &= E_\parallel^{\,r}\sqrt{\varepsilon_2}\,\frac{1+n\beta\cos\chi_r}{1+\beta\cos\chi_i}\,e^{i2\pi\omega_r\left(t-\frac{x\cos\theta_r+y\sin\theta_r}{c_2}\right)}.
\end{aligned}\right\}
$$

..... (12.6)

If we put $\beta = 0$ in (12.5) and (12.6) they degenerate to (12.2) and (12.3) respectively.

Since $E_\parallel^{\,l}$ in (12.5) and $E_\parallel^{\,i}$ in (12.2) are given by $\varkappa_2 E_\parallel^{\,i}$, we see that when $\varkappa_2$ vanishes the natural light is plane polarized by reflexion at a moving surface. Therefore we may say that Brewster's law remains approximately true even when the reflecting surface is in motion.

## Summary.

1. Employing the generalized Lorentz-Einstein transformation equations, the state of the light disturbance in a medium moving in

any direction has been studied. It has been found that we have to use the component of the velocity along the direction of propagation, instead of its absolute value, when it appears linearly in the expression giving Doppler effect and that giving the velocity of propagation of light in the moving medium.

2. The laws of reflexion at a moving surface have been investigated. The frequency and amplitude of the reflected wave and the angle of reflexion in the most general cases have been obtained. The expressions given by Hicks, Harnack, Edser and others, are all contained, as special cases, in the expressions obtained by the author.

3. The corresponding important formulæ for the refracted wave in the general case have been deduced up to the term of order $v/c$.

4. It has been shown that Brewster's law of polarization holds good even when the reflecting surface is in motion, so far as the first order effect is concerned.

In conclusion the author wishes to express his indebtness to Prof. T. Mizuno for his kind suggestions.

# Figures produced on Photographic Plates by Electric Discharges.

By

**Usaburo Yoshida.**

(Received Nov. 24, 1916.)

Of dust figures, known as Lichtenberg's figures, produced on non-conducting plates by electric discharges, many investigations have been made.

Brown[1], however, used photographic plates instead of the powdered non-conducting plate of Lichtenberg's figures, and obtained beautiful figures. He placed a photographic plate upon a sheet of tin foil connected to one terminal of the secondary of an induction coil, and the end of the wire connected to the other terminal was put upon the sensitive film. When one single discharge was caused by breaking the mercury-break by hand, beautiful figures were obtained after developement. As to the figures thus obtained Brown says "..... when the terminal on the plate was negative, the figure consisted of beautiful sharply defined symmetrical palm-like fronds on irregular stems branching out from the center where the wire rested, together with a mass of less distinct irregular straggling lines also branching outwards. When the terminal of the wire was made positive, the figure consisted of irregular branchings sharply defined except near the center."

A little earlier than Brown, E. L. Trouvelot[2] obtained similar figures by a similar method.

In 1896, Nürnberg[3] obtained similar figures with the leyden jar.

Though, since then, similar results have been obtained by Blümel[4] and Nipher[5] by similar method, investigations under various conditions are wanting; and consequently it is not clear why the figures are produced. The writer has experimented under various conditions; and has undertaken a rough explanation of the formation of the figures.

1 Phil. Mag., **26**, 502, (1888).

2 C. R., **107**, 684, (1888). 3 Beiblätter z. d. Ann. d. Phys., **20**, (1896). 4 Beiblätter z. d. Ann. d. Phys., **22**, 596, (1898). 5 ] Beiblätter z. d. Ann. d. Phys., **35**, 1106, (1911).

In the following, the subject is treated, for the sake of clearness, in three parts: 1 mode of discharge; 2 formation of the photographic impression; 3 an explanation of the formation of the figures, and the transition from brush discharge to spark discharge.

## 1. Mode of Discharge.

The apparatus used is represented in the annexed figure. In this figure, *C* is a condenser which is charged with an influence machine, *B* a photographic plate placed upon a sheet of tin foil *A*, *E* and *F* spark gaps, *G* an ebonite rod, and *H* a metal rod connected to the tin foil. When the spark gaps *E*, *F* were brought in contact, a glow of discharge, produced on the sensitive film of the plate about the electrode *D*, could be seen; and a discharge figure was obtained after developement. Positive and negative figures were produced on the same plate when the electrode *H* was disconnected from the tin foil and placed upon the plate. When an induction coil, instead of the influence machine, was used, no condenser was inserted. To determine the sign of the electrodes a light-glow-oscilloscope was connected in series in *CE* or *CF*.

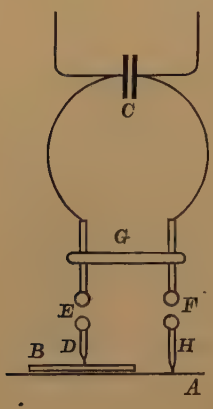


Fig. 1 is a discharge figure obtained with point electrodes connected to both the terminals of an influence machine. The cathode figure consists of regular, sharply defined, straight branches, radiating outwards from the point of the electrode with regular sharply defined intervals between them, their terminals being nearly on the circumference of a circle whose center is the point. The breadth of each branch continuously decreases as we recede from its end to the electrode.

On the other hand, the anode figure consists of sharply defined, irregular branches radiating outwards from the electrode; each branch changes its path irregularly and is divided into further branchings in an irregular manner; it is also irregular in its breadth and its length, and terminates in a sharp point. These characteristic properties of the anode figure will be more clearly seen in Fig. 3. Generally speaking, the extension of the anode figure is greater than that of the cathode figure.

Fig. 2 and 3 are figures obtained when stronger discharges than

By using the lamp described in the preceding section as the source of light, we have tried to examine also the vacuum arc spectra of the above elements. But we did not succeed in obtaining a sufficiently strong source for some elements such as *Fe* or *Pt*; further, some elements showed no intense line in the region of extreme ultra-violet, so that we describe below the vacuum arc spectra of only three elements *Bi*, *Sb* and *Tl*.

For the measurement of wave-lengths, we have taken the values given by Bloch for the following five lines in the spark spectrum of silver as standards, and interpolated the other lines. The values given by Bloch are expressed in the international Ångström unit, and not reduced to vacuum.

Standard silver lines:

| Intensity | $\lambda$ |
|---|---|
| 5 | 1993·65 |
| 5 | 1956·88 |
| 5 | 1916·28 |
| 4 | 1879·60 |
| 2 | 1855·61 |

Owing to the small dispersion of the instrument, the accuracy of our measurement was only to the first decimal of an Ångström unit. In the region under investigation, one division of the drum of the photo-measuring microscope corresponded approximately to 0·1 Å.U. but as in the case of measuring thick or diffuse lines the error of pointing may sometimes amount to 2 or 3 divisions, thus incurring an error of 0·2 or 0·3 Å.U. in unfavourable cases.

We have taken about 90 plates in all, on each of which more than 10 different exposures could be given by displacing the plate. The time of exposure was several minutes in most cases for the spark spectra, and 10 to 20 minutes for those of the vacuum arc.

After each measurement, the lines were carefully examined to eliminate the air lines and also those lines which could be identified as due to impurities. In the case of the vacuum arc spectra, zinc lines sometimes appeared on the photograph, especially when the plati-

num foil burned out during the exposure. But there was no great difficulty in identifying these lines.

The results of the measurement are given below separately for each element, and the values obtained by Bloch, Handke and others are also given for comparison. It is to be remarked that the results of Handke, and also of Saunders, which were expressed in wave-length reduced to vacuum, are changed to those in air for the sake of comparison.

(1) *Ag*

As stated in the paper of Bloch, the spark spectrum of silver shows many lines in the extreme ultra-violet which are evenly distributed, so that the spectrum may conveniently be chosen as the wave-length standard.

In the region between $\lambda$ 2000–1855 Å.U., our results agree quite well with those of Bloch, excepting the following faint lines which appeared on all of our photograms:

Spark spectrum of *Ag* (No. 1).

| Intensity | λ | |
|---|---|---|
| 1 | 1989·6 | |
| 1 | 8·5 | |
| 2 | 30·6 | |
| 4 | 1862·7 | (Handke 1862·3 [Int. 5]) |

The figures given by Handke show some discrepancies as already noted by Bloch.

Below $\lambda$ 1855 Å.U., we have found the following lines:

Spark spectrum of *Ag* (No. 2).

| Takamine and Nitta | | Handke | |
|---|---|---|---|
| Int. | λ | Int. | λ |
| 1 | 1852·9 | 5 | 1852·8 |
| 1 | 48·7 | 5 | 48·8 |
| | — | 5 | 46·1 |
| 3 | 38·6 | 5 | 38·9 |
| 2 | 37·0 | 4 | 37·5 |

| T and N | | Handke | |
|---|---|---|---|
| Int. | λ | Int. | λ |
| | — | 3 | 1835·0 |
| 2 | 1832·6 | 3 | 33·4 |
| 1 | 30·6 | 4 | 31·2 |
| | — | 5 | 28·0 |
| 3 | 26·3 | 4 | 26·5 |

(2) *Al*

It is well known that the spark lines of this element are convenient for the orientation of lines in the region of the extreme ultra-violet. Our results are slightly different from those of the former investigators.

Instead of the single line at λ 1862, we obtained a double line; and a faint new line was observed at 1855 as shown in the following table:

Spark spectrum of *Al*.

| Int. | λ |
|---|---|
| 8 | 1989·8 |
| 7 | 35·2 |
| 2 | 30·3 |
| 4 | 1862·1 |
| 1 | 61·5 |
| 3 | 57·4 |
| 1 | 55·3 |
| 6 | 54·0 |

(3) *Au*

The only investigation hitherto published extending below λ 2000 is that of Handke, who measured the wave-lengths of spark lines in a wider range than ours. As in the case of silver, there are many discrepancies.

Spark spectrum of *Au.*

| T and N | | Handke | |
|---|---|---|---|
| Int. | λ | Int. | λ |
| 8 | 2000·2 | | |
| 2 | 1996·0 | | |
| 8 | 91·8 | | |
| 4 | 89·2 | | |
| 1 | 84·5 | | |
| 8 | 77·5 | | |
| 2 | 72·7 | 2 | 1972·7 |
| | — | 2 | 58·2 |
| 1 | 57·5 | 2 | 57·5 |
| | — | 2 | 56·0 |
| 1 | 55·7 | 3 | 55·6 |
| 1 | 54·5 | | — |
| 3 | 51·8 | 4 | 51·8 |
| 1 | 48·0 | 3 | 48·3 |
| | — | 3 | 47·5 |
| 1 | 46.0 | | — |
| 1 | 44·1 | 3 | 44·0 |
| | — | 2 | 42·9 |
| 1 | 38·8 | 1 | 39·0 |
| 2 | 37·5 | 3 | 38·0 |
| 2 | 35·0 | 3 | 35·4 |
| 1 | 34·0 | 2 | 34·5 |
| 2 | 31·5 | 3 | 31·8 |
| 1 | 30·6 | | — |
| 1 | 29·1 | 2 | 29·3 |
| | — | 1 | 27·0 |
| | — | 1 | 26·0 |
| | 24·5 | 7 | 25·4 |
| 6 | 20·7 | 7 | 21·8 |
| 6 | 18·8 | 6 | 19·4 |

| T and N | | Handke | |
|---|---|---|---|
| Int. | λ | Int. | λ |
| | — | 2 | 1918·0 |
| | — | 1 | 10·9 |
| | — | 3 | 09·4 |
| | — | 1 | 07·6 |
| 3 | 1904·1 | 5 | 05·0 |
| | — | 2 | 00·3 |
| | — | 2 | 1899·4 |
| 4 | 1890·2 | 6 | 90·5 |
| 4 | 86·0 | 6 | 87·0 |
| 1 | 84·6 | | — |
| 1 | 80·3 | | 80·8 |
| 4 | 79·2 | 4 | 79·7 |
| | — | 1 | 74·5 |
| 2 | 71·3 | 6 | 72·0 |
| | — | 2 | 65·6 |
| 4 | 61·8 | 5 | 62·1 |
| | — | 4 | 59·6 |
| 2 | 58·4 | 3 | 58·5 |
| 1 | 57·0 | 4 | 56·7 |
| | — | 4 | 52·7 |
| 1 | 52·0 | 4 | 52·0 |
| 1 | 50·9 | 4 | 50·4 |
| 2 | 49·6 | 3 | 49·2 |
| | — | 1 | 46·7 |
| | — | 4 | 45·3 |
| 1 | 44·0 | | — |
| | | 1 | 41·5 |

The region below $\lambda$ 1925 Å.U., with the comparison spectrum of *Ag* spark, is reproduced in Fig. 3, Pl. I.

(4) *Bi*

In the region between $\lambda$ 2061·7 and 1902·6, Eder and Valenta[1] gave seven lines, to which Bloch added two new lines. Besides the lines obtained by them, we found two more lines. It may be remarked that the line $\lambda$ 1902·4 appeared with considerable intensity in our photograph, a few seconds exposure being sufficient to photograph the line.

Spark spectrum of *Bi*.

| T and N | | Eder and Valenta | | Bloch | |
|---|---|---|---|---|---|
| Int. | λ | Int. | λ | Int. | λ |
| 1 | 1990·2 | | — | | — |
| 4 | 88·9 | 1 | 1988·6 | | — |
| 2 | 73·3 | | — | 3 | 1973·15 |
| 2 | 59·7 | | — | 3 | 59·63 |
| 5 | 53·9 | 1 | 54·5 | | — |
| 2 | 10·2 | | — | | — |
| 10 | 02·6 | 1 | 02·6 | | — |

The extreme ultra-violet part of the vacuum arc spectra of bismuth has not hitherto been investigated. We have found three lines below $\lambda$ 2000, which appear also in the spark spectrum.

Vacuum arc spectrum of *Bi*.

| Int. | λ |
|---|---|
| 2 | 1959·7 |
| 2 | 53·9 |
| 3 | 02·6 |

A reproduction of the vacuum spectra of *Bi* with the comparison spectrum of *Fe* spark is shown in Fig. 8, Pl. II.

(5) *Cd*

The former observations on the spark spectrum of this element are

1 Atlas Typischer Spectren, 148 (1911).

those of Eder and Valenta, Bloch, Saunders, and McLennan and Edwards[1]. The last mentioned authors have employed a spectrograph consisting of a train of fluorite prisms. In the following table, our measurements are compared with those of earlier investigators.

Spark spectrum of *Cd.*

| T and N | | Bloch | | McLennan & Edwards | | T and N | | Bloch | | M and E | |
|---|---|---|---|---|---|---|---|---|---|---|---|
| Int. | λ | Int. | λ | Int. | λ | Int. | λ | Int. | λ | Int. | λ |
| 6 | 1994·8 | 3 | 1994·78 | 3 | 1995·1 | 2 | 1919.6 | 1 | 1919·30 | 3 | 1919·6 |
| 1 | 89·1 | | — | 1 | 89·2 | 1 | 14·4 | 1 | 14·50 | | — |
| | — | | — | 1 | 79·8 | 2 | 00·6 | 2 | 00·70 | 6 | 01·1 |
| 3 | 77·4 | 2 | 76·85 | 2 | 77·1 | | — | 1 | 1898·28 | 2 | 1899·2 |
| 1 | 75·0 | | — | | — | 1 | 1896·7 | 1 | 96·64 | | — |
| | — | | — | 1 | 70·4 | | — | 1 | 87·78 | | — |
| 3 | 65·8 | 1 | 65.44 | 4 | 65·4 | 2 | 84·2 | 1 | 84·08 | 2 | 83·1 |
| 1 | 65·3 | | — | | — | | — | | — | 1 | 77·8 |
| 1 | 62·4 | | — | | — | 6 | 73·2 | 4 | 73·37 | 6 | 73·8 |
| 1 | 61·6 | | — | | — | 1 | 67·7 | 1 | 67·73 | | — |
| 1 | 56·7 | 1 | 56·81 | | — | 1 | 65·3 | 1 | 65·34 | | — |
| | — | | — | 1 | 45·6 | 4 | 55·8 | 3 | 56·10 | 6 | 56·4 |
| 2 | 44·1 | 1 | 43·85 | | — | 4 | 55·2 | 2 | 55.32 | 6 | 55·3 |
| 2 | 42·5 | 1 | 42·61 | 6 | 42·9 | 3 | 50·7 | | — | 7 | 50·6 |
| 4 | 39·2 | 2 | 38·91 | 4 | 39·2 | 2 | 43·7 | | — | 7 | 44·1 |
| 3 | 30 4 | | — | | — | | | | | | |
| 3 | 21·4 | 2 | 21·55 | 4 | 21·9 | | | | | | |

(6) *Co*

For the spark spectrum of this element in the extreme ultra-violet we have only the data given by Bloch in the region λ 2174–1873 Å.U. We have not measured the part above 2000, but as shown in the following table, we have found many lines below 1930 Å.U.

1 Trans. Roy, Soc. Canada, **9**, 167 (1915).

Spark spectrum of *Co.*

| T and N | | Bloch | | T and N | | Bloch | | T and N | | Bloch | | T and N | |
|---|---|---|---|---|---|---|---|---|---|---|---|---|---|
| Int. | λ | Int. | λ | Int. | λ | Int. | λ | Int. | λ | Int. | λ | Int. | λ |
| 4 | 1999·0 | | — | 1 | 1942·0 | | — | 1 | 1907·5 | | — | 3 | 1861·5 |
| 2 | 99·3 | | — | 2 | 41·6 | 2 | 1941·64 | 1 | 06·0 | | — | 2 | 59·9 |
| 2 | 96·2 | 1 | 1996·44 | 8 | 40·2 | 6 | 40·52 | 1 | 05·1 | | — | 2 | 54·2 |
| 2 | 94·7 | 1 | 94·67 | 2 | 39·4 | 3 | 39·41 | 1 | 03·0 | | — | 1 | 53·7 |
| 2 | 93·3 | 1 | 92·52 | 1 | 37·0 | | — | 1 | 01·0 | 1 | 1900·83 | 2 | 53·4 |
| 2 | 90·8 | | — | 4 | 36·6 | 1 | 36·85 | 1 | 00·1 | | — | 3 | 52·0 |
| 5 | 89·0 | 3 | 88·85 | 1 | 36·2 | 2 | 36·26 | 1 | 1899·6 | | — | 1 | 50·8 |
| 3 | 86·5 | 1 | 86·38 | 1 | 35·5 | | — | 1 | 96·1 | | — | 1 | 49·0 |
| 2 | 84·3 | 1 | 84·16 | 2 | 34·5 | 2 | 34·21 | 3 | 95·2 | 1 | 1895·47 | 1 | 47·0 |
| 2 | 83·2 | 1 | 83·24 | 2 | 34·0 | | — | 1 | 93·7 | | — | 1 | 46·3 |
| 2 | 80·3 | 1 | 80·62 | 2 | 33·8 | | — | 2 | 91·4 | | — | 4 | 45·1 |
| 4 | 79·1 | 1 | 79·32 | 1 | 33·0 | 1 | 32·41 | 1 | 90·1 | | — | 1 | 44·0 |
| 2 | 78·0 | 1 | 78·18 | 1 | 30·3 | 1 | 30·20 | 1 | 89·7 | | — | 1 | 43·5 |
| 3 | 76·3 | 3 | 76·25 | 1 | 29·7 | | — | 2 | 88·2 | | — | 2 | 42·5 |
| 5 | 74·2 | 3 | 74·13 | 2 | 29·0 | 2 | 29·06 | 1 | 87.7 | | — | 1 | 39·0 |
| 2 | 72·0 | | — | 6 | 28·0 | 4 | 27·86 | 1 | 86·3 | | — | 3 | 38·4 |
| 3 | 71·1 | 1 | 71·09 | 2 | 27·1 | 1 | 26·97 | 1 | 84·9 | | — | 1 | 36·3 |
| 5 | 69·6 | 4 | 69·25 | 1 | 25·5 | | — | 1 | 84·0 | | — | 1 | 34·7 |
| 2 | 68·3 | 2 | 68·15 | 2 | 24.9 | | — | 1 | 82·4 | | — | 1 | 34·0 |
| 4 | 62·8 | 2 | 62·84 | 1 | 24·0 | | — | 3 | 81·2 | 1 | 81·52 | 1 | 28·0 |
| 3 | 60·6 | 1 | 60·61 | 1 | 23·5 | | — | 1 | 80·7 | | — | | |
| 2 | 58·6 | 5 | 58·58 | 1 | 22·6 | 1 | 22·62 | 1 | 80·0 | | — | | |
| 6 | 56·7 | 5 | 56·58 | 1 | 22·0 | | — | 2 | 78·5 | | — | | |
| 5 | 55·3 | 3 | 55·04 | 1 | 20·2 | | — | 2 | 76·6 | | — | | |
| 4 | 54·3 | 4 | 53·99 | 3 | 18·3 | 3 | 18.44 | 1 | 74·5 | | — | | |
| 3 | 53·4 | 1 | 53·06 | 3 | 16·8 | 2 | 16·98 | 2 | 74·3 | | — | | |
| 2 | 52·4 | 1 | 52·30 | 1 | 15·7 | | — | 1 | 73·7 | | — | | |
| 2 | 51·3 | 1 | 51·31 | 1 | 14·5 | | — | | — | 1 | 72·94 | | |
| 1 | 50·5 | | — | 1 | 13·5 | | — | 1 | 72·0 | | — | | |
| 6 | 49·8 | 3 | 50·09 | 1 | 12·5 | | — | 4 | 71·2 | | — | | |
| 1 | 49·4 | 4 | 48·31 | 1 | 11·5 | | — | 1 | 67·9 | | — | | |
| 1 | 48·5 | | — | 3 | 10·1 | 1 | 10·16 | 3 | 66·6 | | — | | |
| 1 | 46·2 | 2 | 46·00 | 1 | 09·2 | | — | 2 | 63·0 | | — | | |
| 1 | 44·8 | 1 | 44·43 | 3 | 08.3 | | — | 2 | 62·4 | | — | | |
| 2 | 43·7 | 1 | 43·46 | 1 | 07.7 | 1 | 07·85 | 2 | 62·1 | | — | | |

Fig. 4, Pl. I. is the reproduction of *Co* spectrum with *Ag* comparison. It may be noted that this portion is not clearly shown in the publication of Bloch.

(7) *Fe*

As in the visible and ordinary ultra-violet part, so also in the extreme ultra-violet the spark spectrum of iron is very rich in lines and hence suited for comparison of wave-length.

In the region between $\lambda$ 2000 and 1915 Å.U., our results agree quite well with those of Bloch. The slight differences being that, (i) the line 1943·64 (intensity 1) recorded by Bloch did not appear in our photograph; (ii) instead of the close doublet 1939·37 (intensity 2) and 1939·13 (intensity 4), we obtained 1939·3 (2) and 1938·3 (3).

Beyond the line $\lambda$ 1875, which is the most refrangible line in the measurement of Bloch, we have found some more lines.

In the following table, we give the results of our measuremen for the region below $\lambda$ 1915:

Spark spectrum of *Fe*.

| T and N | | Bloch | | T and N | | Bloch | | T and N | |
|---|---|---|---|---|---|---|---|---|---|
| Int. | λ | Int. | λ | Int. | λ | Int. | λ | Int. | λ |
| 4 | 1914·3 | 5 | 1914·43 | 3 | 1891·6 | 2 | 1891·53 | 2 | 1864·6 |
| 6 | 13·3 | 6 | 13·40 | 2 | 91·0 | | — | 2 | 62·5 |
| 1 | 12·3 | | — | 3 | 90·2 | 4 | 90·07 | 1 | 62·0 |
| 1 | 11·0 | 1 | 10·75 | 2 | 88·3 | 2 | 88·15 | 1 | 61·3 |
| 1 | 10·0 | 1 | 10·00 | 3 | 87·4 | | — | 3 | 59·4 |
| 1 | 09·0 | | — | 3 | 86·9 | 2 | 86·55 | 1 | 58·0 |
| 2 | 06·8 | 3 | 06·97 | 2 | 85·8 | | — | 1 | 57·1 |
| 1 | 06·0 | 1 | 06·06 | 3 | 84·8 | | — | 1 | 56·0 |
| 1 | 04·2 | 1 | 04·22 | 3 | 82·0 | 1 | 81·54 | 2 | 54·0 |
| 1 | 03·5 | | — | 2 | 81·1 | | — | 1 | 51·7 |
| 1 | 03·0 | 3 | 02·98 | 2 | 80·7 | 1 | 80·39 | 1 | 50·0 |
| 1 | 02·0 | 1 | 01·30 | 1 | 80·0 | | — | 1 | 48·7 |
| 2 | 00·8 | 2 | 00·44 | 3 | 77·4 | 1 | 77·41 | 1 | 47·5 |
| 1 | 1899·5 | | — | 3 | 76·9 | 1 | 76·86 | 2 | 43·7 |
| 1 | 98·3 | 1 | 1897·96 | 1 | 76·1 | | — | 1 | 42·5 |
| 1 | 97·3 | | — | 1 | 71·8 | | — | 2 | 41·0 |
| 2 | 96·2 | 1 | 96·18 | 2 | 70·7 | | — | 1 | 39·9 |
| 6 | 94·9 | 6 | 94·90 | 3 | 69·5 | | — | | |
| 2 | 93·8 | 2 | 93·44 | 1 | 66·5 | | — | | |
| 2 | 92·5 | | | 1 | 65·8 | | — | | |

in the case of Fig. 1 had taken place. On the whole, these resemble the figures obtained by Brown, but there are no irregular branches near the electrode in the cathode figure as is seen in Brown's figure. Perhaps, as will be noted later, these may be of the anode type, due to an oscillation in the secondary of the induction coil used by Brown.

The principal differences between the figures represented in Fig. 2 and the cathode figure in Fig. 1 are that the former suffered deformation by the appearance of some strong branches, and that further fine branchings occurred.

It is worthy of note that, before the further branching takes place, the intensity in a branch is greater on its sides than in its central portion. This is always observed in cathode figures when further branching of a branch occurs. In the anode figure represented in Fig. 3, the characteristic properties observed in Fig. 1 are more clearly seen, and moreover it is interesting to note the appearance of many stronger branches near the electrode and several small anode figures with independent origins whose formation can not be explained.

Fig. 4 was obtained with an induction coil when a few make and break discharges had taken place. On the whole, in their characteristic properties, both cathode and anode figures resemble the anode figure obtained with the influence machine, but in details they are different. In the cathode figure its irregular, finer branches make a denser group of smaller extension than that of the anode, and there are many branches which run in directions perpendicular to the radial directions.

Fig. 5 was obtained when a little stronger discharge than in the case of Fig. 4 had taken place. At its cathode, the cathode figure get with the influence machine appeared together with the cathode figure in Fig. 4. As it is ambiguous with regard to the distinction between cathode and anode in Fig. 4 and 5, for several make and break discharges occurred, it is better to test with a single make or a single break discharge. Fig. 6 was obtained with a single break discharge which was caused by breaking the mercury-break by hand.

In this figure also, both cathode and anode figures greatly resemble the anode figure produced by the influence machine. In the cathode figure, it is seen that many branches run in directions perpendicular to the radials, as observed in Fig. 4 and 5. Inserting a light-glow-oscilloscope in series in the circuit, and observing by a rotating mirror, the discharge was really seen to be oscillatory. The cathode

electrode is one which was cathode at first; and the anode electrode is one which was anode at first. As, in the next period of oscillation, the electrode which was cathode at first will become anode, an anode figure will be produced from this electrode at this stage. Are the cathode figures in Fig. 4, 5 and 6 not anode figures thus formed? To test this point further, I experimented with oscillatory discharges from the influence machine. The annexed figure indicates the arrangement taken. In this figure, *L* denotes a self induction, *O* the light-glow-oscilloscope, *M* a condenser, and *S* a spark gap.

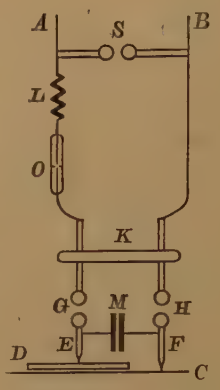


After *A*, *B* were connected to both the terminals of the influence machine, the spark gaps *G*, *H* were respectively brought in contact. After a single spark had passed through the spark gap *S*, the plate was developed. The figures thus obtained are represented in Fig. 7 and 8. Fig. 8 was obtained at the electrode which had been cathode before a spark had passed through the spark gap *S*, and Fig. 7 when the sign was reversed. In their characteristic properties, both figures have much resemblance respectively to the cathode and anode figures obtained with a single discharge of the induction coil.

Before the spark had passed through the spark gap *S*, a weak glow was visible only at the negative pole of the oscilloscope, but just when the spark passed through *S*, an intense glow appeared at both the poles. Though this intense glow could not by a rotating mirror be resolved as an oscillatory discharge, yet, it was doubtless one of short period, because the self induction and the capacity used were small. The reason why the cathode figures obtained with the influence machine did not appear in the above oscillatory figures is probably that cathode figures with the influence machine always have less extension than the anode figures. Consequently we may say that there is a distinct difference between the cathode figure which is composed of regular branches and the anode figure which is composed of irregular branches.

Next, using electrodes of various forms, various discharge figures were obtained with influence machine. Fig. 9 and 10 are respectively the cathode and anode figures got with cylindrical electrode. In these

figures, cathode branches end abruptly on a regular continuous outline as usual, and leave a small circular free portion in the center of the electrode, but the irregular anode branches end irregularly, and do not leave any regular free space at the center of the electrode as that of the cathode branches.

The points where the branches seem to start from the electrode are never regularly distributed, but when an electrode with many regularly distributed small studs along the contour of it, was employed, all the anode and cathode branches seem to start from the studs where electric force was intense. Fig. 11, 12, 13, etc. are obtained with such electrodes.

In Fig. 11 a circular-disc-electrode was used, and in Fig. 12 and 13 a crossed-plate-electrode was used. From these figures we see that all the regular cathode branches, which do never interfere with each other, leaving sharply defined regular dark intervals between them, seem to start at right angles to the contour of the electrode. The facts observed in the case of the point electrode with regard to the mode of branching and of the distribution of intensity in a branch also may be clearly seen in these figures. In Fig. 14, the electrode used consists of a circular cylinder and a smaller concentric disc, both of which were connected to the cathode of the influence machine. The branches which radiated from the disc and those which radiated from the inside of the cylindrical electrode never interfere but leave dark circular portion as their boundary.

Now with regard to the directions of the cathode branches which radiate outwards from the electrode, Fig. 11 and 14 seem to show that they represents the directions of the lines of force due to the electrode; but if we recollect the figure represented in Fig. 2, where a stronger discharge than in the case of Fig. 1 occurred, we shall be led to think that there is considerable repulsion between neighbouring branches. In order to test this point, cathode figure Fig. 15 was taken. This figure was produced when a cathode discharge took place on a photographic plate under which a wooden plate coated with tin foil was placed in the position indicated by the rectangle. Near the electrode the direction of all branches is nearly perpendicular to the contour of the electrode; but, as the branches go a little forward, these above the tin foil grow longer and longer than those under which there is no tin foil, and the latter change their direction continuously by the repulsion due to the former.

The fact that all cathode branches terminate on continuous curves seems to indicate that all branches of a cathode figure start from the electrode and go forward simultaneously, repelling each other with considerable forces. In the cathode figure Fig. 12, each branch which radiates from the neighbouring two sides of a corner is straight along almost its whole path, except in a little portion at its end where it curves a little along the dark boundary of the branch which is the bisector of the angle of the corner. In the anode figure Fig. 13, all branches which seem to radiate from the neighbouring sides of a corner terminate nearly on the bisector of the angle of the corner in an irregular manner.

Consequently, with regard to the formation of the cathode figure, it seems to the writer as if the branches start from the points on the electrode where the electric force is intense, and go forward with nearly equal velosity, leaving sharply defined intervals between them, and repelling each other with considerable force, and finally terminate abruptly on the regular boundary of the figure.

Next the writer investigated the change of the nature of the discharge figures with regard to the height of the sensitive film above the tin foil. Fig. 16 is a cathode figure on a Kodak film, the height of its sensitive film above the tin foil was about 0·15 mm; while with ordinary plate it is about 1–2 mm. The figure consists of very, very fine regular branches, and the intervals between them are also very sharp and fine.

When the height of the sensitive film was increased by placing glass plates or an ebonite plate under the photographic plate, the branches became large and the intervals between them became diffused. Fig. 17 was obtained when an ebonite plate whose thickness is about 1 cm. was placed between the photographic plate and the tin foil which was connected to the positive pole of the influence machine.

Fig. 18, 19, and 20 are anode figures obtained with various heights of the sensitive film above the tin foil. In Fig. 18 the height is least, as a Kodak film was used. Fig. 19 was obtained with a common plate; and in Fig. 20 an ebonite plate whose thickness was about 1 cm. was placed between the plate and the foil, and consequently the height is greatest in this case. From these figures we see that the anode figures become smaller in extension, and that their branches become finer and end more regularly as the height is reduced.

So far as the writer has experimented, the various features of the

discharge figures seem to be unaffected by the metal used as electrode, the metal placed under the photographic plate, and the kind of photographic plates.

## 2. Formation of the Photographic Impression.

With regard to the question as to whether the result obtained was due to a photographic effect of the luminosity of the discharge, or to some more direct action of the discharge on the film, Brown[1] took the latter view. For, according to his experiment, the luminosity of the discharge alone was too weak to produce such fine figures; and, when the discharge was taken with the two terminals on the back or uncoated side of the plate, a photographic effect on both sides of the film was observed.

When the discharge on a photographic plate was observed with the naked eye, only the intense portions of the branches showed their structures, the weak portions of continuous luminosity never showing their details; but, if viewed through a lens, the discharge represented all its details as is depicted on the photographic plate. Moreover, these features of the discharge are not confined to a photographic plate, but can be seen on a glass plate when the luminosity of the discharge is viewed through a lens. This shows that the sensitive film plays, at least, no essential part in the formation of the figure, except that the latent image of the luminosity of the discharge which occurred along its surface is produced in it.

When the discharge was taken with either electrode on the back or uncoated side of a common plate, only a cloudy photographic impression of the branching discharge on the back of the plate was obtained on the back of the sensitive film; but when a Kodak film on a glass plate was used, instead of the common plate, a clear impression of the branching discharge on the back of the film was produced on the back of the sensitive film. And as, in either case, the luminosity of the discharge could be seen on the back of the plate or the film, there seems to be no objection, as far as the above experiment is concerned, to considering that the photographic impression on the back of the sensitive film was made by the luminosity of the discharge on the back of the plate.

In favour of his view, Brown mentioned the fact that he obtained

1 Phil. Mag., **26**, 502, (1888).

a photographic impression on the outer surface of the sensitive film when the discharge took place on the back of the plate which had been placed with its sensitive film downward on a sheet of tin foil. But, if two thin and small glass plates were placed between the sensitive film and the metal plate so that an air space was left between them, the luminosity of the discharge could be seen between them, and a photogtaphic impression be obtained on the outer surface of the sensitive film. Considering this, there is no reason to believe that the luminosity of the discharge did not appear between the film and the foil in the Brown's experiment, and consequently that any direct action produced such an impression on the photographic plate without the intervention of the luminosity of the discharge.

In resumé, so far as the writer has experimented, the sensitive film plays no essential part in the formation of the figure, and it is natural to consider that the photographic impression of the discharge figure is produced by the photographic action of the luminosity of the discharge which occurs along the surface of the sensitive film.

## 3. An Explanation of the Formation of the Figures, and the Transition from Brush Discharge to Spark Discharge.

If we assume that the luminosity of the discharge is due to the ionisation of molecules of gas, the discharge figures obtained will be the path of the ionisation; and, therefore, in the explanation of the figures we need only to consider the path of the ionisation of the gas molecules produced by the electric discharge.

J. J. Thomson, in his theory of the conduction of electricity through gases, regarded the spark discharge as originating in the ionisation of the gas by moving ions, the small negative ions—the corpuscles—being more efficient ionisers than the positive ones, which have a greater mass. And, as the original source of these ions, he considered the ionisation due to the collision of positive ions with the gas molecules near the cathode or with the cathode itself.

As to the difference between the minimum potential for positive and negative points when the electric discharge occurs from a point he says, "...the minimum potential difference is determined by the condition that the electric field near the electrode should be strong enough to enable the positive ions to produce an adequate stream of corpuscles. Now when the point is the cathode the positive ions have two

opportunities of producing corpuscles, (1) by impact with the electrode, (2) by impact with the molecules of the gas; while when the point is the anode only the second of these is available; this would have the effect of making the minimum potential required for point discharge greater."

Now, in our experiment, this consideration of the case of electric discharge from points may be applied; and an explanation of the principal properties of the discharge figures was undertaken by the following assumptions: (1) in a cathode branch, the ionisation in its end portion is caused by the collisions of negative ions with the gas molecules, and the original source of these negative ions is supplied by the ionisation due to the collisions of positive ions with the gas molecules in the neighbourhood of the cathode, or with the cathode itself; (2) in an anode branch, also, the ionisation in its end portion is caused by the collisions of negative ions with the gas molecules, and the ionisation due to the collisions of positive ions occurs in the portion nearer to the anode.

If the potential of the anode is increased sufficiently, the negative ions, which were present just before the formation of the photographic impression by the ionisation commences, will be pushed toward the portions of the electrode where the electric force is strong, and will ionise the gas molecules with which they collide. The negative ions thus produced will also do the same thing; and many positive and negative ions will be produced. The group of positive ions, which will be left behind as the negative ions are pushed toward the anode, will now act as a portion of the anode; and, repeating the same process as before, further branching and elongation of the anode branch will take place. With this explanation, the properties of the anode branches (that they are irregular in their branchings and elongations, and that their branches end in sharp points) will be immediately understood; because the formation of these branches is due to the presence of negative ions which would be distributed irregularly.

When the height of the sensitive film from the tin foil is reduced, the electric force along the film becomes smaller; and, consequently, the range in which the ionisation occurs becomes smaller as is seen in Fig. 18.

*An explanation of the formation of the cathode figure.* When the electric force at a point on the cathode reaches a certain intensity, a short spark passes from this point to the air a little distance away.

Along the path of this spark ions will be produced, positive as well as negative, and the positive ions will be attracted toward the electrode, while the negative ions will be driven away. The prolongation of a branch thus formed will be caused by the ionisation of the negative ions which are driven away from the cathode, as was assumed before. These negative ions on the surface of the sensitive film will be attracted downward by the attraction of the positive charge on the tin foil, and their motion will be retarded as if they suffer a kind of resistance. When many such branches are produced from the cathode on the sensitive film, there will be a portion of least electric force between any two neighbouring branches.

The electric force which acts on the negative ions on the side of a branch will be nearly perpendicular to the side of the branch along the surface of the film, and will be very small due to the repulsion of the charge on the neighbouring branch and the resistance caused by the attraction of the opposite charge on the tin foil ; and therefore the kinetic energy of the negative ions gained under the electric field will become insufficient to ionise the gas molecules before they reach the region of the least electric force between the neighbouring two branches. The property of the cathode branches that they leave sharply defined intervals between neighbouring branches seems thus to be explained.

Next an explanation of why the further branching of a cathode branch occurs will be given. Let *A*, *B*, *C* etc. be the ends of cathode branches before further branching takes place. At the end of any branch the attraction of the tin foil on the negative ions will be greater in its central portion than on its side portion; and, therefore, the resistance which will retard the motion of the negative ions on the end of the branch will be greater in its central portion than on its sides ; and consequently the negative ions on the side portion of the branch will go further and further forward than in its central portion, and at last the branch will be split into two. In Fig. 15, 14 and 21 many such branches can be seen.

When the breadth of a branch is comparatively great, the attraction on the negative ions in its end, due to the tin foil, will be strong and nearly constant in all portions excepting the sides where it will decrease abruptly. And when a certain stage of its elongation is

reached, the end of the branch will bulge out at the sides, leaving the central portion unaffected as indicated in the annexed figure. The repulsive forces which act on the negative ions at various points at the end of the branch thus formed, will be stronger or weaker according as the convexity of the boundary at that point is greater or smaller, or the concavity is smaller or greater. In its next stage the branch will grow out in its central portion as indicated by the dotted line in the figure. Consequently, when its further growth occurs, the branch will at last split up into three. If the branch is still broader, the central branch will also split up into two or more, and consequently, further branching of a branch into many branchlets will take place, as is seen in many cathode figures.

The variation of the intensity of the attraction of the tin foil upon negative ions at various points on the boundary of the end of a branch will be greater when the distance between the sensitive film and the tin foil is reduced, and when the branch is long. This is the reason why the cathode branches become finer as the distance between the sensitive film and the tin foil is reduced, and why the further branching of a branch occurs at a certain distance from the electrode.

Lastly, in order to study in what stage of the brush discharge a direct spark will pass, the writer placed two electrodes on the sensitive film, one being connected to the tin foil under the plate. When the two electrodes were brought into contact respectively to both the terminals of the influence machine, a discharge figure was obtained only at the electrode which was not connected to the tin foil.

When this was cathode, cathode figures were produced at this electrode, as represented in Fig. 21 and 22. In Fig. 21, where no direct spark discharge occurred, the cathade figure did not reach the anode. But in Fig. 22, when a direct spark occurred, the boundary of the cathode figure seemed to have been in contact with the anode. On many figures, not given here, the writer could not observe where no direct spark occurred when the cathode branches reached the anode.

On the other hand, when the sign of the electrode was reversed, anode figures were produced, as represented in Fig. 23, 24 and 25. In Fig. 24, no direct spark occurred, though the end of some branches reached the cathode. This will be explained, if we consider, as was assumed before, that the ionisation by positive ions does not occur in

the end portion of an anode branch, for to make a direct spark pass between the electrodes, the ionisation by positive ions should occur near the cathode as was pointed out by J. J. Thomson. On the other hand, if the ends of cathode branches reach the anode, a direct spark will pass, for every cathode branch has its original source of ions in the neighbourhood of the cathode by the collisions of positive ions, as was assumed before.

In conclusion the auther's sincere thanks are due to Prof. T. Mizuno for the interest he has taken in the work.

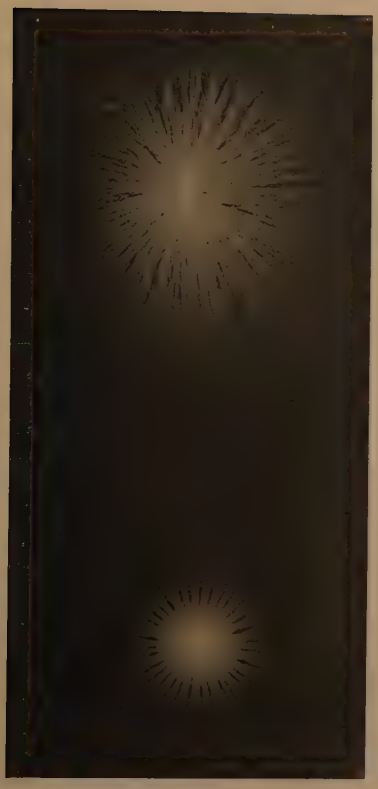

Fig. 1

Fig. 3

Fig. 2

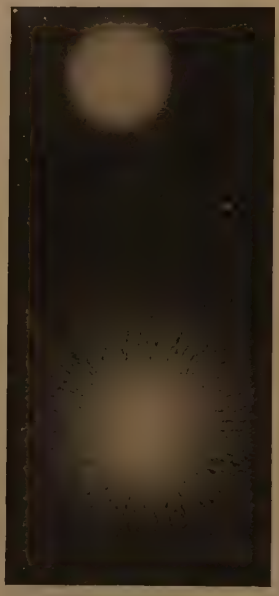

Fig. 4

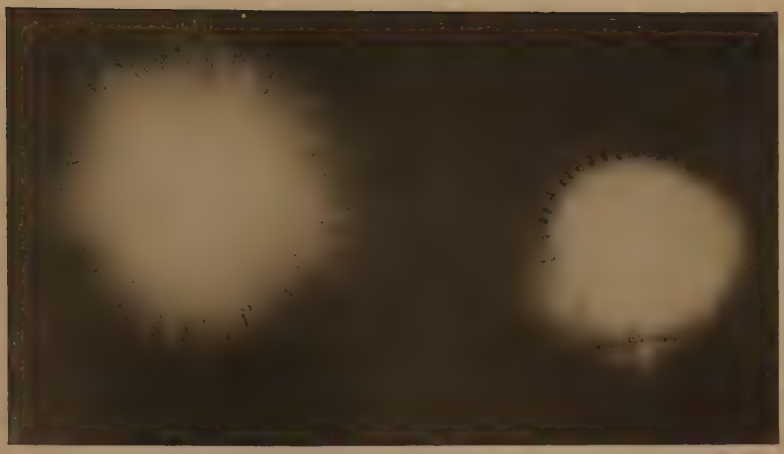

Fig. 5

Fig. 6

Fig. 7

Fig. 8

Fig. 9

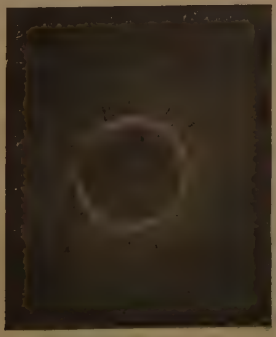

Fig. 10

Fig. 11

Fig. 12

Fig. 13

Fig. 14

Fig. 15

Fig. 16

Fig. 17

Fig. 18

Fig. 19

Fig. 20

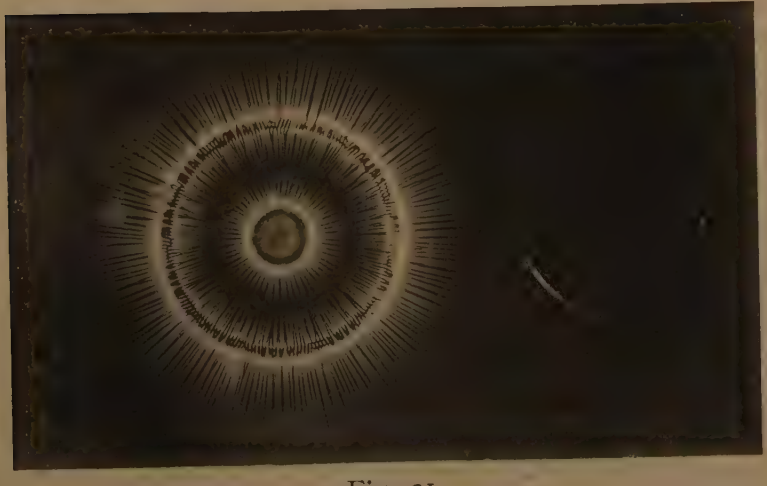

Fig. 21

Fig. 22

Fig. 23

Fig. 24

Fig. 25

# The Spark and the Vacuum Arc Spectra of Some Metals in the Extreme Ultra-Violet.

By

**Toshio Takamine and Shigeharu Nitta.**

(Received Dec. 9, 1916).

## 1. Introduction.

In connexion with the recent progress in the study of photo-electricity, the investigation of arc and spark spectra in the region of ultra-violet emitted by the vapours of various kinds of metals has become of increasing importance.

Owing to the researches of Schumann, Lyman and others, the limit of the spectrum in the extreme ultra-violet has been considerably extended, the excellent literature of these investigations is given by Lyman[1].

The present experiment deals only with the region which can be examined by a quartz spectrograph, the lower limit of wave-length being at about 1839 Å.U., but as most of the wave-length tables given in Kayser's Spectroscopie end at about $\lambda$ 2100 Å.U., and further, as the recent investigations on the spectra in the extreme ultra-violet are not so numerous, we may state that even in this easily accessible region between $\lambda$ 2200 and $\lambda$ 1830, our knowledge of the arc and spark spectra of various metals are far from being complete.

Below we give very brief resumé of the results obtained by a few recent observers.

The results obtained by Lyman for the elements *Al, Ca, Sr, Ba.* and *Mg* are given in the appendix of his monograph above cited, they are mostly confined to the spark spectra of these elements.

In 1909, Handke[2] published the results of his experiments obtained by using a vacuum prism spectrograph of the Schumann type. The elements investigated were *Ag, Al, Au, Cu, Hg, Mg, Sn, Zn.* A

1 The Spectroscopy of the Extreme Ultra-Violet, 1914.

2 Diss. Berlin, 1909.

similar instrument was employed by Wolff[1] who investigated the vacuum arc spectra of *Zn*, *Cd* and *Hg*.

In 1914, L. and E. Bloch[2] published the preliminary report of their investigations on the extreme ultra-violet lines in the spectra of some kinds of metals. In this experiment, they employed a quartz spectrograph having a large Cornu prism. The spectrograph was specially modified for photographing the extreme ultra-violet region, the lower limit of wave-length being at about 1850 Å.U. It is stated in their paper that by employing a vacuum spectrograph, they obtained the photograph extending down to 1400 Å.U.

In all the papers above cited, excepting that of Wolff, the spark spectrum only is investigated. Quite recently Saunders[3] has published his investigations on both the spark and the vacuum arc spectra of several metals in the extreme ultra-violet. Although the arc spectra present a very few lines in the extreme ultra-violet, they are of interest in connexion with series relations.

Previous to these investigations, Eder[4] examined the spark spectra of a greater number of elements in the ultra-viotet region, but excepting the case of aluminium, the region investigated extended only down to 2100 Å.U.

For some kind of metals, further data are to be found in Eder and Valenta's[5] "Atlas Typischer Spectren." Excellent photographs of various spectra in the extreme ultra-violet are reproduced in Tables LII and LIII. But it is to be remarked that in every photograph the intensity begins to fall off very rapidly in the region near $\lambda$ 1900 Å.U.

With a view to extending the aforesaid investigations and also comparing the spark spectra with those of the vacuum arc for some elements in the region above cited, the present investigation was undertaken.

## 2. Arrangements.

Two quartz spectrographs made by Hilger, each furnished with a Cornu prism having faces of $65 \times 41$ mm. (length of three equal sides $\times$ height) and of $21 \times 13$ mm. respectively were at our disposal. The larger one gives a dispersion of 5 Å.U. per mm. at $\lambda$ 2100 Å.U.,

1 Ann. d. Phys., **42**, 836 (1912).
2 Jour. de Phys., **4**, 622 (1914). C. R. **158**, 784, 1416 (1914).
3 Astrophys. Jour., **43**, 234 (1916).
4 Ber. d. k. Akad. d. Wiss., Wien **122**, 607 (1913).
5 Atlas Typischer Spectren, 1911.

while the smaller one a dispersion about 15 Å.U. per mm. at $\lambda$ 2100 and 7 Å.U. per mm. at $\lambda$ 1900 Å.U.

Without a special modification it was impossible for us to photograph the region below $\lambda$ 2100 Å.U. with the larger instrument, while with the smaller one, the spectra down to $\lambda$ 1830 Å.U. appeared with considerable intensity.

For the production of spark, we have employed the sparking apparatus of Hilger, consisting of a ¼ K.W. rotary converter and a transformer raising the potential up to about 10000 volts, a condenser being inserted in parallel with the spark.

As the electrodes, we used in most cases metal rods of 2 or 3 mm. diameter, the spark gap being 3 or 4 mm.

For the purpose of obtaining the vacuum arc spectra, we employed the lamp using a Wehnelt cathode as originally designed by Janicki[1] and afterwards modified by Wali-Mohammad[2].

In order to obtain the photographs of spectra extending to the extreme ultra-violet part, some further modifications were necessary. The lamp is shown in Fig. 1.

The glass tube $AB$ is about 20 cm. long and has a diam, of 35 mm. The upper end of the tube has a rim of 3 mm., to which a quartz circular disc of diam. 4 cm. and thickness 2 mm. is attached and sealed air-tight with sealing wax.

The lower end $B$ is protruded, and comes in contact with the conical ending of $C$, both surfaces being well ground to fit each other. The lower tube is about 5 cm. long. The outer side of the tube $AB$ is covered by another glass tube $A'B'$ with a gap of 1 mm. between them, the outer diameter of $A'B'$ being 40 mm. The upper and lower ends of the gap between $AB$ and $A'B'$ were stopped by rubber tubes, and the inner tube $AB$ was cooled by the water current.

1 Ann. d. Phys., **29**, 833 (1909).

2 Diss. Göttingen, (1912).

Fig. 1.

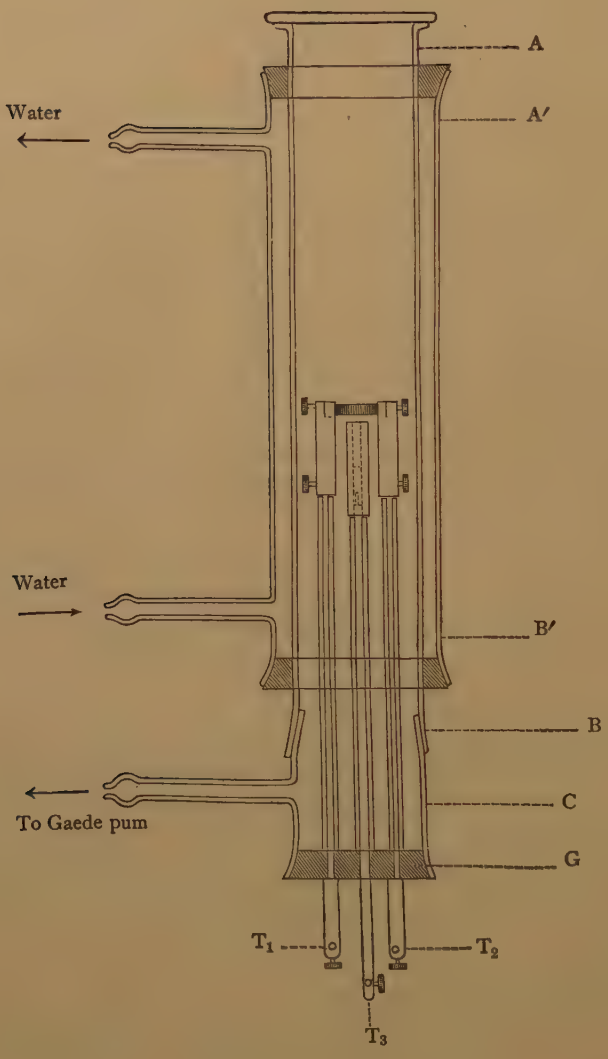


The central portion of Fig. 1, showing the anode and the cathode, is given enlarged in Fig. 2.

The cathode consists of a platinum foil 0·02 mm. thick, 30 mm. long and 5 mm. broad.

By cutting the tops of the two brass rods *D* (of 3 mm. diam.),

narrow slits were made and both ends of the platinum strip were inserted in them, the strip being slightly curved around the anode *A*.

Fig. 2.

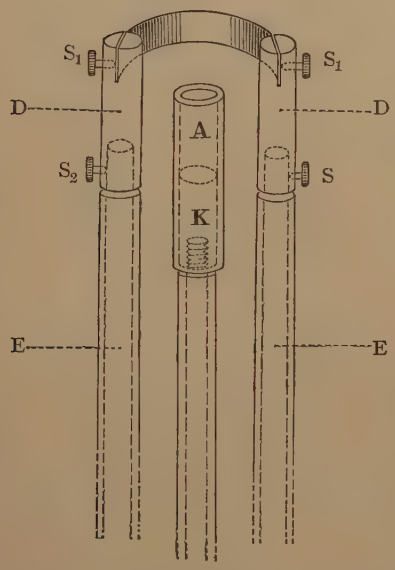


The small screws *S* are to secure good contact of the platinum foil with *D*. With the screw *S*, *D* was fixed to the brass rod *B* of 2 mm. diameter, leading to the terminals $T_1$ and $T_2$ on the ebonite stop *G* as shown in Fig. 1. The rod *E* was covered by a glass tube for the purpose of insulation.

To make the Wehnelt cathode, a mixture of barium nitrate and calcium nitrate was dissolved in water and a small quantity of the deposit was put on the platinum foil and heated with a Bunsen burner. The nitrates are then reduced and the strip become covered with a layer of oxide. When lighting the lamp, the cathode was heated to incandescence by a current of 13 to 17 amp. at 40 volts.

As the anode, the metal to be examined was put in a small tube of fused silica *A* in Fig. 2, either in solid or in powdered state. The dimensions of the tube varied according to the kind of the metal, but in most cases, the external diameter was about 5 mm. and the internal diameter 4 mm. the length of the tube being 2 or 4 cm. The bottom of this silica tube was stopped by the brass rod *K* which was wrapped in a thin asbestos sheet to fit tightly into the silica tube, the lower end of *K* was screwed into the terminal $T_3$ in Fig. 1.

Between the terminals $T_1$ (or $T_2$) and $T_3$, a potential difference of 220 volts was applied with a suitable resistance in series. The process of lighting the lamp may be briefly described as follows. After evacuating the tube for several minutes with a rotary oil pump, the Gaede mercury pump is started and the water current is passed. Then the Wehnelt cathode is made incandescent by the heating current and finally the switch for the main current is closed. The strength of the main current varied from 0·1 to 2·5 amp. at 220 volts. The state of

evacuation was sometimes tested by a discharge in a Geissler tube connected to a side tube.

In the previous investigation carried out by one of the authors[1], the light from the anode was totally reflected by a right-angled prism placed at the top, but in the present experiment it was not desirable to let the ray pass through a large quartz prism owing to its absorption, so that the small spectrograph was placed with its collimator vertical and the lamp was brought with its upper end just below the slit of the collimator.

By cutting suitable windows in the slide put before the slit of the collimator, the spark spectrum of iron, or sometimes that of silver, was photographed in the middle part of each spectrum as shown in the reproduction Figs. 8, 9 in Pl. II.

It was so arranged that after photographing the vacuum arc spectrum of a certain element, the lamp was removed and the iron electrodes of the spark was brought in its place. By interchanging the window in the slide before the slit we were able to photograph the comparison spectrum of iron without touching the photographic plate.

The measurements were carried out by means of a photo-measuring instrument of 15 cm. travel reading to 1 $\mu$, constructed by Hilger. As the spectra of the elements under investigation appeared on the photograph closely in contact with the standard spectrum of iron, we were able to measure both spectra without touching the photographic plate.

As it was of primary importance to use pure materials for the electrodes, great care was taken to avoid impurities. But on account of the war, there was much difficulty in obtaining the pure metals. Of the metals we have investigated *Al, Bi, Cd, Co, Sb* were those prepared by "Kahlbaum", and the others were of "Merck", and were of the guaranteed purity. We are obliged to Professor Chikashige of the Chemical Institute for the loan of several samples of pure metals for which we express our deepest thanks.

The Schumann plates prepared by Hilger were used in photographing the spectra.

## 3. Results of the Experiment.

The spark spectra of the following elements were investigated: *Ag, Al, Au, Bi, Cd, Co, Fe, Mn, Ni, Pt, Sb,* and *Tl.*

1 Takamine, Proc. Tokyo Math.-Phys. Soc., 8, 31, (1915).

The most refrangible part of the above spectrum is reproduced in Fig. 5, Pl. I.

Comparing the results obtained for the iron spectrum with that of the manganese spectrum, we see that the two lines $\lambda$ 1958·59 and 1914·43, which were suspected by Bloch as due to *Mn*, are really due to iron.

(8) *Mn*

We could not find any former observations for this element below $\lambda$ 2100 Å.U. We have found the following lines in the spark spectrum below $\lambda$ 2000 Å.U., but all of them are of feeble intensity.

Spark spectrum of *Mn*.

| Int. | λ |
|---|---|
| 4 | 1993·7 |
| 5 | 92·8 |
| 2 | 90·9 |
| 2 | 90·0 |
| 4 | 89·2 |
| 2 | 86·4 |
| 4 | 85·4 |
| 1 | 85·0 |
| 2 | 82·5 |
| 2 | 78·7 |
| 2 | 75·4 |
| 1 | 71·0 |
| 3 | 69·8 |
| 2 | 69·0 |
| 2 | 63·7 |
| 2 | 62·8 |
| 2 | 61·6 |
| 4 | 58·2 |
| 2 | 55·7 |
| 2 | 54·2 |
| 3 | 53·1 |
| 3 | 52·2 |

| Int. | λ |
|---|---|
| 2 | 1951·0 |
| 2 | 47·9 |
| 3 | 44·2 |
| 4 | 42·6 |
| 3 | 40·9 |
| 2 | 38·8 |
| 2 | 36·0 |
| 2 | 34·5 |
| 2 | 33·0 |
| 2 | 30·8 |
| 3 | 25·8 |
| 2 | 24·7 |
| 3 | 22·3 |
| 4 | 20·2 |
| 2 | 18·7 |
| 2 | 18·0 |
| 1 | 17·0 |
| 6 | 14·8 |
| 3 | 11.1 |
| 2 | 08·5 |
| 1 | 1899·2 |
| 1 | 98·5 |

| Int. | λ |
|---|---|
| 1 | 1897·1 |
| 2 | 93·2 |
| 2 | 92·0 |
| 1 | 77·3 |
| 1 | 76·0 |
| 1 | 75·3 |
| 1 | 72·2 |
| 1 | 67·5 |
| 1 | 65·3 |
| 1 | 64·0 |
| 4 | 62·2 |
| 1 | 61·2 |
| 1 | 60·2 |
| 1 | 57·5 |
| 4 | 54·2 |
| 1 | 53·0 |
| 1 | 52·5 |
| 1 | 51.1 |
| 1 | 50·1 |
| 1 | 44·6 |
| 1 | 43·3 |
| 1 | 42·5 |

(9) *Pt*

For this element also, we were unable to obtain the data of any former observers in the region below $\lambda$ 2000 Å.U. Our results are tabulated below:

Spark spectrum of *Pt.*

| Int. | λ | Int. | λ | Int. | λ | Int. | λ |
|---|---|---|---|---|---|---|---|
| 2 | 1999·2 | 3 | 1958·3 | 3 | 1925·5 | 3 | 1878·6 |
| 2 | 96·9 | 4 | 54·6 | 1 | 19·7 | 1 | 72·5 |
| 3 | 95·2 | 2 | 52·7 | 2 | 18·1 | 1 | 71·5 |
| 1 | 91·7 | 2 | 51·4 | 2 | 17·5 | 1 | 71·0 |
| 1 | 91·0 | 4 | 49·5 | 1 | 14·5 | 2 | 70·6 |
| 5 | 89·8 | 2 | 48·3 | 1 | 13·5 | 1 | 69·7 |
| 1 | 88·7 | 2 | 46·2 | 2 | 12·1 | 5 | 66·5 |
| 5 | 87·5 | 5 | 43·8 | 5 | 11·2 | 1 | 65·4 |
| 1 | 84·2 | 3 | 41·3 | 2 | 08·7 | 1 | 62·3 |
| 5 | 83·2 | 6 | 39·2 | 3 | 03·9 | 1 | 60·2 |
| 4 | 79·3 | 4 | 37·1 | 1 | 03·2 | 1 | 56·8 |
| 2 | 78·5 | 2 | 34·0 | 2 | 01·6 | 1 | 55·5 |
| 1 | 76·5 | 2 | 33·7 | 1 | 1898·7 | 1 | 51·7 |
| 4 | 71·5 | 2 | 33·0 | 1 | 98·0 | 1 | 45·5 |
| 1 | 70·0 | 1 | 31·8 | 2 | 97·0 | 1 | 44·6 |
| 2 | 69·5 | 1 | 31·5 | 4 | 95·8 | 1 | 42·0 |
| 3 | 68·9 | 2 | 30·3 | 3 | 94·6 | 1 | 39·5 |
| 2 | 65·3 | 4 | 29·3 | 3 | 93·9 | 1 | 37·6 |
| 1 | 63·0 | 4 | 28·5 | 1 | 91·0 | | |
| 1 | 62.0 | 4 | 27·7 | 6 | 89·2 | | |
| 1 | 61·3 | 1 | 26·3 | 3 | 82·4 | | |

Reproductions are shown in Figs. 6, 7, Pl. I.

(10) *Sb*

The ultra-violet part of the spark spectrum of this element was examined by Schippers and the arc spectrum by Kayser and Runge; the shortest wave-lengths measured in both cases being above 2000 Å.U. Schumann has photographed the more refrangible part but he did not measure the wave-lengths. L. and E. Bloch were the first to measure the lines from $\lambda$ 2068 to 1871 Å.U. We have added several more lines as shown in the following table.

So far as we are aware, the vacuum arc spectrum of *Sb* in this region was investigated for the first time. It is remarkable that the vacuum arc of this element, which is of very feeble intensity in visible light, produces a number of fairly strong lines in the ultra-violet part extending down to 1850 Å.U.

Spark spectrum of *Sb* Vacuum arc spectrum of *Sb*.

| T and N | | Bloch | | T and N | |
|---|---|---|---|---|---|
| Int. | λ | Int. | λ | Int. | λ |
| 5 | 1989·3 | | — | 5 | 1989·3 |
| 5 | 85·0 | 3 | 1985·36 | 5 | 85·0 |
| 4 | 77·7 | 3 | 77·64 | 3 | 77·7 |
| 3 | 71·9 | | — | 2 | 71·9 |
| 3 | 70·9 | | — | 3 | 70·9 |
| 2 | 56·0 | | — | 1 | 56·0 |
| 6 | 49·8 | 5 | 49·64 | 6 | 49·8 |
| 2 | 45·7 | | — | | — |
| 2 | 37·0 | | — | 2 | 37·0 |
| 5 | 31·1 | 4 | 30·83 | 4 | 31·1 |
| 5 | 26·6 | 4 | 26·61 | 4 | 26·6 |
| 5 | 22·6 | | 22·68 | | — |
| 2 | 1899·7 | | — | 2 | 1899·7 |
| 2 | 98·9 | | — | | — |
| 3 | 91·3 | | — | 1 | 91·3 |
| 3 | 90·3 | | — | 1 | 90·3 |
| 2 | 82·6 | | — | | — |
| 2 | 81·8 | | — | | — |
| 4 | 78·1 | 2 | 1877·91 | | — |
| 1 | 75·8 | | — | | — |

Spark spectrum of *Sb.* (Continued).

| T and N | | Bloch | |
|---|---|---|---|
| Int. | λ | Int. | λ |
| 1 | 74·5 | | — |
| 6 | 70·4 | 1 | 70·58 |
| 3 | 67·3 | | — |
| 1 | 63·3 | | — |
| 2 | 61·4 | | — |
| 3 | 58·0 | | — |

Vacuum arc spectrum of *Sb.* (Continued).

| T and N | |
|---|---|
| Int. | λ |
| 1 | 74·5 |
| 2 | 70·4 |
| 1 | 67·3 |
| 1 | 63·3 |
| 1 | 61·4 |
| 1 | 58·0 |

The vacuum arc spectrum of *Sb*, with *Fe* spark as comparison, is reproduced in Fig. 9, Pl. II.

(11) *Tl*

Both the spark and vacuum arc spectra of this element have been investigated by Saunders[1], the most refrangible line recorded by him being 1812 Å.U. We have found several new lines in the spark spectrum in the region λ 2000–1860 Å.U.

In the vacuum arc spectrum we have found two lines which appear also in the spark spectrum. The element is very convenient for a lamp using a Wehnelt cathode, since the vaporisation of the anode material is exceedingly small.

1 Astrophys. Jour. **43**, 234, (1916).

Spark spectrum of *Tl.*

| T and N | | Saunders | |
|---|---|---|---|
| Int. | λ | Int. | λ |
| 2 | 1994·6 | | — |
| 1 | 89·8 | | — |
| 3 | 89·0 | | — |
| 3 | 71·8 | | — |
| 4 | 37·1 | | — |
| 2 | 30·4 | | — |
| 8 | 08·2 | 5 | 1908·05 |
| 6 | 1892·3 | 3 | 1892·08 |
| 4 | 90·2 | | — |
| 4 | 80·7 | 2 | 80·57 |
| 2 | 71·2 | 1 | 70·85 |
| 2 | 60·0 | | — |
| | | 1 | 37·34 |
| | | 2 | 27·38 |
| | | 4 | 14·11 |

Vacuum arc spectrum of *Tl.*

| T and N | | Saunders | |
|---|---|---|---|
| Int. | λ | Int. | λ |
| 3 | 1971·8 | | — |
| 2 | 08·2 | 10 | 1908·05 |
| | — | 1 | 1892·08 |
| | — | 1 | 14·11 |

## Summary.

1. The spark spectra of *Ag, Al, Au, Bi, Cd, Co, Fe, Mn, Pt, Sb* and *Tl*, in the extreme ultra-violet were investigated by means of a quartz spectograph using Schumann plates. Relying on the data given by L. and E. Bloch for *Ag* and *Fe* spark, the wave-lengths of the spectrum lines were measured for the above elements in the region λ 2000–1830 Å.U.

A number of new lines were found for each element, especially in the most refrangible part. The spark spectra of *Mn* and *Pt* in this region were investigated for the first time.

2. Employing a vacuum arc lamp provided with a Wehnelt cathode, the vacuum arc spectra of *Bi, Sb* and *Tl* were photographed with the same apparatus and several new lines were found for each element in the region λ 2000–1850 Å.U.

# Plate I

Fig. 3

Magnification: 10

Fig. 4

Magnification: 10

Fig. 5

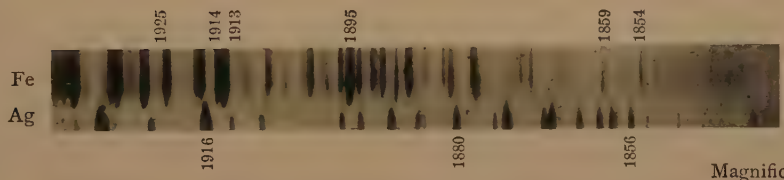


Magnification: 12

Fig. 6

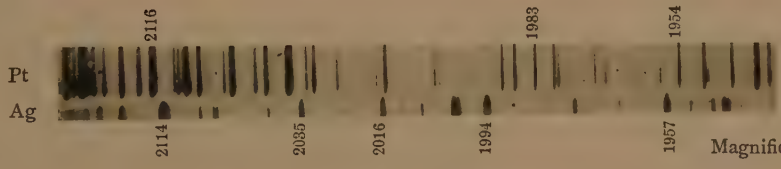


Magnification: 7

Fig. 7

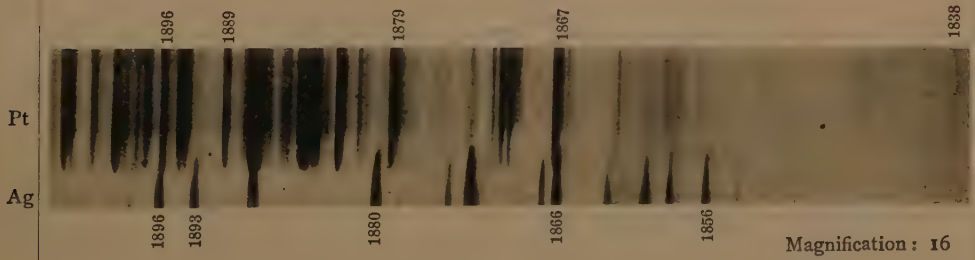


Magnification: 16

Fig. 8

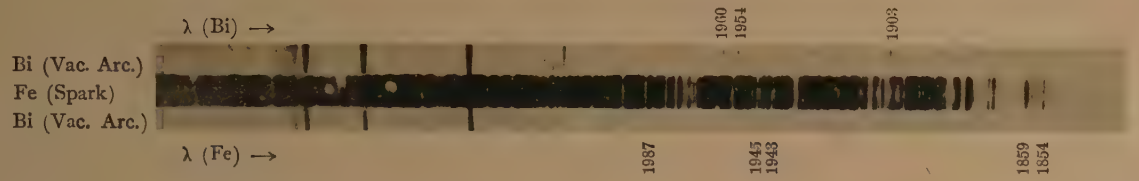


Magnification : 7

Fig. 9

Magnification : 9

# The Effect of an Electric Field on the Spectrum Lines of Hydrogen.

By

**Toshio Takamine and Usaburo Yoshida.**

(Received January 26, 1917.)

## § 1. Introduction.

In 1913, the effect of an electric field on spectrum lines was investigated by Stark[1], and also by Lo Surdo[2] under different experimental conditions.

In a series of subsequent investigations undertaken by Stark and others, several elements beside hydrogen and helium were also examined. The results relating to these researches are collected in Stark's "Elektrische Spektralanalyse chemischer Atome."[3]

In the mean time, many researches were carried out by different workers after the method first employed by Lo Surdo. Among those we may cite Evans and Croxson[4] who have dealt with the helium line $\lambda$ 4686 Å.U.

Quite recently, by adopting Lo Surdo's method, Howell[5] studied the manner of decomposition of certain spectrum lines of lithium and calcium in an electric field.

While Stark used canal rays as the source of light, Lo Surdo employed the glow in the region immediately in front of a cathode where the potential gradient is very large.

In Howell's paper, it is stated that the results obtained by Lo

1 Sitz. Ber., Berlin 932 (1913).
2 Rendiconti d. Lincei, **22** 664 (1913).
3 Leipzig: S. Hirzel, (1914).
4 Phil. Mag., **32** 327 (1916).
5 Astrophys. J., **44** 87 (1916).

Surdo[1] and Puccianti[2] are somewhat different from those of Stark. In fact, instead of the many components observed by Stark, Lo Surdo found two parallel ($p$) components in all the hydrogen lines $H_\alpha$, $H_\beta$, $H_\gamma$, and $H_\delta$, and perpendicular ($s$) components agreeing in number with the term number of the series.

As further research relating to the effect of an electric field on spectrum lines seemed highly desirable, the present experiment was undertaken.

## § 2. Arrangement.

In the present experiment, making use of Lo Surdo's method, we examined the transverse effect relating to the spectrum lines of hydrogen.

The discharge-tube used as the source of light was prepared in the following way :—

One of the electrodes of a fused silica Geissler tube of an ordinary Plücker form was replaced by a long aluminium rod, which completely filled about the half length of the capillary portion whose diameter was 2 mm. This served as the cathode. The other electrode of the tube was taken away, and a glass bulb of nearly spherical form having a capacity of about 1 liter was attached to this end. A long aluminium rod, 2 mm. in diameter, which passed through the bulb and terminated in the broad part of the fused silica tube, was used as the anode. The attachment of the fused silica tube to accessory glass tubes was secured by means of sealing wax. Two side tubes were connected to the bulb, one of which served for the introduction of hydrogen gas and the other for the evacuation by a Gaede mercury pump. The hydrogen was generated by a Kipp's apparatus and was dried by passing it through concentrated sulphuric acid and a tube containing phosphorus pentoxide.

The discharge-tube was excited by an induction coil of 25 cm. spark length, the current in its primary being 3 or 5 amperes at 40 volts. For the interruption of the primary current, and for the rectification of the secondary one, a rotating rectifier attached to a mercury interrupter was employed. The current in the secondary circuit varied from 1·5 to 2·5 milliamperes. During the discharge, a spark gap was always inserted in parallel with the tube.

After repeated evacuation and refilling of the tube, the side tube leading to the Kipp's apparatus was sealed. The evacuation was then

1 Rendiconti d. Lincei, **23** 82, 143, 252, 326 (1914).

2 Ibid., **23** 329, 331 (1914).

carried on under a continuous discharge, until the length of the Crookes dark space had increased to about 3 mm. or more; then the remaining side tube was also sealed. The length of the dark space of the tube thus produced showed a fluctuation amounting to a few tenths of a millimeter when the tube was newly excited; but usually it soon attained a steady state and afterward remained practically constant, even up to the end of 3 or 4 hours of continuous excitation.

Except a portion of about 4 mm. in front of the cathode, the capillary was covered with a thin asbestos paper. After several hours' excitation the inner wall of the capillary just in front of the cathode became coated with a thin film of some white substance due to the disintegration of the cathode, which considerably diminished the intensity of light. So it was found necessary to change the position of the cathode after one or two days' use of the tube.

For photographing the spectrum, we used the following four different instruments:

1. a four-prism spectrograph,
2. a single-prism spectrograph,
3. a spectrograph with a transparent replica grating,
4. a quartz spectrograph.

Between the source and the slit of the collimator of each spectrograph, excepting No. 4, an achromatic lens and a double image prism were placed so that the separated images of the two components of the source of light polarised parallel and perpendicular to the electric field were formed on the same vertical line of the slit.

Now we shall describe each of the instruments mentioned above.

(1). The four-prism spectrograph was constructed by slightly modifying the wave-length spectrometer of Hilger. In addition to a constant deviation prism (height 34 mm., long face 65 mm.), three 60° prisms of dense flint made by Hilger, ($n_D = 1{\cdot}6392$, height 45 mm., length of the base 64 mm.), were each placed in the position of the minimum deviation for $H_\gamma$. The spectrum was photographed with a Zeiss Tessar having a relative aperture of 4·5 and a focal length of 18 cm. The dispersion on the photographic plate was 15·7 Å.U. per mm. at $H_\gamma$. For this line and also for the lines belonging to the secondary spectrum of hydrogen lying between $H_\beta$ and $H_\gamma$, this instrument was specially adapted.

(2). The single-prism spectrograph was made by modifying a large spectrometer of Krüss. For photographing the spectrum, a Zeiss

lens having a relative aperture of 6·5 and a focal length of 40 cm. was used. This instrument was employed for examining the decomposition of $H_\delta$.

3. To examine the decomposition of $H_\alpha$, a plane grating spectrograph was desirable, but as we had no good plane grating at hand, a transparent replica grating of Hilger was used. The arrangement was, however, far from being satisfactory, and only served for a rough comparison of the separation of $H_\alpha$, $H_\beta$ and $H_\gamma$.

4. It is stated in Howell's paper before cited that, in the spectrum of the glow in the Crookes dark space, beside the hydrogen lines, he observed a number of spectrum lines of the metal used as the cathode, and that he searched for the effect of an electric field on these lines, but with a negative result. In our experiment, we also noticed the appearance of the intense aluminium lines $\lambda$ 3962 and 3944 Å.U. To ascertain the results arrived at by Howell, a quartz spectrograph of Hilger provided with a Cornu prism having a base of 65 mm. was employed. But, in the ultra-violet region, we could find no line which would be affected by the electric field.

For the measurement, we used a photo-measuring instrument of Hilger of 15 cm. travel. The ordinary eye-piece was replaced by a micrometer eye-piece having a screw of ½ mm. pitch, so that we could measure the plate in two directions perpendicular to each other.

The photographic plates we used were the panchromatic plate and the double-instantaneous plate of Wratten and Wainwright, and the Ilford special rapid plate. The exposure varied from 1 to 5 hours. In the present experiment, about 40 photographs were taken in all.

## § 3. Results.

The results obtained by the present experiment mainly relate to the mode of separation of $H_\gamma$, and the effect produced on some of the lines of the secondary spectrum of hydrogen.

a). Lines belonging to the Balmer series.

Of the four lines ($H_\alpha$, $H_\beta$, $H_\gamma$, $H_\delta$) we have examined, the most satisfactory result was obtained for the $H_\gamma$ line. A reproduction of the photograph obtained by the four-prism spectrograph is given in Fig. 1, Pl. I, and the portion near $H_\gamma$ is shown more enlarged in Fig. 2, Pl. I.

For $H_\alpha$ we could only measure the $p$-components. For $H_\beta$, the resolution of our instrument was insufficient, and as shown in the

Fig. 1.

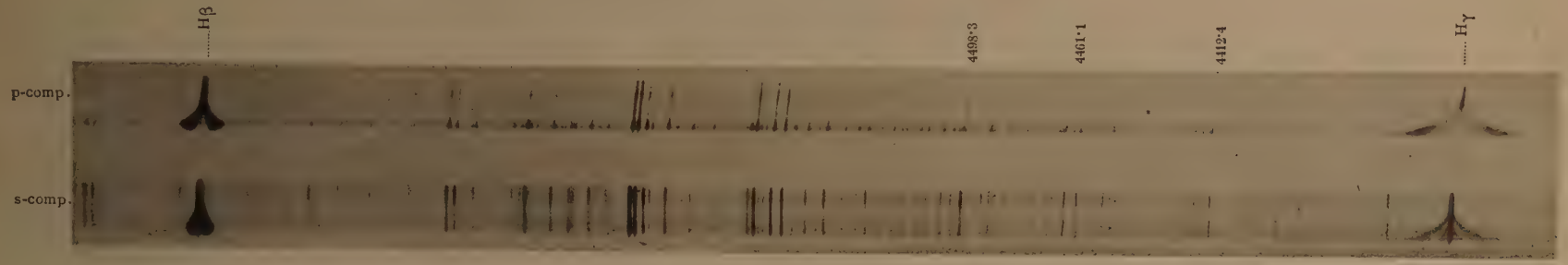


Magnification : 12

Fig. 2.

Exposure : $4^h\ 8^m$.

Magnification : 19

accompanying photogragh (Fig. 1, Pl. I) two *p*- and two *s*-components of $H\beta$ remain unresolved, although they are considerably broadened. For $H\delta$ also, the result was far from being satisfactory. We noticed two *p*-components and four *s*-components on some of the photographs taken with the single-prism spectrograph, and also on those taken with the four-prism spectrograph. In the course of further experiments which are now in progress, we shall re-examine more closely the above three lines.

As shown in Fig. 2, Pl. I, the *p*-components of $H\gamma$ consist of two intense outer components and four inner components of weak intensity; so that there are six components on the whole. The presence of a weak central line which was also given by Stark, may be due to the incomplete rectification of the current in the secondary circuit. In the *s*-components we see, beside a strong central line, two outer and two inner components.

In his later work, Stark found a great number of *p*- and *s*-components for the lines $H\beta$, $H\gamma$ and $H\delta$. But, as remarked by him in one of his papers, it is obvious that with Lo Surdo's method, the difficulty of obtaining a photograph showing such complicated decomposition is very great. Moreover, in Lo Surdo's method, it is not easy to know the intensity of the electric field. Therefore, to determine the field intensity we were obliged to use the following data for the outer components of $H\gamma$ given by Stark in the chapter entitled "Grobzerlegung" of the hydrogen lines.

4·6 Å.U. per $10^4$ volt/cm. for the *p*-components,

3·2 Å.U. per $10^4$ volt/cm. for the *s*-components.

In the first place, we measured the amount of separation of the outer *p*- and *s*-components of $H\gamma$, shown on the photographic plate, at several different points just corresponding to the various distances from the cathode, and from these data, curves were drawn by taking the amount of separation and the distance from the cathode in *x*- and *y*- directions of the rectangular coordinate axes. It is to be remarked that as the appearance of these lines are by no means well defined, especially at the immediate neighbourhood of the cathode, a certain amount of error in determining the point of maximum density must certainly be allowed for.

By using Stark's data given above, we are able to determine the distribution of the electric field in the region just in front of the cathode.

In the case shown in Fig. 1, Pl. I, where the length of the dark space was 2·3 mm., the results shown in Table I was obtained.

TABLE I.

| *p*-component. | | *s*-component. | |
|---|---|---|---|
| Distance from the cathode in mm. | $E$ in $10^4$ volt/cm. | Distance from the cathode in mm. | $E$ in $10^4$ volt/cm. |
| 0 | 5·64 | 0 | 6·15 |
| 0·34 | 4·35 | 0·35 | 4·45 |
| 0·50 | 3·67 | 0·71 | 2·88 |
| 0·67 | 3·07 | 1·06 | 1·90 |
| 1·03 | 2·05 | 1·15 | 1·59 |
| 1·34 | 1·25 | 1·42 | 1·06 |
| 1·68 | 0·70 | 1·77 | 0 56 |
| 2·01 | 0·38 | | |

Fig. 3.

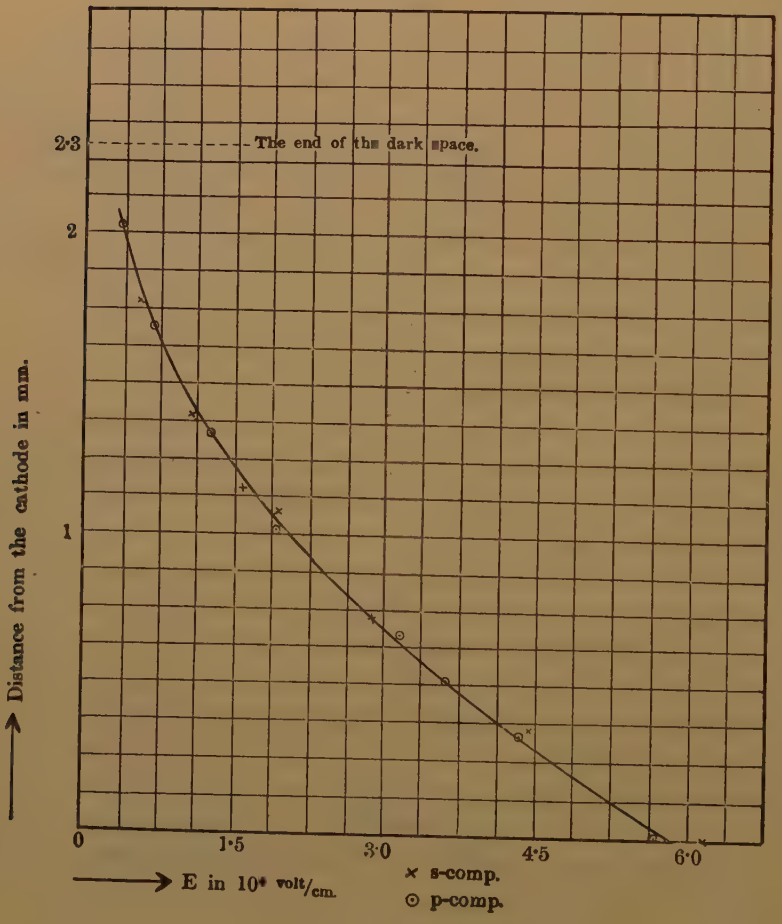

By taking the field intensity $E$ and the distance from the cathode as abscissa and ordinate respectively, and plotting the above results, the curve shown in Fig. 3 was obtained.

It will be seen that if we denote the field intensity at the end of the dark space by $E_0$, the quantity $E-E_0$, so far as the present experiment is concerned, seems to increase nearly proportional to the square of the distance from that end.

For the inner $s$-components of $H_\gamma$, similar measurements were carried out and it was found that, in addition to the fact that the separation is approximately symmetrical, it is proportional to the field strength.

The following table (Table II) gives the ralation between the field intensity $E$ and the amount of displacement $\delta\lambda$ from the position of the undisturbed line.

TABLE II.

| $E$ in $10^4$ volt/cm. | $\delta\lambda$ in Å.U. | $\delta\lambda/E$ |
|---|---|---|
| 1·68 | 0·76 | 0·45 |
| 1·92 | 0·82 | 0·43 |
| 2·96 | 1·19 | 0·40 |
| 4·25 | 1·89 | 0·44 |

It was at once evident that these components corresponded to $(+1)$ and $(-1)$ of Stark, given in the case of "Feinzerlegung" of hydrogen lines.

Quite a similar result was obtained also for the four inner $p$-components of the same line, but in this case, owing to the faintness of the photographic image, the accuracy was much less.

The amount of the displacement were again found to be nearly symmetrical; for $E=5{\cdot}83\times10^4$volt/cm, $\delta\lambda$ was 3·7 Å.U. for the one, and 1·7 Å.U. for the other pair of components. They corresponded almost exactly to $(+2),(+1),(-1),(-2)$ of Stark, given in the case of "Feinzerlegung".

b). Secondary spectrum of hydrogen.

Besides the lines belonging to the Balmer series, Stark found that some of the lines belonging to the secondary spectrum of hydrogen were also affected by the electric field, but in a quite different manner.

The main results obtained on these lines by Stark may be summarized as follows:

(1). Many of the lines belonging to the secondary spectrum of hydrogen are not affected by the electric field.

(2). The effect on the affected lines are one-sided, that is, the lines are displaced either only toward the red, or only toward the violet.

(3). The amount of displacement is very small compared with that of the Balmer lines.

(4). The amount of displacement increases more rapidly than is proportional to the field intensity.

(5). As the type common to the affected lines, one $p$-component and two $s$-components are generally observed, the one of the latter being displaced nearly equal in the amount to the former, while the other is very slightly displaced in the same direction.

In the present experiment, the region in which a number of affected lines were found, extended from $\lambda$ 4390 to $\lambda$ 4530 Å.U. The wave-lengths of the lines in this region, which were determined by photographing the spectrum of an iron arc in comparison, were found to agree fairly well with those obtained by Watson[1] and given in Kayser's Spectroscopie. In the following we have adopted Watson's values to the first decimal of an Å.U.

As the results obtained in the present experiment, we have to note the following facts.

(1). In most cases, the displacement is one sided, just as remarked by Stark; but there seems to be some exceptions. For instance, in the $s$-components of the line $\lambda$ 4417·5, one component is displaced toward the violet, while the other two are displaced toward the red.

In the $p$-components of $\lambda$ 4486·2, one is displaced toward the red, the other toward the violet.

(2). The type described by Stark as common to most of the affected lines, namely, that consisting of one $p$- and two $s$-components, was not observed in the present experiment. But, as the maximum intensity of the electric field calculated from the photograph was about $5{\cdot}83 \times 10^4$volt/cm., and thus inferior to that of Stark ($7{\cdot}40 \times 10^4$volt/cm.), it seems probable that the smaller displacement in the $s$-component could not be detected in our case.

In Fig. 4, we have drawn roughly the curves to show various modes presented by the affected lines. Just as stated by Stark, the amounts of displacement observed were very small for these lines, so that, with the dispersion used in the present experiment, we were unable to measure the amounts of displacement in the region above the dotted line

[1] Proc. Roy. Soc., A 82 189 (1909).

Fig. 4.

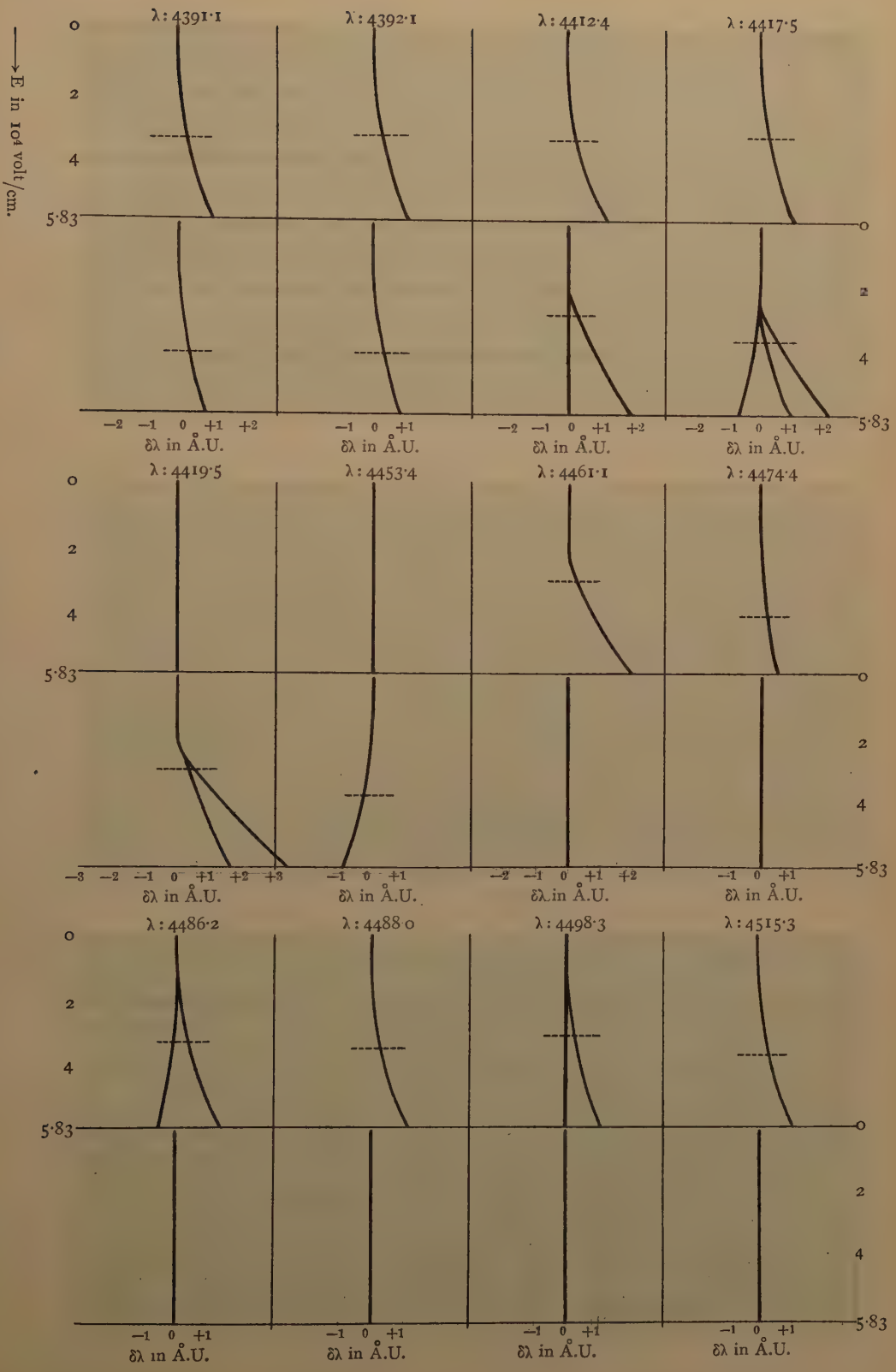
λ : 4391·1
λ : 4392·1
λ : 4412·4
λ : 4417·5
λ : 4419·5
λ : 4453·4
λ : 4461·1
λ : 4474·4
λ : 4486·2
λ : 4488·0
λ : 4498·3
λ : 4515·3
E in 10⁴ volt/cm.
δλ in Å.U.
5·83

The numerical values used for drawing the diagrams given in Fig. 4 are tabulated below:

TABLE III.

| λ in Å.U. | δλ for $p$-comp. | | δλ for $s$-comp. | | Remarks. |
|---|---|---|---|---|---|
| | $E=5{\cdot}8$ | $E=4{\cdot}6$ | $E=5{\cdot}8$ | $E=4{\cdot}6$ | |
| 4391·1 | +1.1 | | +0·8 | +0·5 | Both the $p$- and $s$-components of the line λ: 4392·1 showed similar displacements. |
| 4412·4 | +1·2 | +0·6 | +2·1 | +1·2 | Stark gives for the $p$-comp. of this line: δλ = 1·1 at $E=4{\cdot}8$; δλ = 1·8 at $E=7{\cdot}4$. Both the $p$- and $s$-components of the lines λ: 4414·4, λ: 4415·3 showed similar displacements. |
| 4417·5 | +1·2 | | −0·6<br>+0·9<br>+2·2 | —<br>+0·4<br>+1·3 | |
| 4419·5 | | | +1·5<br>+3·4 | +1·0<br>+2·0 | |
| 4453·4 | | | −0·8 | | |
| 4461·1 | +1·9 | | | | Stark gives for the $p$-comp. of this line: δλ = 1·4 at $E=4{\cdot}8$; δλ = 2·8 at $E=7{\cdot}4$ |
| 4474·4 | +0·6 | | | | |
| 4486·2 | +1·2<br>−0·6 | +0·9<br>— | | | |
| 4488·0 | +1.1 | +0·5 | | | |
| 4498·3 | +1·1 | +0·8 | | | |
| 4515·3 | +1·1 | +0·5 | | | In the $p$-comp. of the lines λ: 4519·3, λ: 4520·1 and λ: 4524·3, similar displacements were observed. |

N.B. In this table, δλ is expressed in Å.U., and $E$ in $10^4$volt/cm.
The + sign means a displacement toward the red, − toward the violet.

It is here to be remarked that in Stark's method we employ a uniform electric field, while in Lo Surdo's method we employ a heterogeneous field. In fact, each method has its own advantage. As a merit of Lo Surdo's method we may state that, in addition to its experimental simplicity, the use of a heterogeneous field has its peculiar advantage in allowing us to follow gradual changes brought on each spectrum line under investigation. The authors believe that this advantage is most highly appreciated when we examine the behaviour of the lines belonging to the secondary spectrum of hydrogen, in which

many lines are clustered closely together. For in such a case, the superposition of one displaced line on the other unaffected one often takes place, just as shown in the photograph accompanying the monograph of Stark. (Fig. 2, Tafel III.)

## § 4. Summary.

1). Employing Lo Surdo's method, the effect of an electric field on the spectrum lines of hydrogen was investigated.

2). For $H_\gamma$, in addition to the two outer *p*-components and the three *s*-components, which were obtained by former investigators adopting Lo Surdo's method, four inner *p*-components and two inner *s*-components were obtained which were clearly identified with certain components obtained by Stark.

3). Relying on the data given by Stark for $H_\gamma$ in the case of " Grobzerlegung ", the field strength was calculated, and the distribution of the electric field in front of the cathode was determined.

4). The proportionality of the amount of separation to the intensity of the electric field was found to hold good for the inner *p*- and *s*-components of $H_\gamma$.

5). The influence of the electric field on certain lines belonging to the secondary spectrum of hydrogen was also investigated and many interesting modes of separation were found.

In conclusion, the authors wish to express their hearty thanks to Prof. Mizuno for placing the resources of the Institute at their disposal, and also for the deep interest he has taken in the present investigation.

The authors' thanks are also due to Prof. Chikashige of the Chemical Institute for his kind advices.

Vol. II., No. 2, Published March 31st, 1917.

*Price - - - Yen 1.20*

These Memoirs are on sale at

MARUZEN COMPANY, LTD.

TOKYO, OSAKA, KYOTO, FUKUOKA & SENDAI.

大正六年三月二十八日印刷

大正六年三月三十一日發行

編纂兼發行者　京都帝國大學理科大學

印刷者　野村宗十郎

東京市京橋區築地三丁目十一番地

印刷所　株式會社 東京築地活版製造所

東京市京橋區築地二丁目十七番地

賣捌所　丸善株式會社

東京、大阪、京都、福岡、仙臺

# CONTENTS.

PAGE.

**Reflexion and Refraction Phenomena relating to Moving Medium.**
By Kajuro Tamaki. - - - - - - - - - - - - 59

**Figures produced on Photographic Plates by Electric Discharges.**
By Usaburo Yoshida. - - - - - - - - - - -

**The Spark and the Vacuum Arc Spectra of Some Metals in the Extreme Ultra Violet.** 105
By Toshio Takamine and Shigeharu Nitta. - - - - - - 117

**The Effect of an Electric Field on the Spectrum Lines of Hydrogen.**
By Toshio Takamine and Usaburo Yoshida. - - - - - - 137